2012

Vehicle lightening with composite materials: Objective performance comparison of material-systems for structural applications

Davide Scuccimarra
University of Windsor

VEHICLE LIGHTENING WITH COMPOSITE MATERIALS: OBJECTIVE PERFORMANCE COMPARISON OF MATERIAL-SYSTEMS FOR STRUCTURAL APPLICATIONS

by

Davide Scuccimarra

A Thesis
Submitted to the Faculty of Graduate Studies
through Mechanical, Automotive, and Materials Engineering
in Partial Fulfillment of the Requirements for
the Degree of Master of Applied Science
at the
University of Windsor

Windsor, Ontario, Canada

2012

VEHICLE LIGHTENING WITH COMPOSITE MATERIALS: OBJECTIVE PERFORMANCE COMPARISON OF MATERIAL-SYSTEMS FOR STRUCTURAL APPLICATIONS

by

Davide Scuccimarra

APPROVED BY:

_____
Dr. Faouzi Ghrib, External Reader
Department of Mechanical, Automotive & Materials Engineering

_____
Dr. Peter Frise, Internal Reader
Department of Mechanical, Automotive & Materials Engineering

_____
Dr. Jennifer Johrendt, Advisor
Department of Mechanical, Automotive & Materials Engineering

_____ _____
Dr. Vesselin Stoilov, Chair of Defense
Department of Mechanical, Automotive & Materials Engineering

September 10th, 2012

DECLARATION OF ORIGINALITY

I hereby certify that I am the sole author of this thesis and that no part of this thesis has been published or submitted for publication.

I certify that, to the best of my knowledge, my thesis does not infringe upon anyone's copyright nor violate any proprietary rights and that any ideas, techniques, quotations, or any other material from the work of other people included in my thesis, published or otherwise, are fully acknowledged in accordance with the standard referencing practices. Furthermore, to the extent that I have included copyrighted material that surpasses the bounds of fair dealing within the meaning of the Canada Copyright Act, I certify that I have obtained a written permission from the copyright owner(s) to include such material(s) in my thesis and have included copies of such copyright clearances to my appendix.

I declare that this is a true copy of my thesis, including any final revisions, as approved by my thesis committee and the Graduate Studies office, and that this thesis has not been submitted for a higher degree to any other University or Institution.

ABSTRACT

In recent years many studies proved that the adoption of polymer composites represents an effective solution to reduce the weight of vehicles.

In this context, the goal of this study is the design of a rear suspension cradle made of composite material, with particular attention to aspects such as recyclability and high volume production of the component.

Starting from the CAD model of the existing aluminum part, a simplified shape that represented it was designed and FEM analysis was conducted using the software ABAQUS; materials, geometry and fiber orientation were changed in order to obtain a composite model with the same performance as the aluminum model but with lower weight. The performance of the composite and aluminum models were compared.

In addition, a manufacturing process and a method of recycling for the optimal composite model solution were provided.

Dedicated to my family

ACKNOWLEDGEMENTS

I wish to express my greatest gratitude for my advisor, Dr. Jennifer Johrendt and my Chrysler tutors Dr. Saad Abouzahr and Dr. Jian Tao in providing continuous support and helpful ideas in the course of my research: I could learn in knowledge and method of research working under their supervision.

I would like to thank my thesis committee members, Dr. Peter Frise and Dr. Faouzi Ghrib for their valuable comments and recommendations.

Finally, I would to express my gratitude to Jan Stewart and Mike Houston for their presence and suggestions during the months I spent here in Canada: I really appreciated your help in every situation.

TABLE OF CONTENTS

LIST OF TABLES

LIST OF FIGURES

CHAPTER I

INTRODUCTION

1.1 Overview

In the recent years the rising trend of oil prices and an increasing awareness of the human contribution to the environmental pollution and global warming lead to an increased interest on fuel-efficient solutions for ground transportation. The result of this new approach has been a thorough search for light weighting options, which consist of the transition to alternative and more fuel-efficient powertrains and activities aimed at reducing vehicle weight [1].

In this context, the adoption of polymer composites represents an effective solution to reduce the weight of vehicles: large vehicle users, such as trailer truck operators, have already tested the benefit of the adoption of such technology for light weighting and their use will increase in this market share.

However, the need for weight reduction was less severe in relatively lighter weight passenger cars in the past and as consequence the introduction and anticipated growth of polymer composites in this market share will be slow.

But the tendency is to size reduction of vehicles and it will bring to a shift of sales away from heavier and less fuel efficient light trucks and SUVs moving towards cars, reversing the trend of the past 20 years, as shown in figure 1 [2].

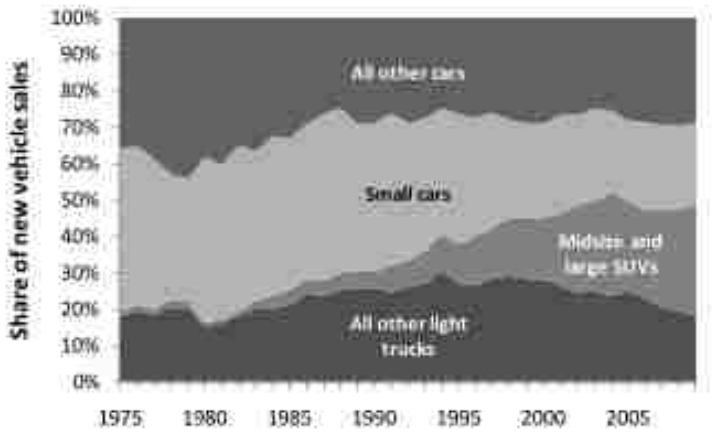

Figure 1: Historical trends of vehicles in the U.S. [2]

For this reason, in recent years automakers' automobile designs have started to incorporate composite solutions in mid-priced automobiles where formerly composites were justified only in very high-end cars, as market drivers such as crashworthiness take precedence over weight savings.

It has been proved through vehicle simulations that fuel consumption is reduced by 0.4 l/100km for cars, and 0.5 l/100 km for light trucks for every 100 kg of weight reduction. In other words, for every 10 % weight reduction, fuel economy increases by 6 % for cars and 8 % for light trucks [2].

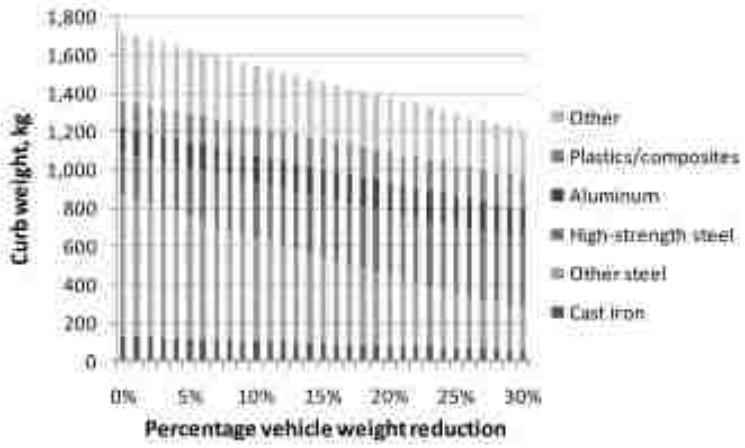

Figure 2: Material composition of 2016 lightweight vehicles [2].

In Figure 2 it is shown how the overall weight of cars will reduce in 2016. According to this prediction, the curb weight of an average new vehicle in 2016 weighs -480 kg than today (i.e. 28% less) [2]. It is possible to notice which materials will increase their percentage in the vehicle, in particular composites, aluminum and high-strength steel will have a steep increase in future years.

The adoption of new kinds of material will also affect the automotive material production energy demand: it is defined as the amount of energy required to produce/process materials embodied in new vehicles sold in each year.

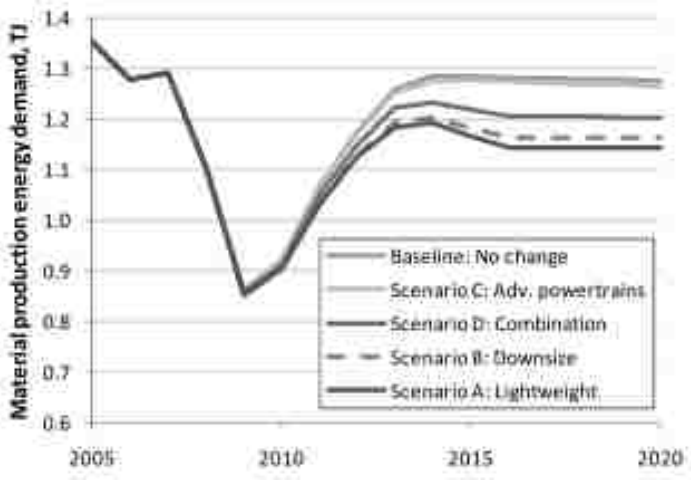

Figure 3a: Annual automotive material processing energy demand under different scenarios [2]

Looking at the trend for future years depicted in Figure 3a, the demand levels off, despite increasing sales, as the effect of accounted efficiency improvements take place. The drop in the energy demand verified around 2009 is due to the decrease in the number of sold vehicles in the same period (Figure 3b). Shaded areas correspond to peaks or drops of sold vehicles.

The production energy demands for four different scenarios are observed to be similar. Obviously, if no improvements are adopted the energy demand will be higher similarly with the adoption of more advanced power trains that weigh more and require more energy to process.

Figure 3b: Number of vehicles sold from 1975 to 2012 [Source: ALTSALES-US Department of Commerce]

Figure 3a shows that pursuing a lightweight strategy implies a lower production impact, despite greater use of more energy-intensive aluminum. A further improvement to this result can be obtained by the adoption of alternative lightweight materials pathways, such as composite materials.

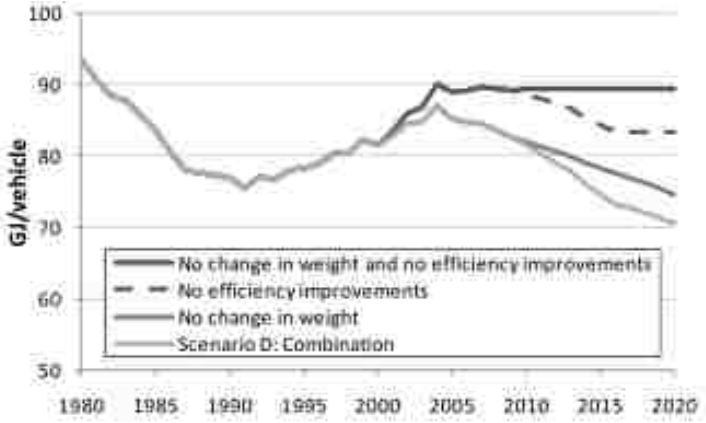

Figure 4: Material processing energy demand per vehicle sold [2]

In the future, the decline in material processing energy demand can be explained by efficiency improvements in materials processing, and due to the 15 % average new vehicle weight reduction depicted in the scenario. The relative magnitude of these two effects is shown on the same figure (Figure 4) by considering their effects separately. This reveals that the material processing improvements are responsible for most of the decline in the production impact.

1.2 Objective and Outline of the Thesis

The goal of the present research is the design of a rear suspension cradle made of composite material, with particular attention to aspects such as recyclability and high volume production of the component.

Starting from the production part mounted on the 2011 Dodge Dart 2.0 WGE Tigershark, a new model will be designed in order to study the feasibility of the conversion of the component from aluminum to composite material, obtaining the same or higher mechanical performance of the existing part but with lower weight.

The first step of this work will be the choice of the material and process more suitable to have a recyclable component for high volume production.

Then, depending on the previous choice, the design phase will be conducted: starting from the CAD model of the existing part, a simplified shape will be designed that reproduces it and FEM analysis will be conducted using the software ABAQUS, applying the same load conditions of the original case. A comparison between solutions with aluminum and composite material will be done, highlighting the results of the composite solution with respect to the metal one.

As explained before, the goals of the work will be a composite component that has a comparable mechanical performance as the aluminum solution, but with a lower weight.

Once the best solution in terms of design and material has been selected, a suitable manufacturing process for the component will be chosen, without providing specific information regarding the times and cost necessary for the production.

A method to recycle the component will be proposed according to the available information about recyclability and most common techniques used nowadays.

CHAPTER II

REVIEW OF LITERATURE

2.1 Composite Materials – Overview

Fiber reinforced polymer composites (FRP) are being widely used for structural applications where high mechanical properties together with low weight are required, and they constitute a valid alternative in comparison with metal materials.

The key point of composite materials is that they optimize the performance of conventional materials, in terms of mechanical behavior and lightness. This benefit is obtained through the combination of more than one material; for example, a matrix material with certain properties can be combined with a fiber that has different properties and the result is a material that highlights the best characteristics of both. Generally, a composite material is composed of at least two components or phases which are combined in different proportions and shapes.

Fiber reinforced polymer materials (FRP) are made of a continuous polymeric phase, the matrix, which assures a certain shape to the component and especially transmits the load uniformly to the reinforcement phase, the fiber, which has to absorb the amount of mechanical solicitations. Fibers can be of several types and shape, but the most common are glass fiber (GRP) or carbon fibers (CRP).

Due to the presence of a continuous (matrix) and a discontinuous (fiber) phase, composite materials have anisotropic characteristics in terms of elastic properties and mechanical resistance. The anisotropic grade depends on the orientation of the fibers inside the matrix: in particular it is higher for those composites which have a parallel disposition of the fibers, while it is lower if they are disposed with varying or random orientations.

The simplest type of fiber-matrix system is the ply, which is a layer of composite material where all the fibers are parallel and they define the longitudinal direction of the same ply. The union of more plies with different orientation forms a multiply: it is possible to define the axis of the multiply with respect to all the plies' orientation.

According to the previous definition, the mechanical response of the single ply will differ depending on the direction of the load, parallel or orthogonal to it, and on the number of plies adopted.

In Figure 5 it is shown how the presence of the fiber in the polymer matrix leads to a material with improved mechanical properties (especially tensile strength) when compared to a material made of only the polymeric matrix.

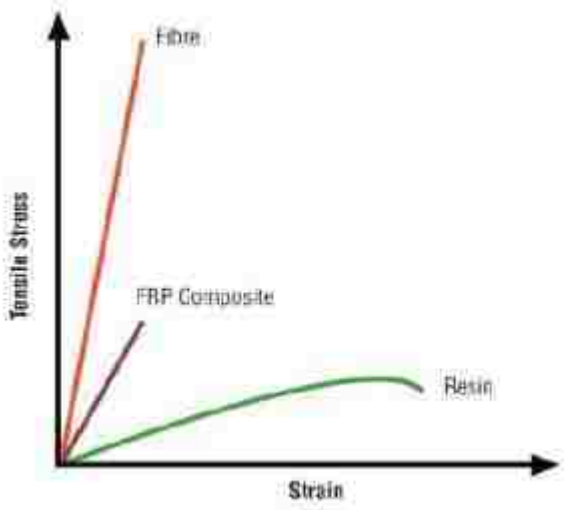

Figure 5: Mechanical properties of fiber, resin and FRP composite [13]

In order to exploit the mechanical properties of the fiber and improve both the resistance and the stiffness of the composite structure, it is fundamental to realize a good bonding along the surface of the interface between matrix and fiber. The external load is applied to the matrix but it is transmitted to the fiber through the shear friction along the surface mentioned previously (especially for those fibers that are not extended for all the length of the matrix).

The critical length for the fiber is defined as that beyond which the axial load is considered constant (this critical length is function of the type of the fiber, the interface and the matrix).

Regarding the mechanical properties of the FRP, it is possible to indicate two critical points for the mechanical behavior of such materials. As it can be seen in Figure 6, there is a maximum load beyond which the structure completely collapses. In this situation both the fiber and the matrix fail [13].

Nevertheless, before this point a laminate can reach a stress condition that leads to the formation of micro cracks in the matrix, which are detrimental for the mechanical properties of the composite material. For this reason, it is fundamental to ensure that a structure that has plies which do not exceed this point in presence of regular loads. The maximum stress that a laminate can withstand before the occurrence of micro-cracking depends on the adhesive properties of the resin.

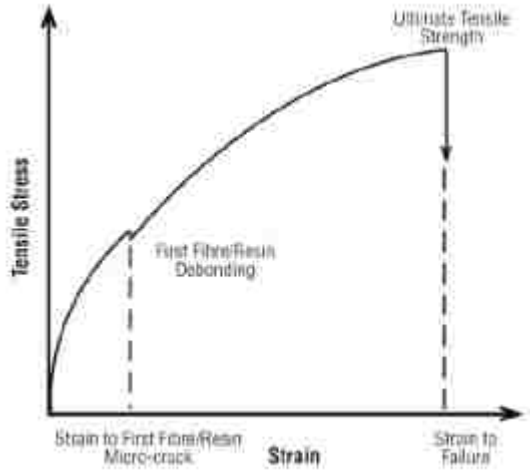

Figure 6: Stress-strain curve for FRP composites [13]

The fatigue behavior of FRP composites is influenced by the hardness of the resin, its resistance to micro-cracking and the grade of adhesion between matrix and fibers.

The bonding property of the system matrix-fiber is determined by the nature of the resin and can be improved through surface treatments of the fibers, namely applying a proper agent on the surface of the fibers.

Another way to improve the adhesion between matrix and fibers has been exploited in recent years through carbon nanotubes (CNT): their initial development faced difficulties

in dispersing CNT in polymers at high weight fractions while achieving uniform and strong interactions with the polymer matrix. Moreover, studies of hybrid composites using unoriented CNTs dispersed in polymers reported only negligible mechanical property improvements at low CNT loadings.

The solution for these problems consisted of aligning the CNTs and organizing them with long-range order, realizing mechanical improvements [14].

One method to establishing such order is by spinning ropes of discontinuous CNT as a new type of advanced carbon fiber. Another solution is to modify existing advanced composite systems to create hybrids; dispersion and alignment challenges for nano-composites are even more pronounced when the CNT is processed into matrix with a high volume fraction (approximately 60%) of advanced fibers.

Since the interface between plies in advanced composites is more accessible from the processing aspect than the laminate interior, several studies have realized marginal to nano-modified interfacial properties using carbon nano-fibers (CNF) and CNT at laminate interfaces [14].

One approach could be to integrate aligned CNT with existing carbon fiber prepreg materials and processing.

This is accomplished by growing a vertically-aligned CNT (VACNT) forest at high temperature, and then 'transfer-printing' the CNT to prepreg at room temperature, taking advantage of the tack of the prepreg to separate the CNT from the growth substrate.

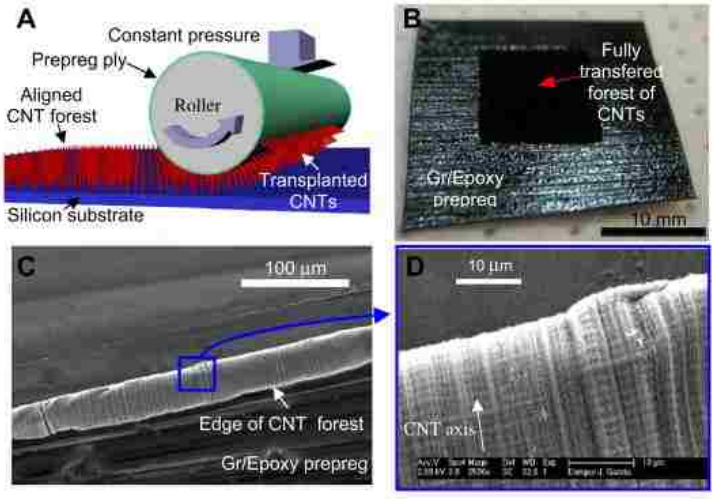

Figure 7: Transfer printing of VACNTs to prepreg [14]

The process used to transplant the VACNT to a prepreg is shown in Figure 7A. The prepreg is attached to a cylinder that is rolled and pressure is applied across the substrate containing the CNT forest to transfer the CNT to the prepreg: the transfer rate, pressure, and geometry are set until full transplantation of the CNT forest is achieved.
Figure 8 shows how the VACNTs are placed between composite plies and how they contribute to bridge the cracks.

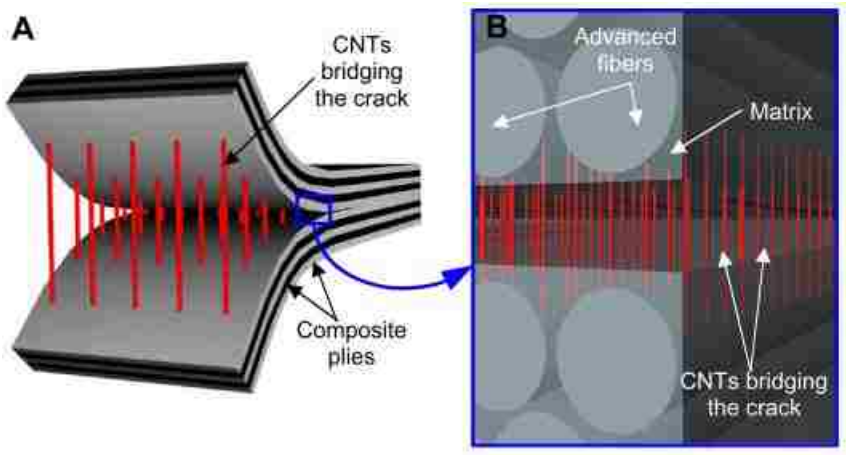

Figure 8: Hybrid interlaminar architecture: (A) VACNTs placed in between two plies and (B) effect of VACNTs bridging the crack between two plies [14]

Further developments of CNT will lead to a great interest fabricating shorter aligned CNT forests to reduce the interlayer thickness and thereby focus on bridging.

2.2 Fiber Materials

In Figure 9 the raw materials pipeline is depicted: starting from raw fibers and resins, they are manufactured and several types of composite products can be achieved, depending on the specific application. Focusing the attention on the fiber manufacturing section of the pipeline of Figure 9, in the production of composite materials many different types of fiber can be used; the most common are carbon fibers, glass or aramid fibers. In the following a brief presentation of their characteristics will follow

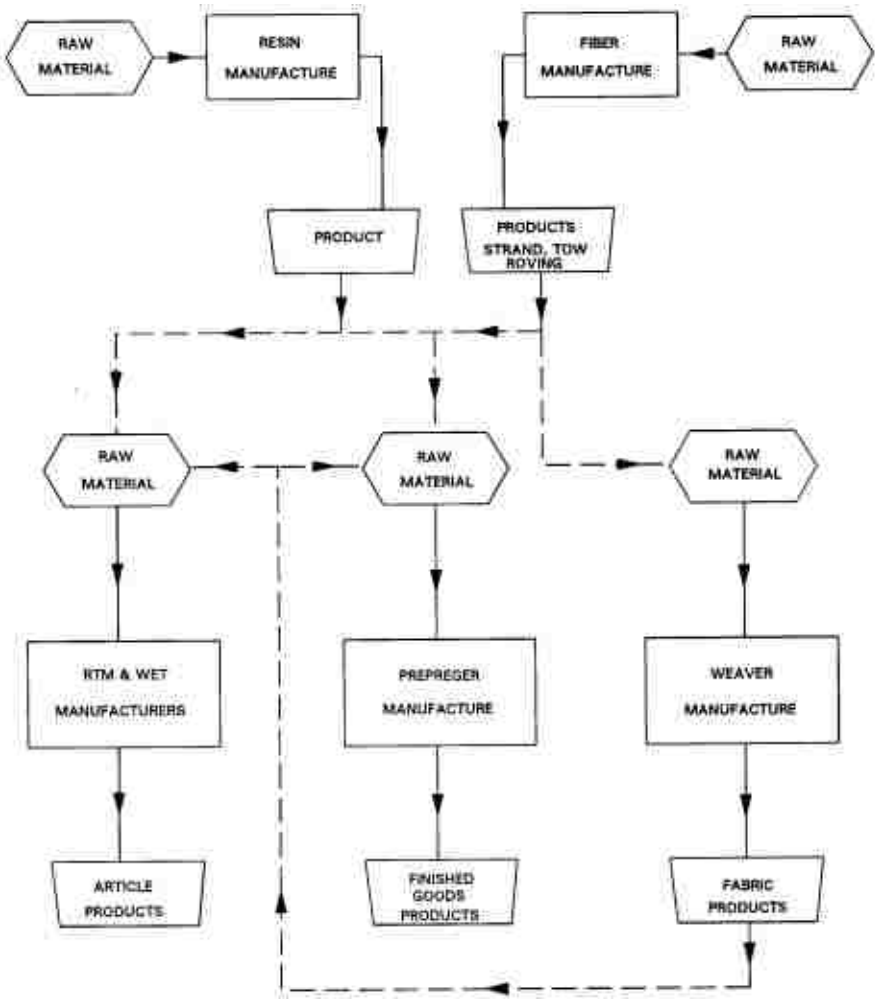

Figure 9: Raw materials process [18]

2.2.1 Carbon Fibers

The interest in carbon fibers for structural materials was initiated in the late 1950s when first experiments were conducted to carbonize synthesized rayon in textile form to produce carbon fibers for high temperature applications.

One of the first distinctions to be made for this kind of fibers is the difference between carbon and graphite fibers, although the terms are frequently used interchangeably.

Carbon and graphite fibers are both based on graphene (hexagonal) layer networks present in carbon: the material is defined as graphite if the graphene layers stack with three dimensional orders. Usually for graphite fibers extended time and temperature processing are required to form this three dimensional order, and this aspect makes these fibers more expensive. Nevertheless, disorder frequently occurs in the layers because the bonding property between planes is weak, so only the two dimensional ordering within the layers is present: this kind of material is defined as carbon. There are several other conditions which contribute to differentiate carbon from graphite fibers, and even graphite fibers retain some disorder in their structure, while some differences are implied [18].

In order to produce carbon fibers three different precursor materials are commonly used: rayon, polyacrylonitrile (PAN), and isotropic and liquid crystalline pitches. Among the previous materials, PAN is the most common: carbon fibers are made mainly from its carbonization [18]. The fiber graphite with basal planes tends to align along the fiber axis and this forms an internal structure that is similar to an onion skin, while pitch fibers may have a different internal structure, reminding to sheaves or spokes.

This kind of materials present high levels of anisotropy due to their morphology and this leads to a great variability in the moduli range: they vary from 200 to 750 GPa along the direction parallel to the fiber long axis, while they are lower in the normal direction of the fiber axis, around 20 GPa. To make a comparison, a single crystal of graphite is about 1060 and 3 GPa, for the directions parallel and normal to the axis of the fiber, but these properties are not attainable in fiber form and these values are lower after the processing [18]. Nevertheless, ultra high modulus fibers can be prepared from liquid-crystalline mesophase pitch; they give higher moduli because the precursor material has a higher degree of orientation and this translates through to the final carbonized fiber generating larger and more oriented graphite crystallites [18].

As a consequence of previous considerations, carbon fiber properties are dependent on the fiber microstructure, which is deeply affected by the process which is adopted; in this way, such that properties of fibers can be highly different even if their precursor materials are the same but a different process has been used to their production. In this context, precursors and processes are chosen in order to optimize the mechanical properties of the

fiber, taking into account the application of the fiber and the costs involved in their production.

For example, carbon fibers from PAN have a lower cost respect to the other precursors, which makes them more competitive in the market maintaining a good compromise between cost and quality of the fiber [18].

In the following it will be described the manufacturing process for carbon fiber for the PAN variant, which is one of the most common and, as told before, most cost effective. The manufacture of PAN based carbon fiber can be divided into the white fiber and black fiber stages: they are generally described in the following [18].

The production of PAN precursor, or white fiber, is considered a technology in itself due to its complexity; for this stage conventional fiber processes are performed: polymerization, spinning, drawing, and washing, even if additional drawing steps may be added in the process. It is important to notice that the characteristics of the white fiber deeply influence the processing and results for the black fiber processing, so it is fundamental to achieve a good quality of the same.

The black fiber process consists of several steps: oxidation (or thermosetting), pyrolysis (or carbonizing), surface treatment, and sizing. In the oxidation process the PAN fiber is converted to a thermoset from a thermoplastic. For this oxidation process the fiber diameter is limited by waste gas diffusion. In the pyrolysis process, which is performed under an inert atmosphere, most of the non-carbon material is expelled, forming ribbons of carbon aligned with the fiber axis [18].

In the surface treatment step the fiber may be etched in either gas or liquid phase to improve the wet ability for the resin and enhance the formation of a strong bond; this can be realized through oxidizing agents such as chlorine, bromine, nitric acid or chlorates. Some additional improvement may also be realized through removal of surface flaws. The carbon fibers are often treated with solution of unmodified epoxy resin and/or other products as a size. The sizing prevents fiber abrasion, improves handling, and can provide an epoxy matrix compatible surface. From the experience in this field, it has been proved that PAN precursor can provide higher strength carbon fibers, while pitch can provide higher moduli. In Figure 10 white fiber and black fiber processes are schematized.

Another precursor material for carbon fibers is the Rayon: nevertheless, Rayon based

fibers tend to be less expensive but have lower performance. In Figure 11 this characteristic of Rayon based fibers can be noticed; in addition, differences between pitch and PAN fibers are evident in terms of tensile modulus, tensile strength and cost. In the past pitch fiber composites have been prepared with elastic moduli superior even to steel and electrical conductivity higher than copper conductor even if the shear strengths and impact resistance are degraded. The yield for PAN is approximately 50%, but for pitch can reach 90%.

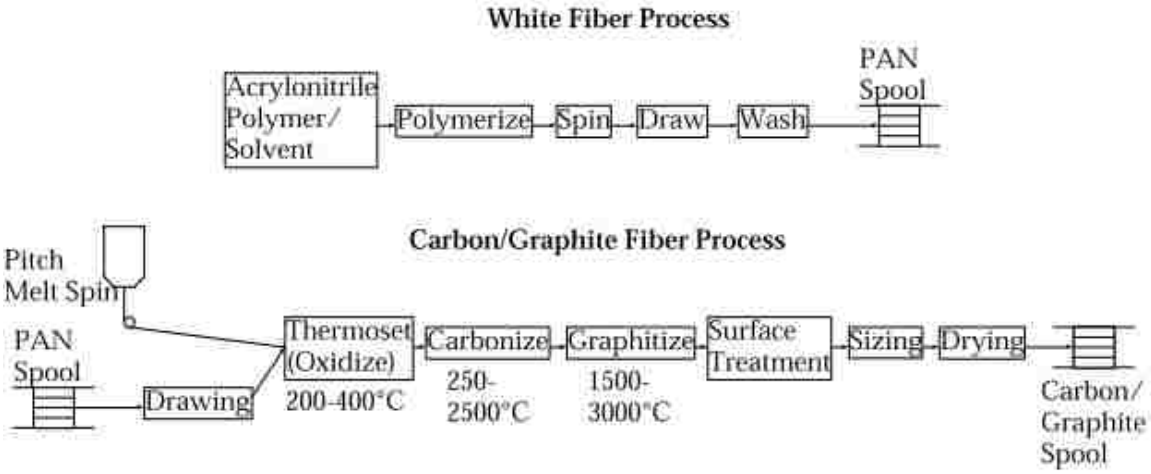

Figure 10: Carbon fiber typical process flow diagram [18]

	Tensile Modulus, Msi	Tensile Strength, ksi	Density, g/cm^3	Fiber Diameter, micron	Cost, $/#
Carbon (PAN)	30-50	350-1000	1.75-1.90	4-8	20-100
Carbon (Pitch)	25-110	200-450	1.90-2.15	8-11	40-200
Carbon (Rayon)	6	150	1.6	8-9	5-25
Glass	10-12.5	440-670	2.48-2.62	30	5-40
Aramid	20	410	1.44	--	25-75
Boron	58	730-1000	2.3-2.6	100-200	100-250

Figure 11: Properties of carbon fibers (from different precursor materials) and other types of fibers [18]

2.2.2 Glass Fibers

Glass fiber are characterized by an elevated strength (at least double if compared with the best steel), good stiffness (similar to aluminum), low cost, low thermal and electrical conductivity, high maximum temperature of operation (between 500 and 1000 °C).
There are principally two different kinds of glass fiber for the manufacture of composite materials:

- E: it is the most utilized and economic type of glass fiber. It is composed of silica (50 %), alumina (15 %) and calcium and boron oxides; it has low electric conductivity and originally it was employed in the electric sector;
- S: it is essentially constituted of silica (65%), alumina (25 %) and magnesia (10%) and it is characterized by a high strength.

Then there are several other types of glass fibers that are utilized for special and dedicated purposes.
For many years glass composites have had a distinct strength to weight advantage. Although the rapid evolution of carbon and aramid fibers has gained advantages, glass composite products have still prevailed in certain applications.
In particular, the advantages related to glass fibers are a low cost per weight or volume, chemical or galvanic corrosion resistance, good electrical properties, and the possibility to realize many product forms. While the typical disadvantages of these fibers compared to carbon ones are the coefficient of thermal expansion and modulus properties, while respect to aramid fibers the glass ones have worse tensile properties but better behavior under compression , higher shear properties and moisture pick-up [19].
Typical commercial applications for glass products are filtration devices, thermal and electrical insulation, pressure and fluid vessels, and structural products for automotive and recreation vehicles. Many uses are applicable to military and aerospace products as well. As told before, with this wide range of applications it can be seen how glass fiber composite can be produced with different forms for different applications, and also

structural applications can be considered limitless to fabricate (choosing the proper process for the particular application) [18]. Compared to other fibers, they have some limitations linked to their low thermal and electrical conductivity and different melting temperatures when compared to carbon fibers.

Regarding the manufacture methods for their production, glass fibers are mostly produced from raw products with additives that are mixed and are premelted into marbles. This form presents a raw product form for automated feeding to the individual melt furnaces, diminishing the time of the process. Another method is to feed, via hoppers, dried raw products directly to batch cans.

Independently from the raw form, the material is fed into furnaces to become molten at approximately 1500°C. The molten mass flows into plates which contain many bushings with small orifices from which the individual filaments are drawn. The diameter of the filaments is controlled by the viscosity of the glass melt and the rate of extrusion. Cooling or solidification occurs rapidly as the glass leaves the bushings in filament form under ambient conditions and it is realized through water spray and/or application of the binders. The individual untwisted filaments are gathered and then high speed wound on tubes or "cakes". Sometimes finishes are applied after the strands are wound on the tubes then dried. In order to produce rovings, the strands are then creeled, unwound and gathered again to form ends or multiple untwisted strands. This process of gathering or combining is again repeated to form rovings of desired yields (yards per pound).If they have to be used for weaving of fabrics and braiding, the strands are twisted to form yarns. Single yarns are composed of single strands twisted by it. Two strand constructions are two strands twisted to produce a single yarn, while plied yarns are made from twisting two or more yarns together. Twisting and plying is often referred to as "throwing". During this process of continuous filament one of the most important variables is the repeated tensioning required during the numerous product forms fabrication. For this purpose, tensioning devices are used, such as: disc-type or "whirls", gate-type, tension bars or staple bars, and compensating rolls in the delivery from the creels. Humidity is another controlled variable in the twisting, plying, and braiding, warping, slashing, gulling and weaving areas. The common value of the relative humidity is of 60 to 70 percent range. During the glass processing operations surface abrasion is a factor which

must be monitored, especially for devices such as: guide eyes, spacer bars, rollers and such are subject to wear and must be maintained. These contact devices are manufactured from materials including: stainless steel, chromium plating, and ceramics [18].

2.2.3 Aramid Fibers

Aramid fibers have a great interest for applications in composite materials due to the following factors: low density (the density of aramid is 1.44 g/cm^{3,} about 40% lower than glass and about 20% lower than commonly used carbon), high tensile strength, high tensile stiffness, low compressive properties (nonlinear), and exceptional toughness characteristics. Moreover, aramid fibers do not melt and they decompose at about 500°C. The tensile strength of yarn can be varied from 3.4 - 4.1 GPa (in twisting direction) by choosing different types of aramids. The nominal coefficient of thermal expansion is -5x10^{-6} m/m/C° in the axial direction. Since aramid fibers are aromatic polyamide polymers, they have high thermal stability and dielectric and chemical properties, in addition to excellent ballistic performance and general damage tolerance derived from fiber toughness. Moreover, composite systems reinforced with aramid have excellent vibration-damping characteristics and they resist shattering upon impact. Temperature of use in composite form with polymer matrix ranges from -36 - 200°C. At 60% fiber volume fraction, composites of epoxy reinforced with aramid fibers have nominal tensile strength at room temperature of 1.4 GPa and nominal tensile modulus of 76 GPa.

These composites are ductile under compression and flexure and, as a consequence, their ultimate strength is lower than glass or carbon composites under compression and flexure. Composite systems, reinforced with aramid, are resistant to fatigue and stress rupture: under tension/tension fatigue, unidirectional specimens survive 3,000,000 cycles at 50% of their ultimate stress [18]. Recently, thermoplastic resin composites reinforced with aramid have been developed and they have exhibited equivalent mechanical properties compared to similar thermoset systems. In addition, thermoplastic systems provide potential advantages in economical processing, bonding, and repair. These are also used for composites where maximum impact and damage tolerance is critical and

stiffness is less important. Kevlar™49 is predominantly used in reinforced plastics - both in thermoplastic and thermoset resin systems. It is also used in soft composites like core of fiber optic cable and mechanical rubber good systems.
Typical applications of aramid fibers are to brake, clutch, and gasket due to their stability and frictional properties at high temperatures; low coefficient of thermal expansion is being used in printed wiring boards and exceptional wear resistance is being engineered into injection-molded thermoplastic industrial parts. Melt-impregnated thermoplastic composites, reinforced with aramids, offer unique processing advantages -e.g., in-situ consolidation of filament-wound parts: these can be used for manufacturing thick parts where processing is otherwise very difficult.
Aramid fiber is relatively flexible and tough. Thus it can be combined with resins and processed into composites by most of the methods established for glass [18].

2.3 Resin Materials

Resin is a generic term used to designate the polymer, polymer precursor material, and/or mixture with various additives or chemically reactive components. The resin, its chemical composition and physical properties, deeply affect the processing, fabrication and ultimate properties of composite materials. Some variations in the composition, physical state, or morphology of a resin and the presence of impurities or contaminants in the same resin may affect handle ability and process ability, lamina/laminate properties, and composite material performance and long-term durability [18].
Resin for composite material can be divided in two types: thermoset or thermoplastic. In the following these two types of matrixes are described.

2.3.1 Thermoset Resin

2.3.1.1 Epoxy

The term epoxy is a general description of a family of polymers which are based on molecules that contain epoxide groups. An epoxide group is an oxirane structure, a three-member ring with one oxygen and two carbon atoms. Epoxies are thermosetting resins that can be polymerizable and contain one or more epoxide groups curable by reaction

with amines, acids, amides, alcohols, phenols, acid anhydrides, or mercaptans. The polymers are available in a variety of viscosities from liquid to solid.

Epoxies are used widely in resins for prepregs and structural adhesives. The advantages of epoxies are high strength and modulus, low levels of volatiles, excellent adhesion, low shrinkage, good chemical resistance, and ease of processing. Their major disadvantages are brittleness and the reduction of properties in the presence of moisture. The processing or curing of epoxies is slower than polyester resins.

The cost of the resin is also higher than the polyesters. Processing techniques include autoclave molding, filament winding, press molding, vacuum bag molding, resin transfer molding, and pultrusion. Curing temperatures vary from room temperature to approximately 180°C. The most common cure temperatures range between 120° and 180°C. The use temperatures of the cured structure will also vary with the cure temperature, while higher temperature cures generally yield greater temperature resistance. Cure pressures are generally considered as low pressure molding from vacuum to approximately 700 kPa [18].

2.3.1.2 Polyester

The term thermosetting polyester resin is a general term used for orthophthalic polyester resin or isophthalic polyester resin. Polyester resins are relatively inexpensive respect to epoxy ones and fast processing resins used generally for low-cost applications. In combination with certain fillers, they can exhibit resistance to breakdown under electrical arc and tracking conditions. Isophthalic polyester resins exhibit higher thermal stability, dimensional stability, and creep resistance respect to orthophthalic ones. In general, for a fiber-reinforced resin system, the advantage of polyester is its low cost and its ability to be processed quickly [18].

Fiber-reinforced polyesters can be processed by many methods. Common processing methods include matched metal molding, wet lay-up, press (vacuum bag) molding, injection molding, filament winding, pultrusion, and autoclaving [18].

2.3.2 Thermoplastic

The majority of thermoplastic polymers are composed of a random molecular orientation and are named amorphous. Amorphous thermoplastics are available in several physical forms, including films, filaments, and powders. Combined with reinforcing fibers, they are also available in injection molding compounds, compressive moldable random sheets, unidirectional tapes and woven prepregs. With this kind of resins the fibers used are primarily carbon, aramid, and glass.

The use of amorphous thermoplastics as matrix materials for continuous fiber reinforced composites is a recent development: in particular, the properties of these resins have led to their consideration for primary and secondary aircraft structures, including interior components, flooring, fairings, wing skins, and fuselage sections.

The specific advantages of amorphous thermoplastics depend upon the polymer. Typically, the resins are noted for their processing ease and speed, high temperature capability, good mechanical properties, excellent toughness and impact strength, and chemical stability. The stability results in unlimited shelf life, eliminating the cold storage requirements of thermoset prepregs. Several amorphous thermoplastics also have good electrical properties, low flammability and smoke emission, long term thermal stability, and hydrolytic stability.

The primary advantages of amorphous thermoplastics in continuous fiber reinforced composites are potential low cost process at high production rates, high temperature capability, and good mechanical properties before and after impact, and chemical stability. High temperature capability and retention of mechanical properties after impact have made amorphous thermoplastics attractive to the aerospace and automotive industry. A service temperature of 350°F and toughness two to three times that of conventional thermoset polymers is typical. The most significant advantage of thermoplastics is the speed of processing, resulting in lower costs: typically, cycle times in production are less than for thermosets since no chemical reaction occurs during the forming process.

The costs of amorphous thermoplastics prepreg used for advanced composites are higher than equivalent performance epoxies. Finished part costs may be lower due to the

processing advantages discussed above. The ability to re-process the material results in reduced scrap rates, translating into additional cost savings. For example, the same sheet laminate can be thermoformed several times until the desired configuration is achieved, and in addition certain forms can be recycled.

2.3.3 B – Stage Epoxy

Composites using epoxy resins can be formed and reformed whenever they are heated above their glass transition temperature (T_g). The reform ability decreases as the degree of conversion nears the ultimate for that particular epoxy polymer. An epoxy reinforcement in the B-staged condition can be treated as a thermoplastic material and can be melted and thermoformed.

The degree of cure can be increased in steps or progressions without significant detrimental effect to the mechanical properties of the composite material. Tailored blanks can be CNC cut, laminated, rapidly formed and B/staged. These formed and B/staged blanks can then be fed into the progression molding operation.

There is a point in the epoxy degree of conversion when the cooled lamination is dimensionally stable enough to withstand unsupported post-cure. This post-molding heat treatment will yield maximum degree of conversion for each specific epoxy.

Epoxy resins arrive at a prepregger in normally a solid form, typically powdered, granular or in large chunks; these are then typically dissolved in a solvent (normally acetone), then mixed with catalysts and the fiber reinforcement is dipped into baths, excess resin is squeezed off and then the solvent is evaporated away in heating towers or tunnel ovens. These tunnel ovens drive the state of cure of the epoxy further, but not to completion. This process is called B-staging the epoxy material [22].

Another method used to mix the solid epoxy resins is by heating and melting them in reactors or mix vessels effectively reducing the viscosity to a point where the other key ingredients can be compounded into the mixture. At this stage in the cross-linkage process the epoxy resin is technically still a thermoplastic and it can be melted, although the molecular weight of the polymer is steadily increasing. The molten resin is then cast

into paper or can be directly applied to the reinforcement at this time. When cooled the resin hardens and returns to the original semi-solid form. The sticky or tacky characteristics can be controlled by the amount of time at temperature and directly correlates to the degree of conversion of cure. [23] [25]

However, in the previous description the gradual increase in viscosity of the polymer as the molecular weight increases during the cure process is not considered and the process results more complicated and difficult to realize. B-staged epoxy prepregs are normally characterized by aerospace composites manufacturers by their degree of resin flow, stickiness, drape, formability or sag. Some manufacturers utilize press molding grades of epoxy prepreg.

Some applications of B-stage epoxy are: the Gatling Gun Ammo Handling Helix, where a FG/epoxy prepreg disk has been manufactured through compression molding, and the Lite-Flex Springs, which are in use on over 15 million vehicles, including GM, Ford, Range Rover, Chrysler, Iveco, Navistar and others. Especially for the second application, the fact that this supplier has been able to compression mold very high volumes of thick walled composite springs is proof that the epoxy chemistry can be utilized for an ever greater percentage of a typical vehicle or truck chassis [24].

2.4 Processes

2.4.1 Braiding

The braiding process fabricates a preform or final shape at the same time that it generates the woven form. This product form is a unique fiber reinforcement which can use preimpregnated yarn as well as dry fibers. The main advantage of the braiding process is its ability to realize odd shapes and maintain fiber continuity while developing high damage tolerance compared to unidirectional and laminated products [18]. This particular characteristic is useful to realize square, oval, and more in general shapes with constant cross-section. The three dimensional form of braiding has evolved in last years and it is possible to fabricate non-uniform cross sections too, still maintaining weaving in all three

planes [18].

A demonstration of its versatility is the open-wheel race car body which was fabricated by braiding.

In the application of biaxial and triaxial braiding, a mandrel is usually used to form the braid. The mandrel also acts as the mold for the final product. The braiding machine controls the rate of feed of the mandrel and the rotational speed of the carriers. The combination of these parameters and the size of the mandrel control the braid angle. The braid angle, along with the effective yarn, tape, or tow width (width of the specific size yarn, tape, or tow on the mandrel as placed by the braiding process), ultimately controls the coverage of the braid on the surface of the fabricated form. As the braid angle increases, the maximum size of the mandrel which can be covered with a specific yarn, tape, or tow size decreases. For complicated forms, expendable mandrels may be used. These include mandrels made from low melting temperature metal alloys and water-dissolvable casting materials, and collapsible mandrels [18].

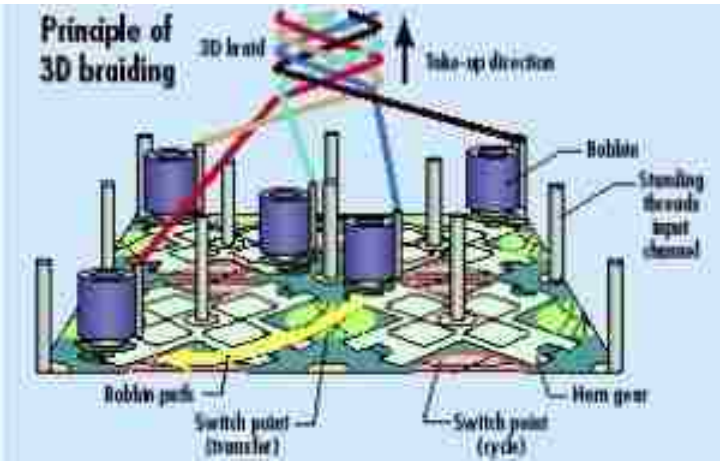

Figure 12: Scheme of 3D braiding process [26]

In three-dimensional (3D) braiding process schematized in Figure 12, the weaving process itself is used to control the shape of the fabricated product. The typical 3D braiding process involves a bed of cops, or weaving loops, which are moved in a systematic manner. This systematic movement creates an interwoven product in the x-y plane. As the yarns, tapes, or tows are pulled into the weaving process, the z-direction is

also intertwined. The resulting product is essentially self-supporting because it interweaves in three directions. For precision exterior dimension, matched metal molds can be used during the resin matrix curing process. The following are the general steps involved in the braiding process [18]:

1. Decide the feed speed, cop speed, and weave pattern (for 3D braiding).
2. Run the braiding machine until the product is finished.
3. If prepreg material is not being used, use an appropriate resin impregnation process (RTM, wet resin impregnation, and so on).
4. Cure according to the appropriate process determined by the impregnation method (autoclave cure, vacuum bag, RTM, and so on).
5. Remove the part from the mold or mandrel.

2.4.2 Thermoforming

The thermoforming process, as applied to thermoplastic composite materials, is generally divided into two categories: melt-phase forming (MPF) and solid phase forming (SPF). Thermoforming exploits the rapid processing characteristics of thermoplastics. The composite thermoforming process can be divided into four basic steps: firstly, the material is heated to its processing temperature external to the forming tool (through radiant heat). Then the oven-heated material is rapidly and accurately transferred to the forming tool and is pressure-formed with matched die set tooling into desired shape. Finally, the formed laminate is cooled and its shape is set by sinking the heat into the tooling [18].

The melt-phase forming is performed at the melting point of the thermoplastic matrix and requires sufficient pressure and vacuum application during the forming process in order to provide complete consolidation. In Figure 13 the steps of vacuum thermoforming are depicted: the plastic sheet is previously heated and then formed with application of vacuum.

In general, the MPF process is preferred when the geometry of the part that has to be

produced presents sharp contour changes that require some level of resin flow.

SPF is generally performed at temperatures between the onset of crystallization and below the peak melting point. This temperature range provides sufficient formability while the material remains in a solid form. SPF allows forming of preconsolidated sheet to be performed without a consolidation phase, but it is limited to part geometries exhibiting gentle curvatures [18].

The processing time for thermoforming is governed by the rates at which heat can be added to the material and then removed. This is primarily a function of the material thermal properties, material thickness, forming temperature, and tooling temperature. The pressures required to shape the material are dependent on various factors including part geometry, material thickness, and formability.

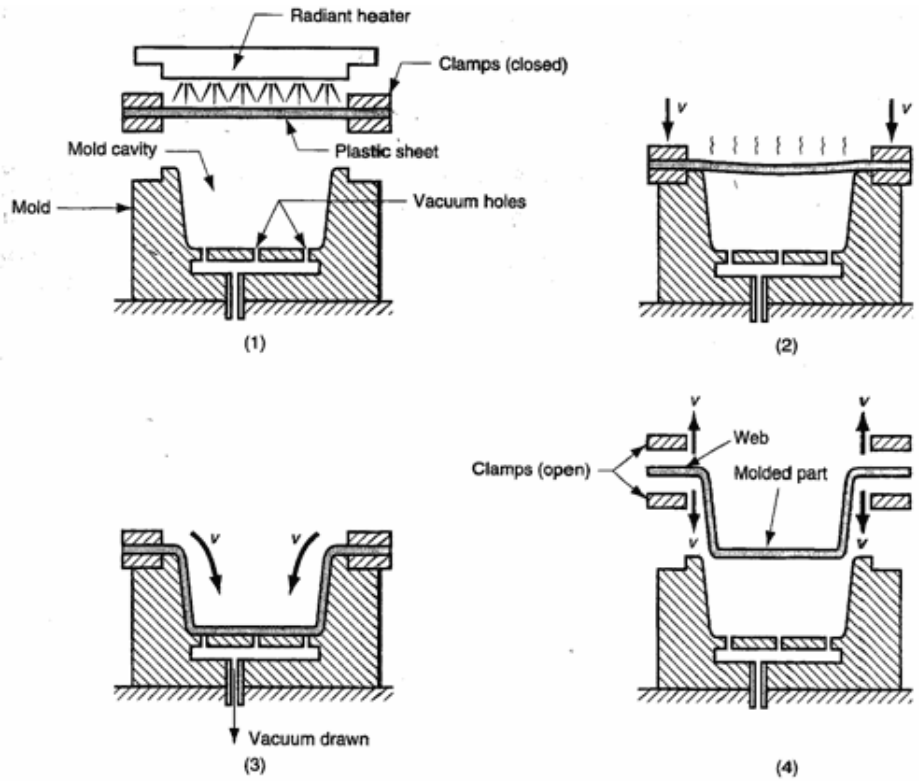

Figure 13: Steps of vacuum thermoforming process [27]

The general deformability behavior of thermoplastics also depends on the strain-rate used during forming and the thermal history of the thermoplastic matrix. The forming process can affect such final properties as:

- Mechanical properties;
- Dimensional tolerances;
- Fiber orientation/alignment;
- Residual stress;
- Uniformity of the fiber to resin ratio;
- Degree of crystallinity;
- Glass transition temperature.

The forming process has a significant effect on the quality of the finished part, so high quality parts with predictable engineering properties require that a well-controlled thermoforming process developed for specific applications [18].

2.4.3 Compression Molding

Compression molding is a process in which the molding material is generally preheated and then is placed in an open and heated mold cavity. A plug member applied on the top closes the mold and exerts a pressure that forces the material into contact with all mold areas, while heat and pressure are maintained to cure the molding material [28]. In the Figure 14 the process is schematized.

The materials employed with this process are mostly thermosetting resins in a partially cured stage, either in the form of granules, putty-like masses, or preforms [28]. Compression molding is a process suitable for composite materials with high-strength fiberglass reinforcements that require high-volume productions; advanced composite thermoplastics can also be compression molded with unidirectional tapes, woven fabrics, randomly oriented fiber mat or chopped strand.

In addition to the advantages listed before, it is one of the lowest cost molding methods compared with other methods such as transfer molding and injection molding; it wastes relatively little material, representing an advantage when working with expensive compounds. However, the drawback of compression molding stands in producing parts with poor consistency and it is difficult to control flashing with this process, and it is not suitable for some types of parts.

Fewer knit lines are produced and a smaller amount of fiber-length degradation is noticeable when compared to injection molding. Compression-molding is also suitable for ultra-large basic shape production in sizes that overcome the capacity of extrusion techniques. Materials that are typically manufactured through compression molding are: polyester fiberglass resin systems (SMC/BMC), Torlon, Vespel, PPS, and many grades of PEEK [29].

At the first stages of its application, compression molding was developed to manufacture composite parts for metal replacement applications, especially to make larger flat or moderately curved parts. Nowadays, this method of molding is greatly used in manufacturing automotive parts such as hoods, fenders, scoops, spoilers, as well as smaller more intricate parts.

The material to be molded is positioned in the mold cavity and the heated platens are closed by a hydraulic ram. Bulk molding compound (BMC) or sheet molding compound (SMC) are conformed to the mold form by the applied pressure and heated until the curing reaction occurs. SMC feed material is cut to conform to the surface area of the mold; then the mold is then cooled and the part removed [28].

SMC is both a process and reinforced composite material. This is manufactured by dispersing long strands (greater than 1 inch) of chopped glass fibers (usually, but also carbon fiber can be used) on a bath of polyester resin. The longer glass fibers in SMC result in better strength properties than standard bulk molding compound (BMC) products.

Compared to similar methods, SMC benefits from a very high volume production ability, excellent part reproducibility, it is cost effective as low labor requirements per production level is very good and industry scrap is reduced substantially. Weight reduction is also advantageous, because there are lower dimensional requirements and the ability to consolidate many parts into one.

Bulk molding compound (BMC) or bulk molding composite is a ready to mold, fiber reinforced thermoset polyester material primarily used in injection molding and compression molding. The material is provided in bulk or logs. BMC is manufactured by mixing strands (greater than 1 inch) of chopped glass fibers in a mixer with polyester resin. The glass fibers in BMC result in better strength properties than

standard thermoplastic products. Typical applications include demanding electrical applications, corrosion resistant needs, appliance, automotive, and transit [28].

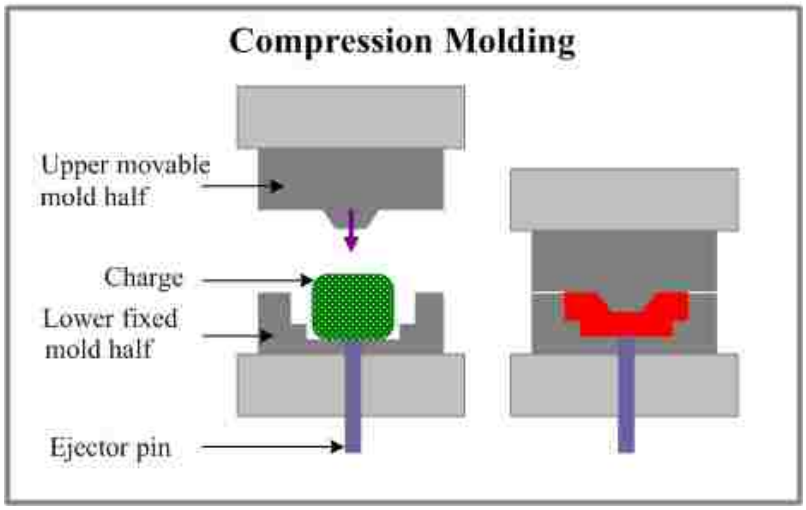

Figure 14: Compression molding process [30]

The material that has to be processed can be loaded into the mold in the form of sheet or pellets; then the charge material is heated above its melting point, formed and cooled. The more evenly the feed material is distributed over the mold surface, the less flow orientation occurs during the compression stage [29].

Some most critical aspects that must be considered for the development of the compression molding process are the following ones:

- Determining the proper amount of material.
- Determining the minimum amount of energy required to heat the material.
- Determining the minimum time required to heat the material.
- Determining the appropriate heating technique.
- Predicting the required force, to ensure that shot attains the proper shape.
- Designing the mold for rapid cooling after the material has been compressed into the mold.

2.4.4 Injection Molding

Injection molding is a manufacturing process for both thermoplastic and thermosetting materials. In this process, material is fed into a heated barrel, mixed, and forced into a mold cavity where it cools and hardens until it assumes the shape of the cavity [28].

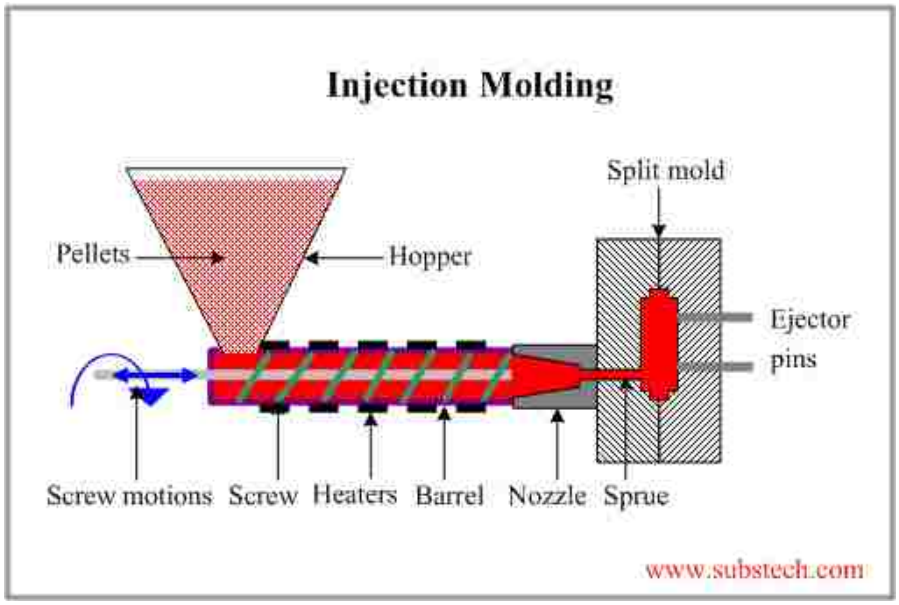

Figure 15: Scheme of injection molding process [31]

A scheme of the injection molding process is depicted in Figure 15.

With this process many polymers (resins) may be used, including all thermoplastics, some thermosets, and some elastomers; as a matter of fact, in 1995 there were approximately 18,000 different materials available for injection molding and that number was increasing at an average rate of 750 per year [28].

The available materials for the process are chosen depending on the required mechanical characteristics for the final product, but when the material has to be chosen the different molding parameters must be taken into account. In fact, even if they have good mechanical properties, if they cannot be molded they cannot be used for the process. For

injection molding, some of the most common polymers used are epoxy and phenolic thermosetting plastics but also thermoplastic plastics such as nylon, polyethylene, and polystyrene.

The mold consists of two primary components, the injection mold (the A plate) and the ejector mold (the B plate). Plastic resin enters the mold through a sprue (a sort of channel) in the injection mold; the function of the sprue bushing is to seal tightly against the nozzle of the injection barrel of the molding machine and to allow molten plastic to flow from the barrel into the mold. The sprue bushing directs the molten plastic to the cavity images through channels that are machined into the faces of the A and B plates. These channels allow plastic to run along them and for their function they are referred to as runners. The molten plastic flows through the runner and enters one or more specialized gates and into the cavity geometry to assume the desired shape of the component [28].

In case of more complex parts, more complex molds are used. These may have sections (slides) which move into a cavity perpendicular to the draw direction to form overhanging part features. When the mold is opened, the slides are pulled away from the plastic part by using “angle pins” on the stationary mold half. These pins enter a slot in the slides and cause the slides to move backward when the moving half of the mold opens. After this operation, the part is ejected and the mold closes. The closing action of the mold causes the slides to move forward along the angle pins [28].

The advantages of injection molding are high production rates, repeatable high tolerances, the ability to use a wide range of materials, low labor cost, minimal scrap losses, and little need to finish parts after molding. Some disadvantages of this process are expensive equipment investment, potentially high running costs, and the need to design moldable parts.

Method	Raw materials	Maximum size	Minimum size
Injection molding (thermo-plastic)	Granules, pellets, powders	700 oz. / 20 kg	Less than 1 oz. / 28 g
Injection molding (thermo-setting)	Granules, pellets, powders	200 oz. / 5.5 kg	Less than 1 oz. / 28 g

Figure 16: Some ranges of the sizes of materials for injection molding process [28]

In Figure 16 raw materials for injection molding are shown, with distinction between the processes for thermoplastic or thermoset materials. It can be noticed that the main difference stands in the maximum size allowed for the specific process: injection molding for thermoplastic composites can be done with materials that weigh up to 20 kg while in case of thermoset materials the raw material cannot exceed about 5.5 kg [28].

2.4.5 RTM (Resin Transfer Molding)

Resin Transfer molding is a process where the amount of molding material (that is usually a thermoset plastic) is measured and inserted before the molding takes place, as in the compression molding process. It is an automated operation that combines compression-molding and transfer-molding processes. This combination leads to good surface finish, dimensional stability, and mechanical properties proper of compression molding and the high-automation capability and low cost of injection molding and transfer molding.

Transfer molding (TM) (or resin transfer molding, RTM) differs from compression molding in that in TM the resin is inserted into the mold (or tool) which contains the

layers of fibers or a preform, whereas in compression molding prepregs or molding compounds are in the mold which is then heated and pressure is applied [28]. The molding material is preheated and loaded into a chamber called *pot*. A plunger is used to force the material from the pot through channels called sprue and runner system into the mold cavities. The mold remains closed as the material is inserted and is opened to release the part from the sprue and runner. The mold walls are heated to a temperature above the melting point of the mold material; this allows a faster flow of material through the cavities [28]. Transfer Molding has a "piston and cylinder"-like device built into the mold so that the rubber is squirted into the cavity through small holes. A piece of uncured rubber is placed into a portion of the transfer mold called the "pot." The mold is closed and under hydraulic pressure the rubber or plastic is forced through a small hole (the "gate") into the cavity. The mold is held closed while the plastic or rubber cures [28]. The plunger is raised up and the "transfer pad" material may be removed and thrown away. The transfer mold is opened and the part can be removed. The flash and the gate may need to be trimmed. Another key point is that a premeasured amount of thermosetting plastic in powder, preform, and even granular form can be placed into the heating chamber. The molds in both compression and transfer molding remain closed until the curing reaction within the material is complete. Ejector pins are usually incorporated into the design of the molding tool and are used to push the part from the mold once it has hardened. These types of molding are ideal for high production runs as they have short production cycles. Transfer molding, unlike compression molding uses a closed mold, so smaller tolerances and more intricate parts can be achieved [28]. The fixed cost of the tooling in transfer molding is greater than in compression molding and as both methods produce waste material, whether it be flash or the material remaining in the sprue and runners, transfer molding is the more expensive process.

Transfer molding (TM) (or resin transfer molding, RTM) differs from compression molding in that in TM the resin is inserted into the mold (or tool) which contains the layers of fibers or a preform, whereas in compression molding prepregs or molding compounds are in the mold which is then heated and pressure is applied [28].

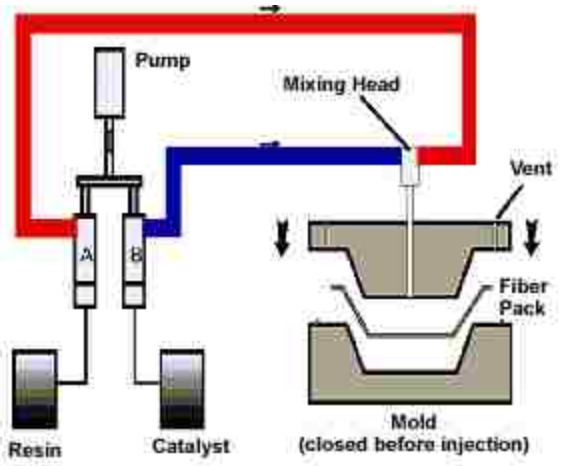

Figure 17: Resin Transfer Molding Process [33]

In RTM the resin is injected or drawn into a mold, which contains the fibers, from a homogenizer under low pressure. The mold can be made from composites for low production cycles or with aluminum or steel for larger production. The differences between the two types being that metal has better heat transfer, hence quicker cycle times; metal lasts longer and deforms less, but at a higher cost. The main problem with this production route is that air can be trapped in mold and hence a method must be incorporated for allowing this air to escape. A number of solutions to the problem exist including extending one level of reinforcement beyond the cavity (with a 25% resin loss), appropriate vents and creating a vacuum in the mold (which also improves quality). Larger structures, better properties (less movement of fibers), increased flexibility of design and lower cost are some of the advantage this process has over compression molding due mainly to the low pressure injection. Other benefits include rapid manufacture, not labor intensive, ability to vary reinforcements easily or include cores such as foam and produce low and high quality products [28].

Plunger molding is a variation on transfer molding, where an auxiliary ram exerts pressure on the material being molded. This approach often performs better in fully automatic operation.

2.4.6 Melding

The conventional joining methods used for metallic airframes, rivets, leave stress concentrations that significantly weaken composite structures, while adhesive bonding of carbon fiber reinforced polymers is difficult, time consuming and unreliable. In this context, melding, called in this way since it is a union of melting and welding, offers an effective alternative to creating seamless bonds by partially curing two laminates and combining them. One of the most recent processes that realize the melding concept is the Quickstep process, developed by Australian researchers [35]. Through a precise temperature control, it is possible to partially cure composites: for example fully cure one part of the laminate stack while leaving the remainder completely uncured and chemically active. Uncured parts are then co-cured together without adhesive so that chemical cross linking can occur; this creates a seamless join without mechanical fasteners or adhesive bonds [35]. In Figure 18 the melding process is shown:

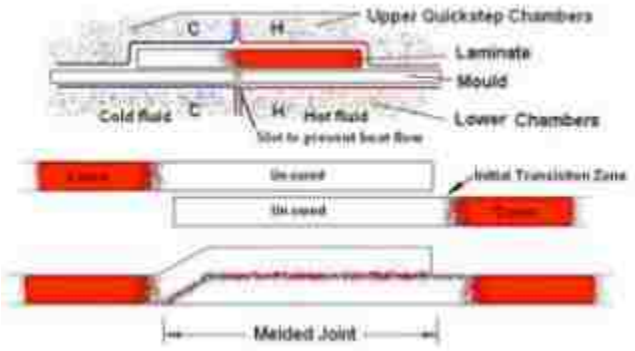

Figure 18: Melding procedure [35]

The Quickstep technique utilizes a glycol heat transfer fluid (HTF) to conduct heat to the uncured laminate stack more efficiently than is possible in the autoclave. This precise temperature control, in conjunction with increased heat transfer, allows for a significant reduction in the cure-cycle time. Advanced carbon fiber reinforced polymers (CFRP) have not been used as widely within manufacturing as would be predicted from their

superior mechanical and structural performances because of complexity, time and energy costs required to create the consistently uniform parts available with most processing techniques. Therefore the use of advanced CFRP has been essentially limited to industries that already have a high product cost, such as the aerospace industry, or industries in which cost is not as much an issue, such as high-end sporting equipment [34]. For Quickstep, the uncured laminate stack is prepared using a vacuum bagging technique similar to that used in autoclaves or composites processing ovens. A silicone bladder contains the HTF and provides a flexible membrane that conforms to the shape of the vacuum bagged laminate. Precise temperature control is maintained by circulating HTF through the bladders from one of three storage tanks; one tank full of room temperature HTF, one full of intermediate-dwell temperature HTF and one of full cure temperature HTF. Typically, the over-pressure is about 10 kPa, which is much lower than that produced in an autoclave, however, as the viscosity of the resin can be reduced to its working viscosity much quicker during the initial stages of cure, however, this low pressure is sufficient to enable consolidation with a minimum of voids. Laminates produced in the Quickstep have been shown to compare favorably with those produced in an autoclave [34]. A hot press applies heat and pressure through two hot plates that are controlled by a hydraulic ram. This is the simplest method to process high quality composite parts with low void content. Its major limitation is that pressure may only be applied uni-axially. While shaped molds are often used to process shapes with simple curves or bends, complex shapes are all but impossible to make. Further, the heating and cooling rates are dependent on the hot press' capability to heat and cool the plates.

2.5 Sandwich Structures

In recent years, sandwich structures are being used more and more frequently in the aeronautic and automotive sector. The purpose is to achieve high stiffness levels together with low weight respect to traditional materials.

A sandwich structure is composed of a central core and two external skins. Generally, skins are made of FRP plies and they characterize the mechanical properties of the

material; the core is a low density material in order to minimize the weight and has to keep together the skins and transfer the loads to them [13].

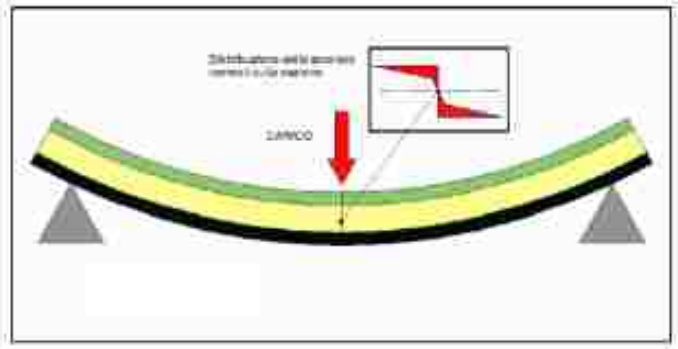

Figure 19: Bending behavior of a sandwich structure [13]

The bending behavior of a sandwich structure is shown in Figure 19: in order to increase the bending stiffness of the structure, the thickness of the external parts is increased, while the internal one can be lighter (as for double-T beams).

In this way the sandwich structure can be considered an extension of this model to a bi-dimensional structural element that mostly undergoes bending loads.

The possibility to utilize a low density material for the core allows the adoption of thicker width for the internal part increasing the moment of inertia of the section and so diminishing the tensions on the external parts.

The adoption of sandwich composite structures leads to weight savings up to 75% respect to other conventional materials (metals and fiber glass laminates).

Other advantages linked to sandwich structures are thermal and acoustic insulation, good crash and impact behavior, chemical resistance, recyclability and thermoform ability. Moreover, they do not require stiffeners elements.

In the contrary, drawbacks are high costs of production and difficulties of processing [13].

In sandwich structures the role of the core is essential: the material that constitutes the core must have high shear stiffness and resistance in order to guarantee the structural continuity with the skins. In fact, in presence of bending as the result of an orthogonal

load respect to the direction of the lamina, skins do not have to slip over the core.

Moreover, core materials must have good compression stiffness to keep the distance between skins constant when they undergo localized loads. For this aspect, foam cores present poor performances presenting a non-linear compression behavior (transversely soft core).

One of the most common solutions for the core is the honeycomb, as shown in Figure 20 and 22: their density varies from 20/200 kg/m^3 and can be made of different materials, such as FRP and metals (between metals aluminum is the most common).

Between FRP on of the most used is the Nomex (produced by DuPont) constituted by reinforced paper where fibers are not cellulose but aramidic resin [13]. The chemical structure of this material is illustrated in Figure 21.

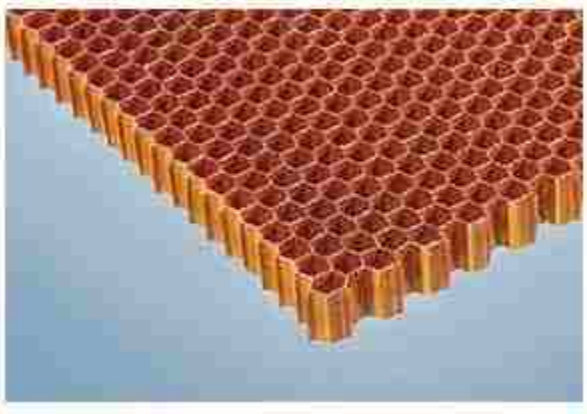

Figure 20: Honeycomb structure with phenolic resin [13]

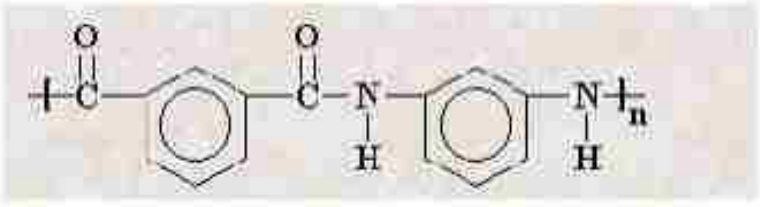

Figure 21: Chemical structure of Nomex [13]

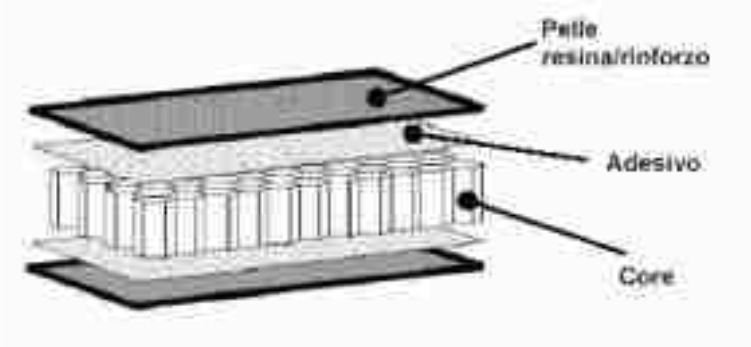

Figure 22: Sandwich structure with honeycomb [13]

In order to obtain the maximum flexural rigidity and bending strength it has been proved that the weight of the honeycomb must be in the range of 50/66.7 % the weight of the panels which constitute the skins [13]. Changing the percentage in weight of the core provides different mechanical properties of the structure.

Honeycomb materials have excellent mechanical properties per weight, even if the bonding with the skins is quite difficult. This kind of solution is applied in sectors where costs are not a priority, but the main goal is to achieve high performance of the component, such as aerospace industry and sportive goods.

Recently, it has been developed another material for the honeycomb: the SynCore. Respect to conventional composite materials, SynCore has better durability in presence of water or moisture, enhancing the corrosion resistance of the whole sandwich structure.

The optimal core thickness for bending behavior is given by [37]:

$$c_{opt}^{B} = 2\left(\frac{\rho_f}{\rho_c}\frac{D_1}{E_f}\right)^{1/3} \tag{1}$$

while for torsion behavior the optimal core stiffness is equal to [37]:

$$c_{opt}^{T} = 2\left(\frac{\rho_f}{\rho_c}\frac{K_1}{G_f}\right)^{1/3} \quad (2)$$

2.6 Recyclability

The increasing use of carbon fiber reinforced polymers (CFRP) has raised an environmental and economic awareness for the need to recycle the CFRP waste. The world-wide demand for carbon fibers (CF) reached approximately 35,000 t in 2008; this number is expected to double by 2014, representing a growth rate of over 12% per year [38]. CFRP is now used in a widening range of applications, and in growing content in most of them. Despite all advantages associated with CFRP, the increasing use generates also an increasing amount of CFRP waste. Common sources of waste include out-of-date prepregs, manufacturing cut-offs, testing materials, production tools and end-of-life (EoL) components; manufacturing waste is approximately 40% of all the CFRP waste generated, while woven trimmings contribute with more than 60% to this number [38]. Recycling composites is inherently difficult because of:

- their complex composition (fiber, matrix and fillers),
- the cross linked nature of thermoset resins (which cannot be remolded),
- the combination with other materials (metal fixings, honeycombs, hybrid composites).

Presently, most of the CFRP waste is landfilled; the airframe of EoL (End of Life) vehicles is usually placed in desert graveyards, airports, or by landfilling. However, these are unsatisfactory solutions for several reasons:

- Environmental impact: the increasing amount of CFRP produced raises concerns on waste disposal and consumption of non-renewable resources.
- Legislation: recent European legislation is enforcing a strict control of composite disposal; the responsibility of disposing EoL composites is now on the

component's manufacturer, legal landfilling of CFRP is limited, and for instance it is required that automotive vehicles disposed after 2015 are 85% recyclable (EU 1999/31/EC; EU 2000/53/EC).

- Production cost: CF are expensive products, both in terms of energy consumed during manufacturing (up to 165 kWh/kg) and material price (up to 40 £/kg) [39].
- Management of resources: demand of virgin (v-) CF usually surpasses supply-capacity [40], so recycled (r-) CF could be re-introduced in the market for non-critical applications [41].
- Economic opportunity: disposing of CFRP by landfilling, where not illegal, can cost approximately 0,20 £/kg; recycling would convert an expensive waste disposal into a profitable reusable material.

It is clear that turning CFRP waste into a valuable resource and closing the loop in the CFRP life-cycle is vital for the continued use of the material in some applications, e.g. the automotive industry.

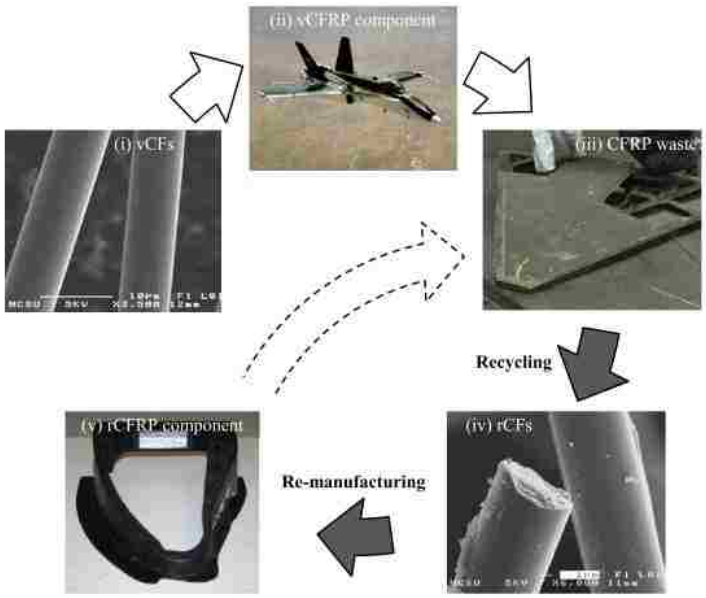

Figure 23: Closed life-cycle of CFRP [38]

2.6.1 Carbon Fiber Recycling Processes

Two technology families have been proposed to recycle CFRP: mechanical recycling and fiber reclamation. Both are addressed in the following, and a critical comparison is summarized in the table below. Most efforts have been focusing on thermoset composites (e.g. carbon–epoxy systems), as their cross-linked matrix cannot be reprocessed simply by remelting.

Summary analysis of different recycling processes.

Process	Advantages	Drawbacks	Implementation	
			Recycler	Process scale*
Mechanical (see Section 2.1.2)	• Recovery of both fibres and resin[a] • No use or production of hazardous materials	– Significant degradation of mechanical properties[a] – Unstructured, coarse and non-consistent fibre architecture[b] – Limited possibilities for re-manufacturing	• ECRC (2003)[c] • Kouparitsas et al. (2002) • Takahashi et al. (2007) • Ogi et al. (2007) • Others[d]	P (10 t/year) L L L L
Pyrolysis (see Section 2.2)	• High retention of mechanical properties • Potential to recover chemical feedstock from the resin[d]. • No use of chemical solvents	– Possible deposition of char on fibre surface[e,f] – Sensitivity of properties of recycled fibres to processing parameters[g] – Environmentally hazardous off-gases[g]	• RCFL (2009) • JCMA (2006)[h] • MIT-RCF (2010)[i] • CFK (2007) • Karborek (1999)[j] • Firebird (2005)[h,k] • HADEG (1995) • Others (Lester et al., 2004, Meyer et al., 2009)	C (2000 t/year) C (1000 t/year) C (500 t/year) P (u/p for 2010) P (u/p to 1000 t/year) P (u/p for 2010) P L
Fluidised bed (see Section 2.3)	• High tolerance to contamination[a,l] • No presence of residual char on fibre surface[m] • Well established and documented process	– Strength degradation between 25% and 50%[o] – Fibre length degradation[n,o] – Unstructured ("fluffy") fibre architecture[o,p,q] – Impossibility for material-recovery from resin[l,r]	• Kennerley et al. (1998), Pickering et al. (2000), Yip et al. (2002), Pickering (2006), Jiang et al. (2007, 2008), Wong et al. (2007b), Turner et al. (2009)	P (under continuous development)
Chemical (see Section 2.4)	• Very high retention of mechanical properties and fibre length[s,t] • High potential for material-recovery from resin[u]	– Common reduced adhesion to polymeric resins[s] – Low contamination tolerance[u,v] – Reduced scalability of most methods[q,u] – Possible environmental impact if hazardous solvents are used[w]	• ATI (1994)[v,x,y] • Nakagawa et al. (2009)[z] • Hyde et al. (2006), Pinero-Hernanz et al. (2008a,b), Jiang et al. (2009), using SCF[w] • Others (Buggy et al., 1995, Liu et al., 2004, 2009)	P (u/p to 1000 t/year) P L L

* Key for process scale: P, pilot-scale plant; L, laboratory scale; C, commercial-scale plant; u/p, upgrade planned.

Table 1: Summary analysis of different recycling processes [38]

2.6.1.1 Mechanical Recycling

Mechanical recycling involves breaking-down the composite by shredding, crushing, milling, or other similar mechanical process; the resulting scrap pieces can then be segregated by sieving into powdered products (rich in resin) and fibrous products (rich in fibers) [38]. Typical applications for mechanically-recycled composites include their re-incorporation in new composites (as filler or reinforcement,) and use in construction

industry (e.g. as fillers for artificial woods or asphalt, or as mineral-sources for cement). However, these products represent low-value applications; mechanical recycling is therefore mostly used for glass fiber reinforced polymers (GFRP), although applications to thermoplastic and thermoset CFRP can be found as well [38].

2.6.1.2 Fiber Reclamation

Fiber reclamation consists of recovering the fiber from the CFRP, by employing an aggressive thermal or chemical process to break-down the matrix (typically a thermoset); the fibers are released and collected, and either energy or molecules can be recovered from the matrix. Fiber reclamation may be preceded by preliminary operations, e.g. cleaning and mechanical size-reduction of the waste.

Fiber reclamation processes are particularly suitable to CFRP: carbon fibers have high thermal and chemical stability so usually their excellent mechanical properties are not significantly degraded (especially regarding stiffness) [38].

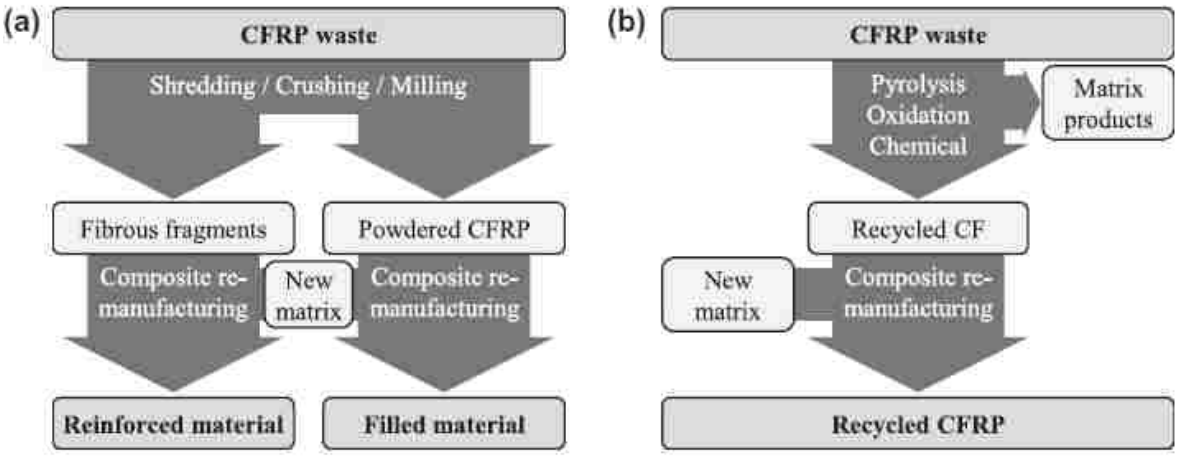

Figure 24: Main technologies for CFRP recycling. (a) Mechanical recycling (b) Fiber reclamation [38]

2.6.1.3 Pyrolisis

Pyrolysis is one of the most widespread recycling processes for CFRP and consists of the thermal decomposition of organic molecules in an inert atmosphere. During pyrolysis, the CFRP is heated up to 450 °C to 700 °C in the (nearly) absence of oxygen; the polymeric matrix is volatilized into lower-weight molecules, while the CF remain inert and are eventually recovered [38].

2.6.1.4 Oxidation in Fluidized Bed

Oxidation is another thermal process for CFRP recycling; it consists in combusting the polymeric matrix in a hot and oxygen-rich flow (e.g. air at 450 °C to 550 °C). During recycling, CFRP scrap (reduced to fragments approximately 25 mm large) is fed into a bed of silica on a metallic mesh. As the hot air stream passes through the bed and decomposes the resin, both the oxidized molecules and the fiber filaments are carried up within the air stream, while heavier metallic components sink in the bed; this natural segregation makes the FBP particularly suitable for contaminated EoL components. The fibers are separated from the air stream in a cyclone, and the resin is fully-oxidized in an afterburner; energy-recovery to feed the process is feasible.

2.6.2 Chemical Recycling

Chemical methods for CFRP recycling are based on a reactive medium such as catalytic solutions, benzyl alcohol, and supercritical fluids under low temperature (typically less than 350 °C). The polymeric resin is decomposed into relatively large and high value oligomers, while the CF remains inert and is subsequently collected.

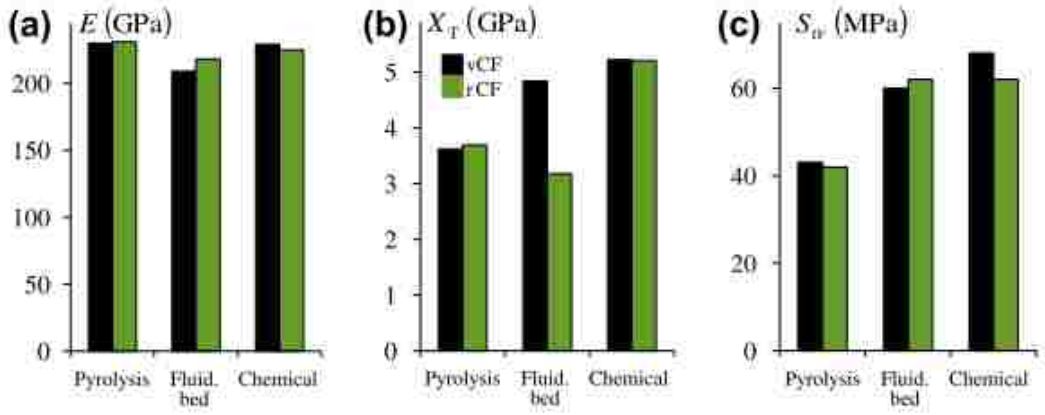

Figure 25: Mechanical properties of recycled carbon fibers and their virgin precursors [38]

The figure (a) represents the Young modulus, (b) shows the strength of carbon fibers and (c) is the interfacial shears strength with epoxy resin.

With the black column virgin fibers are represented, while the green one stands for recycled ones.

Table 3
Mechanical properties of recycled CFs reclaimed through different processes.

Process	Recycler[a]	Fibre type	E^f (GPa)[b]	X_T^f (GPa)[b]	S_{IF} (MPa)[b]
Pyrolysis	RCFL (2009)[c]	Hexcel AS4	231(+0.4%)	3.69(+2%)	42(−2%)
	Meyer et al. (2009)	Toho HTA		3.57(−4%)	
	Karborek (1999)[d]	Toray T800	222(−12%)	4.62(−10%)	99(+41%)
	Lester et al. (2004)	Grafil 34-700	210(−13%)	3.26(−20%)	
Fluidised bed	Jiang et al. (2008); Wong et al. (2007b)	Toray T600S	218(+4%)	3.18(−34%)	62(+3%)
Chemical	Allred et al. (2001)	Hexcel AS4		3.37(−9%)	
	Pinero-Hernanz et al. (2008a)	Toray T600S	205(−15%)	4.00(−2%)	
	Jiang et al. (2009)	Toray T700S	225(−2%)	5.20(−0.3%)	62(−9%)

[a] See Sections 2.2 (pyrolysis), 2.3 (fluidised bed process), and 2.4 (chemical recycling).
[b] Values between brackets represent relative difference to virgin fibre.
[c] Mechanical properties measured by Connor (2008).
[d] Mechanical properties measured by Heil et al. (2009).

Table 2: Mechanical properties of recycled CFs reclaimed through different processes [38]

2.6.3 Composites Re-Manufacturing

The existing manufacturing processes, developed for virgin materials must be adapted to the unique recycled-fiber form.

2.6.3.1 Injection Molding

During injection molding, a mixture of resin (typically a thermoplastic), rCF (short or milled) and fillers/additives is pre-compounded into pellets, which are subsequently injected into a mold (at 10 MPa to 100 MPa) [42].

The rCF (from FBP) can be injected with polypropylene (PP) [43]. The addition of coupling agents (maleic anhydride grafted polypropylene, MAPP) improved fiber–matrix adhesion and thus the overall mechanical properties.

The performance of two injected CFRP, one with virgin and another with recycled (from RCFL) carbon fibers can be done [44]. The recycled was 25% less stiff than the virgin control; strength reduction was less pronounced (12%), likely due to an improved fiber–matrix adhesion in the recycled.

2.6.3.2 BMC Compression

BMCs are intermediate products made by mixing resin (typically a thermoset), rCFs, fillers and curing agents into bulky charges; this premix is subsequently compression molded (under 3:5 MPa to 35 MPa) into a component [42] [45].

Several BMCs with rCFs have been molded from the FBP and SCFs [47] [48]. The formulation of the BMC was tuned so as to overcome the poor flow properties of the resin and the intricated form of the fibers. The main factors affecting the mechanical performance of the rCFRPs (especially the strength) were the fractions of fillers and of rCFs. The mechanical performance of the rCFRPs was superior to that of commercial glass BMCs [48]; however, it is not clear whether these rCFRPs can compete in price.

2.6.3.3 Compression Molding

The production and subsequent re-impregnation of 2D or 3D rCF non-woven dry products (with short and random reinforcement architecture) is one of the most widely used manufacturing processes for rCFRPs. The 2D or 3D non-woven dry products are then either compression molded with resin layers or re-impregnated through a liquid process. Current work focuses on improving the mat-flow properties (e.g. by using thin mats down to 10 gsm, performing pre-compaction, reducing binder levels, filling the resin, [47] [48], and studying alternatives to compression molding (such as autoclave and out of-autoclave curing) [46].

Fiber alignment is a key point to improve the mechanical performance of composites manufactured with discontinuous rCFs [46]: not only the composite's mechanical properties improve along preferential fiber direction, as manufacturing requires lower molding pressures and smoother fiber-to-fiber interactions.

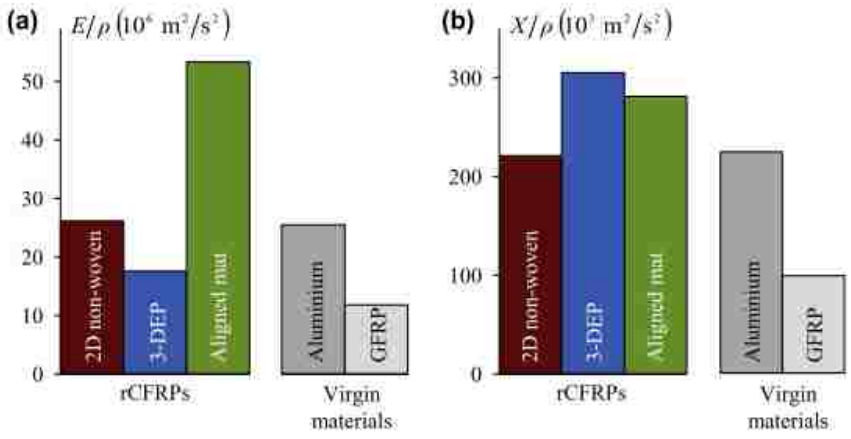

Figure 26: Mechanical Properties of rCFRPs vs. conventional structural virgin materials [38]

In the part (a) of Figure 26 the specific stiffness is shown, while in the part (b) the specific strength [38]. Table 3 resumes the mechanical properties of recycled CFRPs with

different processes.

Table 5
Mechanical properties of recycled CFRPs manufactured through different processes.

Process	Manufacturer[a]	Matrix	V^f (%)	E_T (GPa)	X_T (MPa)	U_{imp} (kJ/m²)
Mechanical recycling	Takahashi et al. (2007)	PP	24	21[b]	101[b]	
	Ogi et al. (2007)	ABS	24	12	102	19
Injection moulding	Wong et al. (2007a)	PP[c]	19	16	126	27
	Connor (2008)	PC	16	14	124	
BMC compression	Turner et al. (2009)	EP[d]	10	20	71	8
Compression moulding of non-woven products	Wong et al. (2009a)	EP	30	25	207	
	Nakagawa et al. (2009)[e]	UP	16	5.5	90	
	Janney et al. (2009)	EP	34	23[f]	400[f]	
Compression moulding of alig. mats	Turner et al. (2009)	EP	44	80	422	35

[a] See Sections 2.1.2 (mechanical recycling), 3.2.2 (injection moulding), 3.2.3 (BMC compression), 3.3 (compr. mould. of non-woven products), and 3.4 (compr. mould. of aligned mats).
[b] Along preferential fibre direction.
[c] With 5% (over fibre weight fraction) of G3003 MAPP coupling agent.
[d] Filled with calcium carbonate, moulded at 2 MPa.
[e] Recycled-CF feedstock with $l^f = 25$ mm.
[f] Flexural properties.

Table 3: Mechanical Properties of recycled CFRPs manufactured through different processes [38]

2.6.3.4 Woven rCFRP

As some recycling processes can preserve the reinforcement architecture of the waste, it is possible to recover the structured weave from large woven items, e.g. out-of-date prepreg rolls, EoL aircraft fuselage, or prepreg trimmings from large components; re-impregnating (through e.g. resin transfer molding (RTM) or resin infusion) the recycled weave fabrics then produces woven rCFRPs. With currently available recycling processes, stiffness and strength could theoretically reach more than 70 GPa and 700 MPa respectively; moreover, fabrics reclaimed from prepreg rolls would be fully traceable [38].

In addition to the technical challenges identified previously, the major current challenge to CFRP recycling operations is the establishment of a sound CFRP recycling chain supporting the effective commercialization of recycling processes and products.

2.6.4 Issues of Carbon Fiber Recycling

The main issues to overcome, as identified by academics, recyclers, end-users and governments are:

- Global strategy: organized networks for CFRP recycling, bringing together suppliers/users (composite-related industries), recyclers and researchers, must be created, so as to understand the current state of the art and plan for future developments on the topic according to industrial needs [49].
- Incentives for recycling: governments should support the option of recycling; this could involve not only penalties for non-recyclers (e.g. landfilling taxes) but also direct privileges (e.g. carbon credits) for companies recycling their CFRP waste [50].
- Implementing suitable legislation: there is currently a void in specific legislation covering the CFRP recycling operations. For instance, the classification of pyrolysis processes for CFRP recycling should be distinguished from that of traditional pyrolysis processes [51]; a suitable classification of CFRP waste for international transport to recycling units needs to be approved.
- Logistics and cooperation in the supplying chain: waste suppliers must cooperate with recyclers, which includes supplying the waste in a continued and suitable form [53] [53]and providing the recyclers with material certificates whenever possible (e.g. for expired prepreg rolls) [50]. Conversely, recyclers must ensure that materials and components supplied will not undergo reverse engineering.
- Market identification and product pricing: this requires that (i) characteristics and properties of different rCFRPs are known, (ii) their processing times and costs are assessed, and (iii) the value for the recycled label is established [50].
- Life-cycle analysis: the environmental, economic and technical advantages of rCFRPs over other materials and disposal methods can be estimated only through cradle-to-grave analyses of the whole CFRP life-cycle.
- Market establishment: ultimately, the major current challenge for the success of CFRP recycling is the establishment of a market for the recyclates; this is

recognized by leading researchers [46] [47], CF recyclers [50], CF user [54], and analysts [55] [56]. Creating a market requires all the previous issues to be overcome, so rCFs are accepted as an environment-friendly and cost-effective material.

Table 8
Demonstrators manufactured with recycled CFs.

rCFRP demonstrator[a]	Virgin component	CF recycler (see Section 2)	rCFRP manufacturer (see Section 3)	rCFRP matrix[b]
Wing mirror cover	Unknown	Unknown	Warrior et al. (2009)	UP
Car door panel	Unknown	Unknown	Warrior et al. (2009)	EP
Corvette wheelhouse	EoL F-18 aircraft stabiliser	RCFL (2009)	Janney et al. (2009)	UP
Aircraft seat arm rest (George, 2009)	Aircraft testing & manufact. waste	Janney et al. (2009)	Janney et al. (2009)	EP
Driver's seat of a Student Formula SAE car	Tennis rackets	Nakagawa et al. (2009)	Nakagawa et al. (2009)	UP
Rear structure of WorldFirst F3 *green* car	Outdated woven pre-preg	RCFL (2009)	Meredith (2009)	EP
Tool for composite lay-up	Outdated woven pre-preg	RCFL (2009)	George (2009)	un.

[a] Additional information can be found in the reference associated with the rCFRP manufacturer, unless otherwise here specified.
[b] Key for rCFRP matrix: EP, epoxy resin; UP, unsaturated polyester; un., unknown.

Table 4: Demonstrators manufactured with recycled CF [38]

Table 7
Estimated values for the cost of carbon fibres (Carberry, 2008).

Fibre type	Manufacturing energy (kWh/kg)	Price (£/kg)
vCF	55–165	20–40
rCF	3–10	11–16

Table 5: Estimated values for the cost of carbon fibers [38]

2.6.5 Applications for rCFRP

One of the most promising applications for rCFRPs consists of non-critical structural components [47] [47]. Although there are currently non-structural applications for rCFs (e.g. industrial paints, construction materials, electro-magnetic shielding, high performance ceramic brake discs, fuel cells [57] [58] [59] [60] structural applications would fully exploit the mechanical performance of the fibers, thus increasing the final value of recycled products.

There is also scope to manufacture automotive components with rCFRPs, not only for technical or economic reasons, but also to boost green credentials. As legislation tightened regarding recyclability and sustainability (EU 2000/53/EC), the automotive industry's interest grew for natural composites [61], which are nowadays widely used in mass production despite some associated problems (e.g. consistency of feedstock); rCFRPs could follow as an environmental-friendly material with improved mechanical performance.

Currently, structural demonstrators manufactured with rCFRPs are aimed at aircraft or automotive industries; other markets have also been identified, such as construction industry, sports and household goods, and wind turbines [60] [62]. Table 6 provides a comprehensive overview of potential applications for several types of rCFRPs; this is complemented by specific applications currently manufactured with virgin materials, to allow for a direct comparison regarding manufacturing methods and mechanical properties.

Understanding the relations between microstructure, mechanical properties and damage mechanisms of rCFRPs provides informed guidance for reclaimers and manufacturers towards recyclates with optimal structural performance. Moreover, this understanding supports design methods for rCFRPs, which are essential for the establishment of a structural applications market. Given the urgency in closing the loop on the CFRP life-cycle, analyzing the mechanical response of rCFRPs at the micro and macro mechanical levels has become critical for the continued use of composites.

A detailed mechanical study of a state-of-the-art rCFRP (manufactured at the University

of Nottingham with fibers reclaimed at RCFL) was performed at Imperial College London [38]; microstructure, mechanical properties, and failure and toughening mechanisms were investigated, and the influence of recycling and re-manufacturing processes analyzed. The study showed that the extensive breakage of fibers during re-manufacturing led to a considerable degradation of tensile strength at the composite level; in addition, it was found that fiber bundles, held together by minimal amounts of residual matrix not completely pyrolysed, increase the in-plane fracture toughness of the material.

The work by Pimenta et al. [38] proved that a feature usually seen as a recycling defect (incomplete removal of matrix) can actually enhance the mechanical response of the recyclates, which illustrates the need for a comprehensive approach towards the optimization of processes. In addition, the experimental observations were used to develop multiscale analytical models to predict the properties of recycled composites, which can be used in the design of rCFRP structural components.

A critical comparison between recycling processes proved each of them to have specific advantages and drawbacks, suggesting complementarities rather than competition. Most of recycling processes yield rCFs with high retention of mechanical properties, and a few commercial-scale plants already exist. The mechanical performance of some rCFRPs overcomes that of some conventional structural materials, and a few structural demonstrators for the automotive and aircraft industries have been manufactured.

Research wise, more detailed, multiscale and systematic studies on the mechanical performance of rCFs and rCFRPs are needed, so as to increase the acceptance of recyclates as structural materials by engineers and designers. It is also essential to perform life-cycle analyses of the several recycling and re-manufacturing methods, to assess cost effectiveness and environmental impact of using rCFs.

Table 9
Potential structural applications for rCFRPs.

Type of rCFRP[a]	Possible processes		Foreseen markets for rCFRP	Examples of current solutions with virgin materials			
	Recycling (see Table 2)	Manufacturing (see Table 4)		Component	Material[b]	E_T (GPa)	X_T (MPa)
Reinforced TP	• Pyrolysis • Fluidised bed • Chemical	• Injection moulding • Compression moulding of non-woven mats	• Automotive semi-structural parts • Construction materials • Leisure and sports goods	• Car dashboard[c] • Car underbody shielding[d] • Plywood replacement[e] • Swimming googles[f]	GF + PP GF + PP GF + PP CF + PA	5.3 4.5 15	100 60 200
Low-reinforced TS	• Pyrolysis • Fluidised bed • Chemical	• BMC compression • Compression moulding of non-woven mats	• Automotive semi-structural parts • Equipment housing	• Car door panel[g] • Carburator housing[h] • Car headlamp reflectors[i] • Fridge handler[j]	GF + UP GF + UP GF + UP GF + UP	14 13 12[o] 12[o]	36 37 48 44
Medium-reinforced TS	• Pyrolysis • Fluidised bed • Chemical	• Compression moulding of non-woven mats	• Automotive non-critical structures • Aircraft interiors	• Car rear wing[k] • Car decklid[l] • Aircraft seat structure[m] • Aircraft overhead bin[m]	CF + VE GF + un. Al 2024 GF + PF	27[p] 12 73[q] 20	152[p] 120 469[q] 167
Aligned TS	• Pyrolysis • Chemical	• Compression moulding of aligned mats • Lay-up of aligned pre-pregs	• Automotive non-critical structures • Aircraft interiors • Wind turbine non-critical structures	• Car roof shell[k] • Wind turbine non-critical layers[n]	CF + EP GF + EP	31[p] 22	234[p] 367
Woven TS	• Pyrolysis (pre-preg rolls)	• Resin infusion • RTM	• Automotive structures • Wind-turbine structures	• Car body panels[k] • Wind turbine non-critical layers[n]	CF + EP GF + EP	53[p] 38	450[p] 711

[a] Key for type of rCFRP: TP, thermoplastic matrix; TS, thermosetting matrix.
[b] Key for materials: GF, glass fibre; PP, polypropylene; CF, carbon fibre; PA, polyamide; UP, unsaturated polyester; VE, vinylester resin; un., unknown; Al, aluminium; PF, phenolic resin; EP, epoxy resin.

Table 6: Potential structural applications for rCFRPs [38]

2.7 Applications of Composite for Structural Components

This work concerns the conversion of a rear suspension cradle from steel/aluminum to a composite material. In this section some previous solutions adopted for the conversion of structural component from steel to composite are investigated, taking into account that, even if they are not direct examples of a rear suspension cradle conversion, they can still be a useful term of comparison because it is possible to look at the methodology of work adopted by other researchers.

In the first case, a structural composite underbody capable of carrying crash loads has been designed, fabricated, assembled into a structure, and tested by the Automotive Composites Consortium.

The composite underbody design was developed to replace the steel assembly from a

donor large, rear-wheel-drive vehicle. The key development load case was found to be the EuroNCAP/IIHS 40 mph Frontal Offset Deformable Barrier (ODB), with the NCAP 35 mph Full Frontal Impact as the second most important load test. The vehicle level stiffness performance with the composite underbody was required to have equivalent performance to the donor, while crash performance was required to meet applicable government and industry requirements. In this design, one molded composite part replaced 14 steel components as well as pieces of 4 others, as shown in Figure 27. The design presented several different thicknesses and cored sections, as well as several ribbed sections [63].

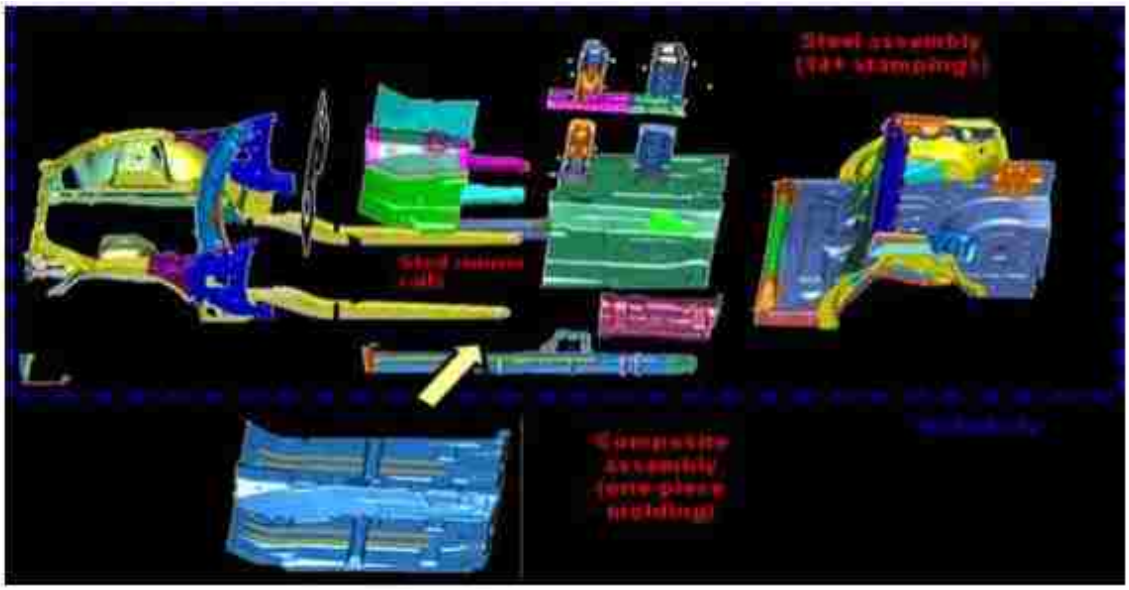

Figure 27: Preliminary composite underbody design [63]

Three material and process systems were investigated: SMC, long-fiber thermoplastic, and urethane long-fiber injection, with several subsets of each characterized. Based on the ability of each to meet program requirements and a technical cost model of these material and process systems, glass fabric SMC with a low density SMC core and some chopped-fiber SMC was selected as material and process system.

To meet the timing for the prototype underbody mold tool, only the most severe load case, the ODB, was assessed and the underbody thicknesses and layups were revised to

provide reasonable performance at this stage in the design.

At the time when the CAD model was released for tooling, the mass status of tooled underbody design was predicted to be ~26% lighter than the equivalent baseline steel design, a savings of 11.3 kg [63].

Using the glass fabric SMC for this complex part required significant fabric deformation and this involved experimental characterization of the material, mesoscopic modeling, and experimental verification in a small shaped part.

In order for a structural composite to perform in a predominately steel automotive body, a methodology for structurally attaching the composite underbody to the steel body-in-white (BIW) was required. For this reason they developed a composite-to-steel weld bonding: this technology involved using a steel doubler strip for the "top" layer, sandwiching the composite in the middle, with the steel structure on the bottom, as shown in Figure 28.

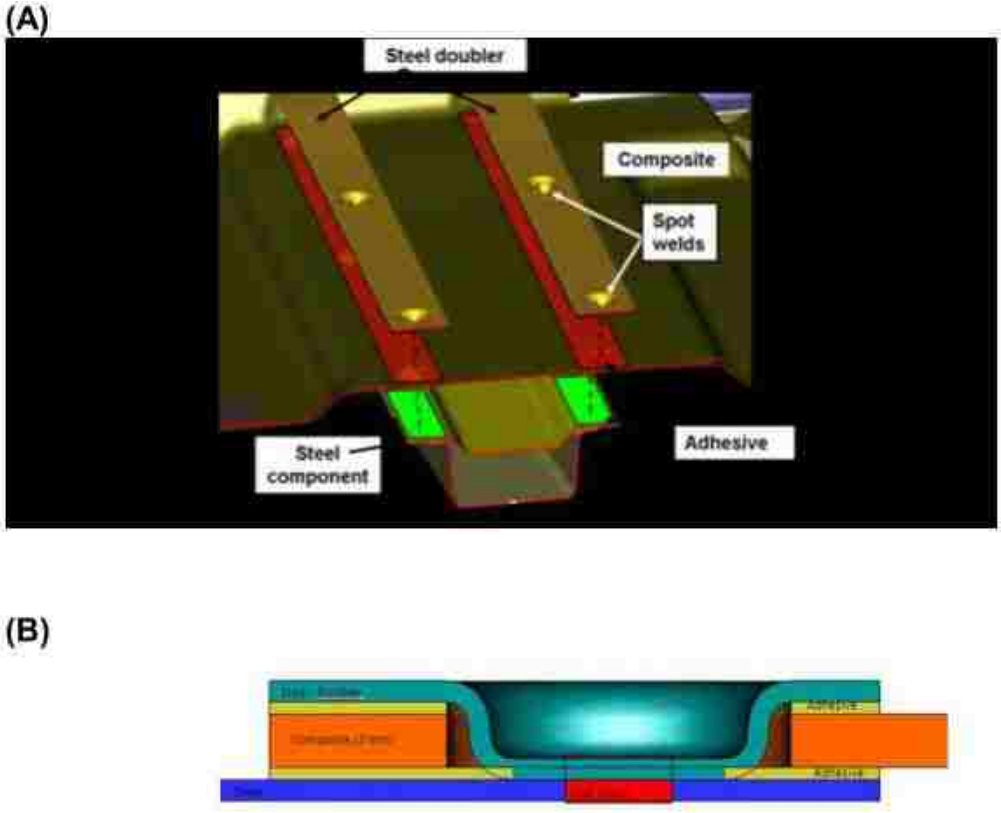

Figure 28: Composite-to-steel weld bond joint. (a) Steel rail weld bonded below composite underbody, with a dimpled steel doubler plate on top. (b) Cross section through one of the dimpled spot weld regions [63]

The composite had holes drilled or cut at predefined intervals, and the double strip had dimples corresponding to these holes. Adhesive has been applied to the composite, and then the composite was placed between the steel layers, with the dimples of the doubler meeting the steel structure through the holes. The double strip was spot welded to the steel structure. The assembled part was then placed in an oven (such as an e-coat or paint oven) for adhesive cure, fixtured by the welds. In addition to the fixturing, the weld also helped protect the structure from peel stresses.

Several non-destructive evaluations have been conducted to ensure the structural integrity of the composite: finally vibrothermography has been chosen to characterize the system and they evaluate ultraviolet dye penetrants for a technique suitable in the field.

The fabrication of the composite underbody started with the compounding of the glass fabric SMC. This was compounded on a normal SMC compounding line, except that the fiber chopping mechanism was replaced by a roll rack for fabric (Figure 29).

Figure 8: Fabric Mat being fed into SMC Compounder at CSP in Van Wert, Ohio

Figure 29: Fabric Mat fed into SMC Compounder [63]

After maturation, the fabric was cut into kits with an automated cutter, then sealed in styrene resistant plastic, and shipped to the molder. These underbodies were molded at Century Tool in Fenton, MI. A molding buck was fabricated from an early tooling break-in part. For each part, the molding buck was covered with glass veil, and the pieces of fabric SMC were placed on it and pressed into position, usually requiring some deformation. In this particular case the geometry was very complex, and the 14 layers of material contained about 60 pieces, including several pieces of structural chopped SMC, placed on top of or below the preform for the ribs. The preform was transferred to the molding tool, and the tool was closed and the material cured. Cure was 3 minutes at 150°C. At the end of manufacturing process, the molded part was found to be thicker and heavier than design.

The particular challenge in validating the design of the composite underbody consisted of the fact that the composite assembly was integral to the vehicle structure. As a result, the durability and impact load inputs were complex, so that it was difficult to conduct simple component level tests. As mentioned above, the primary design driver for the composite structure was the 40mph front ODB test. Automotive OEMs conducted this type of dynamic vehicle impact test using costly fully instrumented prototype vehicles. Because of the cost and complexity of doing full-vehicle testing for a concept component, it was decided to conduct the final testing on a subassembly. The proposed testing plan involved weld bond joining to a steel frame made up from the steel parts that would surround the underbody in production, then inducing loads through that frame, thus testing both the molded component and the joints. The purpose of this testing was validating the CAE methodology used to design the structure. Since CAE analysis showed that, even for the 40 mph ODB test, the loads were introduced to the underbody at very close to quasi-static rates, quasi-static testing methods were used to minimize the test complexity and cost.

Several simple quasi-static non-destructive bending and torsional stiffness and modal tests were used to evaluate the basic molded component performance [63].

After this testing (Figure 30), the molded underbodies were weld bonded into a subassembly consisting of the underbody and the surrounding structure from the donor vehicle, including the rockers, front rails, dash panel, and rear floor.

Figure 30: Molded underbody hung from bungee cord for modal testing [63]

This was then subjected to quasi-static testing to mimic the loads on the underbody in the ODB, as shown in Figure 31. The quasi-static testing consisted of longitudinal loading on the driver's side front rail and the face of the transmission housing. The initial tests resulted in a slight redesign of the fixtures to further direct the loads into the composite, as the fixturing and steel assembly failed first.

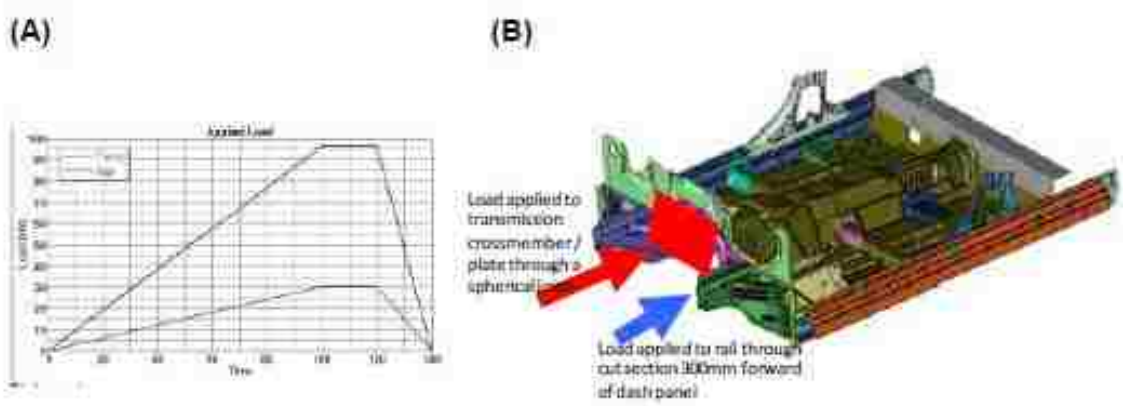

Figure 31: Underbody quasi-static ODB subassembly test. (a) applied load profile (b) subassembly geometry [63]

The test results were then correlated with both the initial predictions of the underbody, and predictions based on the actual mass and thickness of the molded underbody. This allowed evaluating the CAE methodologies for the structural composite, as well as for the assembly into a steel structure [63].

In another study case, a lightweight glass fiber composite structure was fabricated for applications where high bending strength and stiffness are needed.

For this application, composite sandwich panels were fabricated with chopped strand glass reinforcement and polyester resin matrix, due to the low cost of both the reinforcement and matrix resin. The three-point-bending tests were performed both experimentally and numerically on the composite sandwich coupons.

The sandwich specimen was supported by two rigid bodies at the lower surface; another rigid body was moved down to apply the bending, as shown in Figure 32. To establish the contact relationship, an initial displacement was applied to the model. The reaction force and displacements were output to compare with the experiment result [64].

Figure 32: Three points bending tests on the corrugated sandwich composite coupon [64]

Figure 33 presents the experimental load-displacement curves under loading in the machine-direction and the cross-direction. In the parallel-direction, the downfall load reached 50 kN, which is the limit of the testing machine, after the adhesion between face sheet and core failed. In the case of the cross-direction, the sudden load drop became less significant and the loss of linearity was more progressive.

The first load-drop occurred at 41 kN and the second at 33 kN, which correspond to the failure between face sheet and core and the failure in the up face sheet, respectively.

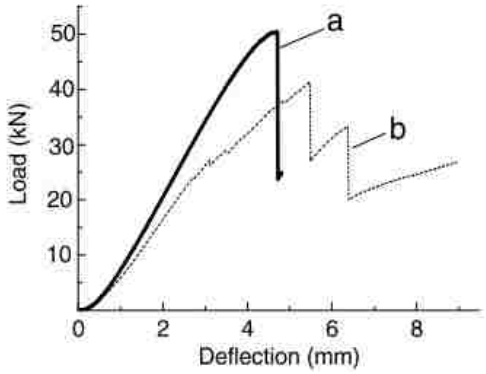

Figure 33: Experimental load-displacement curves of the corrugated composite sandwich coupon s under bending conditions [64]

In order to simulate the mechanical behavior of corrugated sandwich structure, a FE model was created using Abaqus (Figure 34). The FE simulation is an effective tool to reduce the development costs and accelerate the development of the optimized structure in the early stage of design. At that stage, the adhesion between the core and the face sheets was ignored. As it can be seen from Figure 34, the stress concentration occurred on the corrugation core part and the region where the core and the face sheet meet. The model was able to simulate the load-displacement curves at the initial loading stage.

The spaces between core and face sheets provide opportunities for integrating energy resources into the vehicle floor that is a safe and secure location for this purpose.

In the future stages of the work, optimization of the sandwich structure should be conducted and factors such as corrugation angle, thickness of core and face sheets, fiber alignment and hybridization should be considered for maximizing the bending performance with minimum weight.

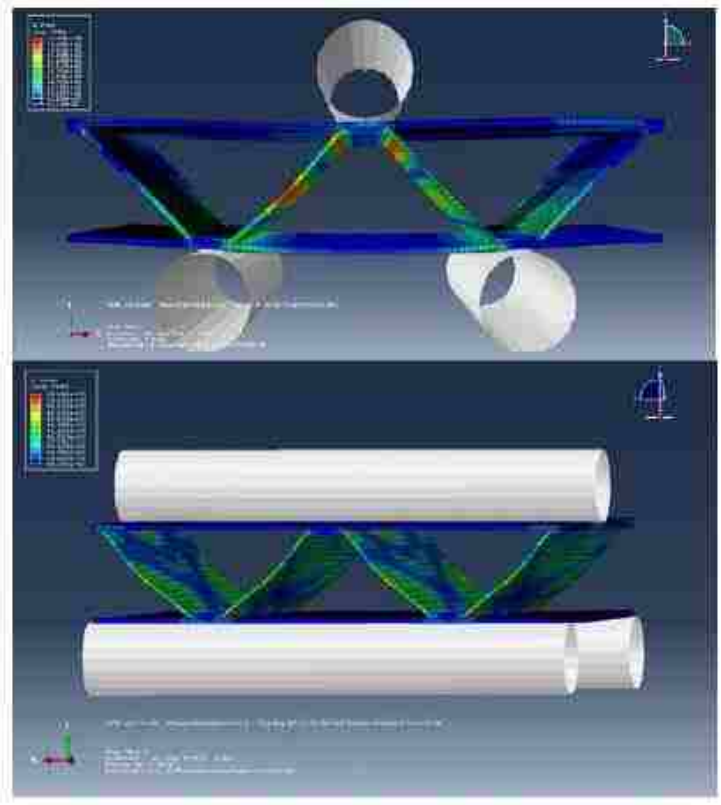

Figure 34: Stress distribution of composite sandwich coupons loaded in both (a) the machine direction and (b) the cross-direction [64]

CHAPTER III

DESIGN AND METHODOLOGY

3.1 Problem Statement

The aim of this thesis research is to evaluate the possibility of realizing a rear suspension cradle with composite materials that will provide comparable performance to an aluminum solution at a fraction of the weight.

The original model taken into consideration is the cradle of the 2011 Dodge Dart 2.0 WGE Tigershark in aluminum. Figure 35 shows the CAD model of the cradle and it is possible to see its installed location inside the vehicle and its function related to the suspension arms.

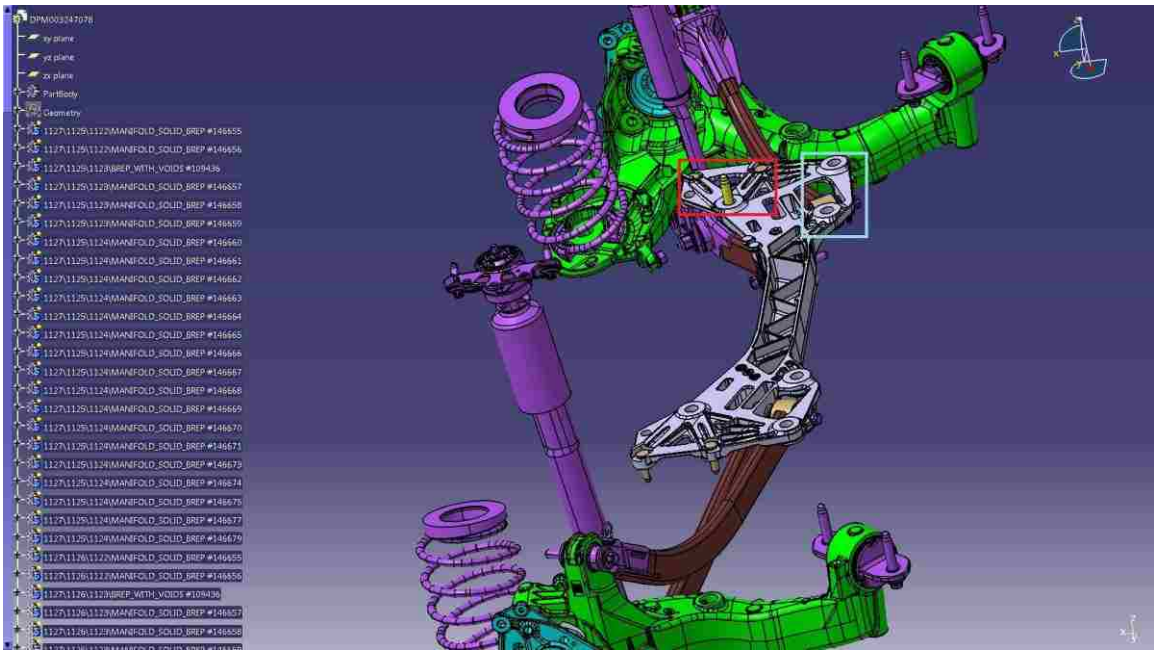

Figure 35: Rear suspension cradle-CAD model

The cradle is the grey part with the attachment points identified with the red box, while the stabilizer bar attachment points are shown in the cyan box (Figure 35). In the evaluation of the stiffness of the component these points have not been considered, while attention has been focused on the brackets where the arms of the suspension are attached, as shown in Figure 36.

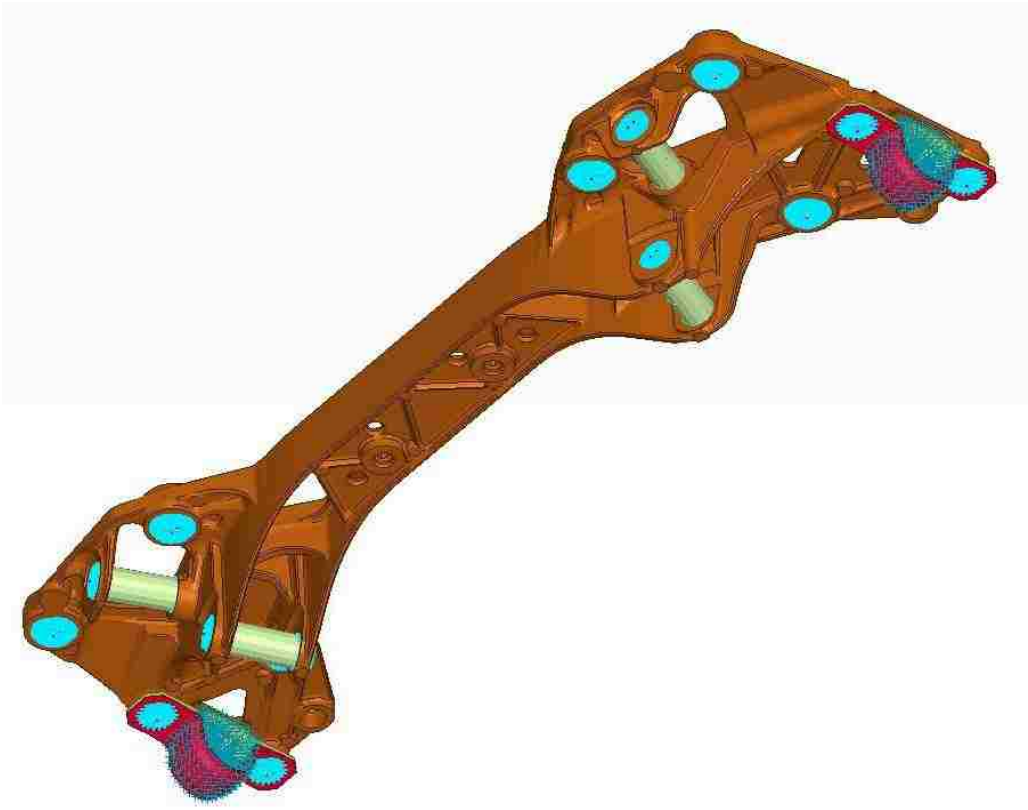

Figure 36: Cradle: attachment points and load points. Source: Material provided by Chrysler

The information relative to the original component is reported with data relative to the values of stiffness reached by this component.

In the column "Direction" of Table 7 the direction used to evaluate the stiffness is shown (linear or angular directions). Note that the values of the left side relative to linear displacements are slightly different from the right side (a bit higher) while the values linked to the torsional behavior are the same.

	Direction	Units	Left	Right
Lower Lateral Link	x	N/mm	120336	119303
	y	N/mm	91435	91130
	z	N/mm	222413	220455
	rx	Nmm/rad	1.60E+08	1.60E+08
	ry	Nmm/rad	9.27E+07	9.26E+07
	rz	Nmm/rad	1.33E+08	1.33E+08
Upper Lateral Link	x	N/mm	315687	315640
	y	N/mm	247613	246840
	z	N/mm	147959	148097
	rx	Nmm/rad	1.14E+08	1.14E+08
	ry	Nmm/rad	9.75E+07	9.76E+07
	rz	Nmm/rad	2.04E+08	2.04E+08
Stabilizer Bar	x	N/mm	23300	23300
	y	N/mm	43267	43305
	z	N/mm	55380	55999
	rx	Nmm/rad	2.60E+07	2.60E+07
	ry	Nmm/rad	1.20E+07	1.20E+07
	rz	Nmm/rad	6.44E+07	6.44E+07

Table 7: Stiffness values of the original aluminum component. Source: Material provided by Chrysler

The weight of the conventional aluminum component is 3.8 kg (E=70000 MPa).

The specific method to calculate the stiffness was not known, so for the design of the composite model the following method was used for all the models that will be presented: for the stiffness along the x, y and z directions a concentrated force of 100 N is applied at the points where the stiffness is to be calculated (lower and upper links); while to evaluate the torsional stiffness a concentrated moment along the three directions (rx, ry and rz) is applied (the details of torsion evaluation are provided in Section 4.4).

3.2 Proposed research

In order to conduct the study of the conversion of the cradle into a composite solution, a simplified version of the aluminum cradle has been realized; this simplified model takes into account the following criteria:

- develop a composite component without the constraints of complex geometry present in the original component;
- develop a method to convert a structural component from metal to composite.

The constraints considered to realize the model are:

- maintain the overall dimensions of the original component;
- maintain the attachment points of the original cradle to the suspension arms and to the body of the vehicle;
- reduce the weight of the original component (original cradle weighs 3.8 kg while the simplified model weighs 4.12 kg).

The material adopted for the simplified version of the cradle is the same conventional aluminum (E= 70000 MPa). The geometry has been kept as simple as possible without the adoption of stiffener members such as stiffening ribs, as shown in Figure 37.
Obviously, this model can be improved and optimized, but in this first stage it is useful to consider it in its simple shape as a starting point for the conversion to composite.

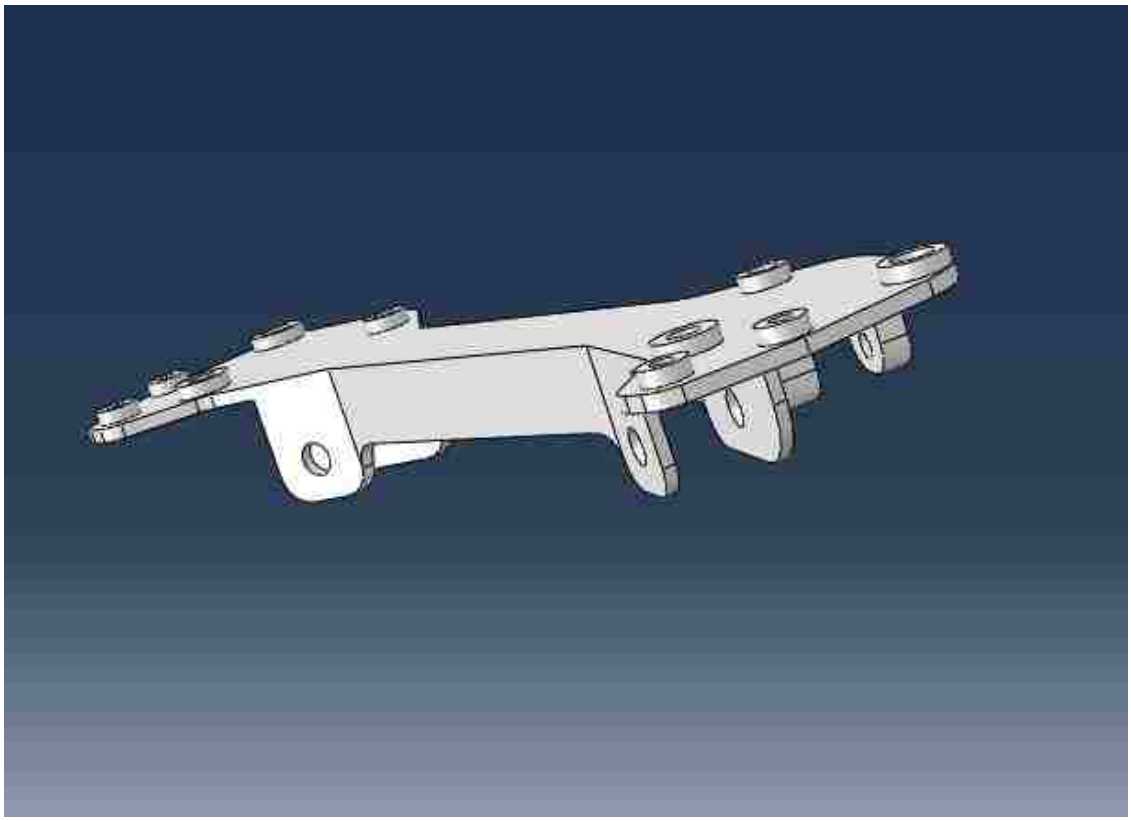

Figure 37: Simplified model of cradle with aluminum material

Figures 38 and 39 show how the component has been constrained and where the loads have been applied: the cradle is constrained to the body of the vehicle in the six points shown in Figure 38 through bolts and screws; for this reason it has been decided to constrain these points as “encastre” in the definition of the load step of the model: all the six degrees of freedom have been locked for these points.

The software used to conduct the simulations is Abaqus; from Figures 41 to 52 displacement fields and stress distributions of the aluminum model are shown for each load configuration; these results constitute the benchmark model for comparison with the redesigned composite model.

In Table 8, stiffness and displacement values of the simplified aluminum model are shown.

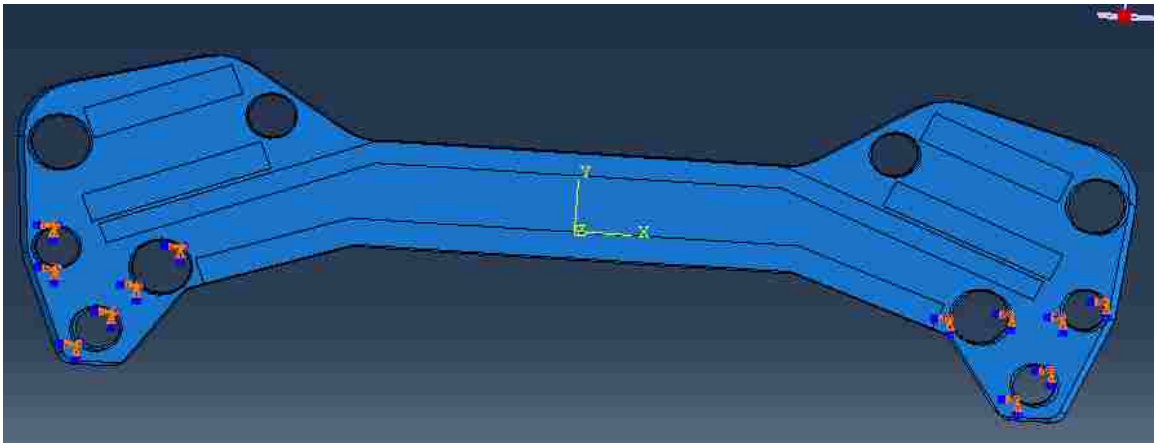

Figure 38: Location of constrained points

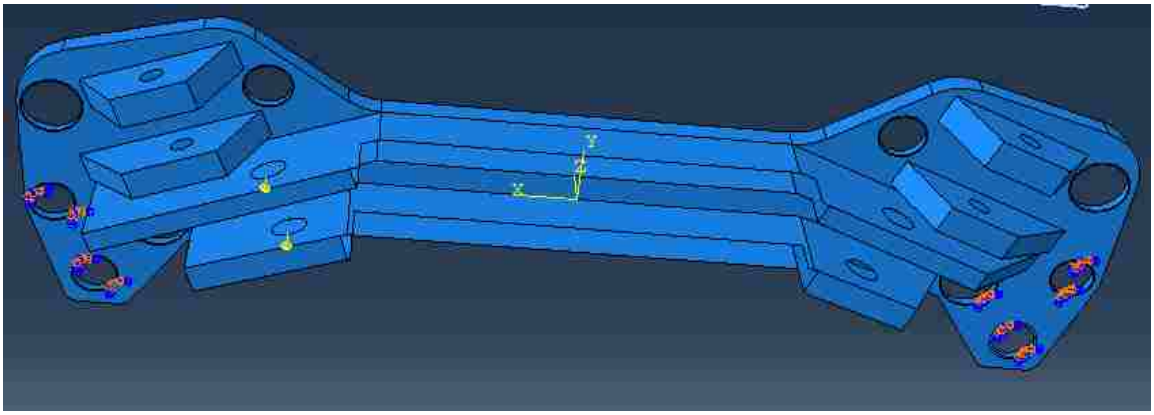

Figure 39: Location of applied loads- Force acting on Lower Link

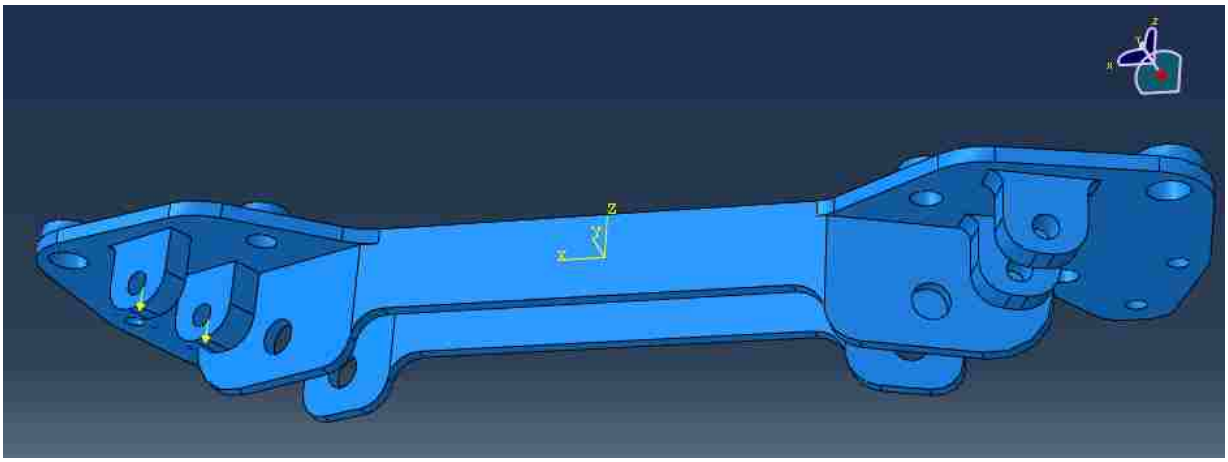

Figure 40: Location of applied loads-Force acting on Upper Link

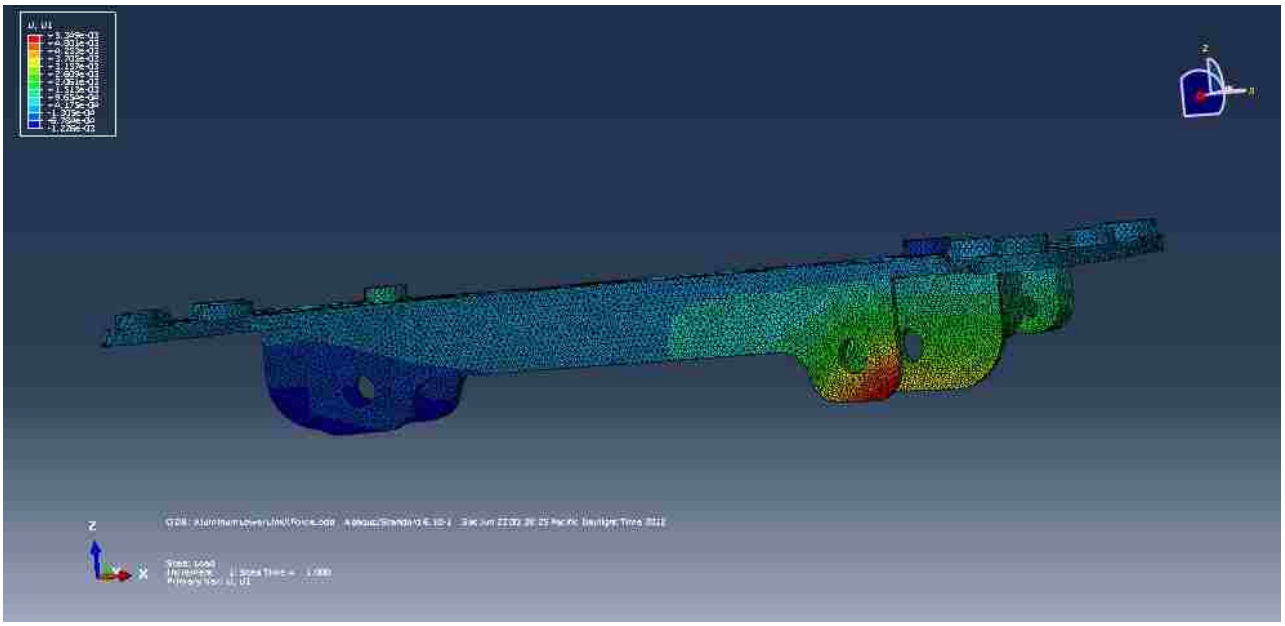

Figure 41: Aluminum model Lower lateral link - Displacements with force applied along x-direction

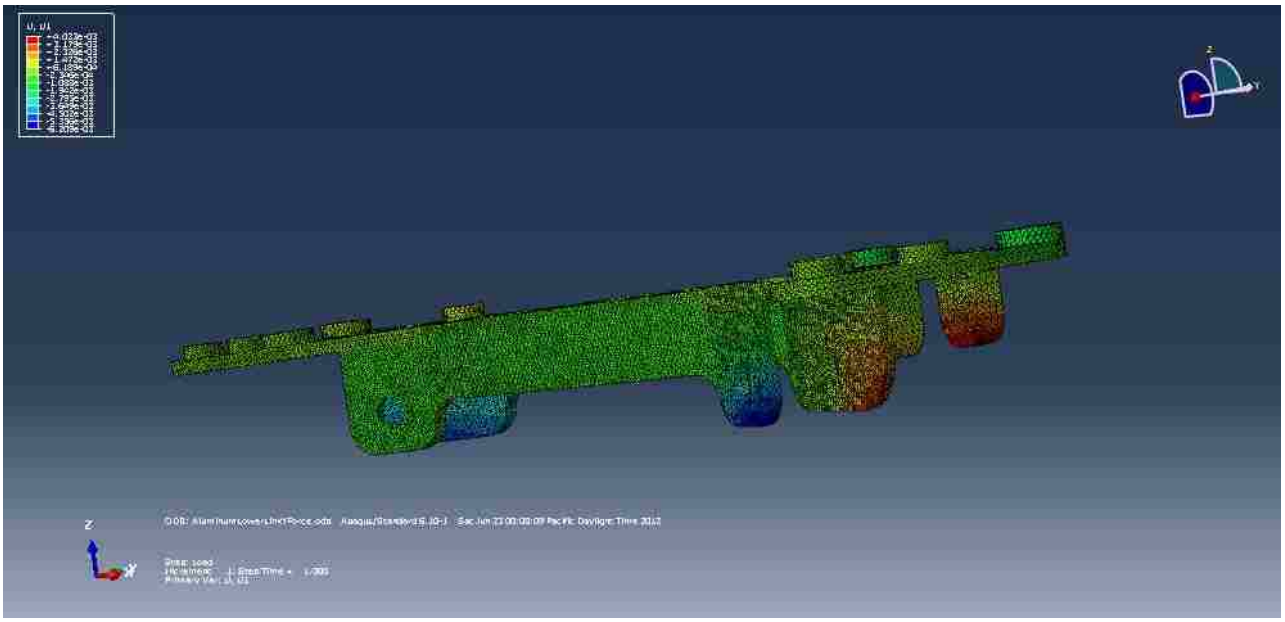

Figure 42: Aluminum model Lower lateral link - Displacements with force applied along y-direction

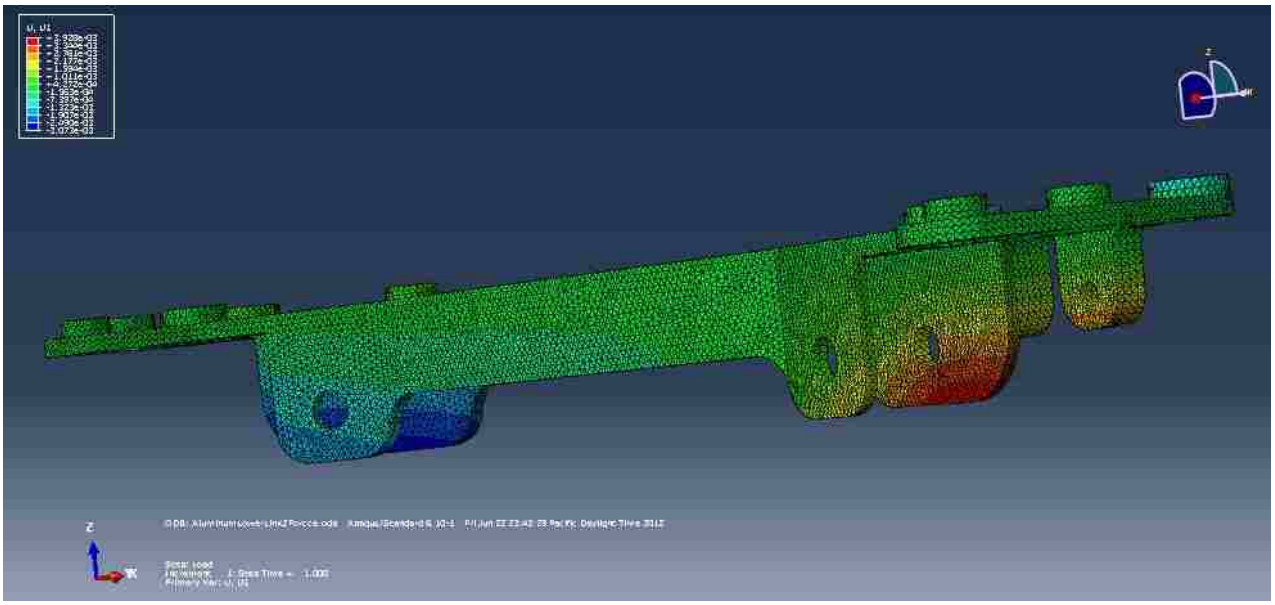

Figure 43: Aluminum model Lower lateral link - Displacements with force applied along z-direction

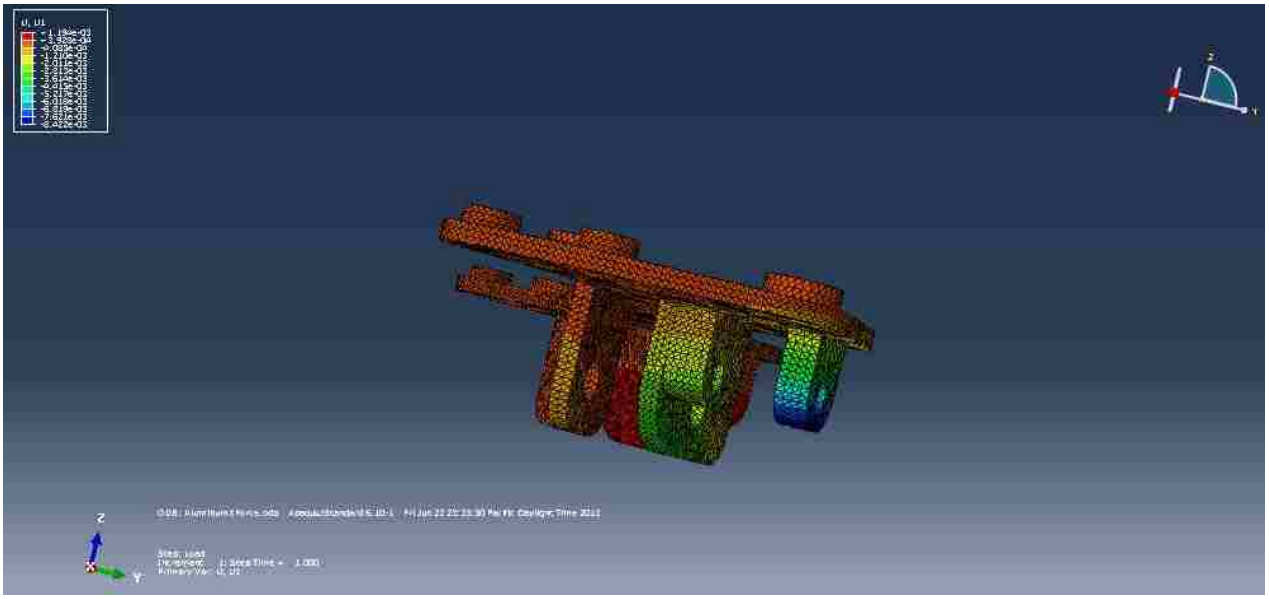

Figure 44: Aluminum model Upper lateral link - Displacements with force applied along x-direction

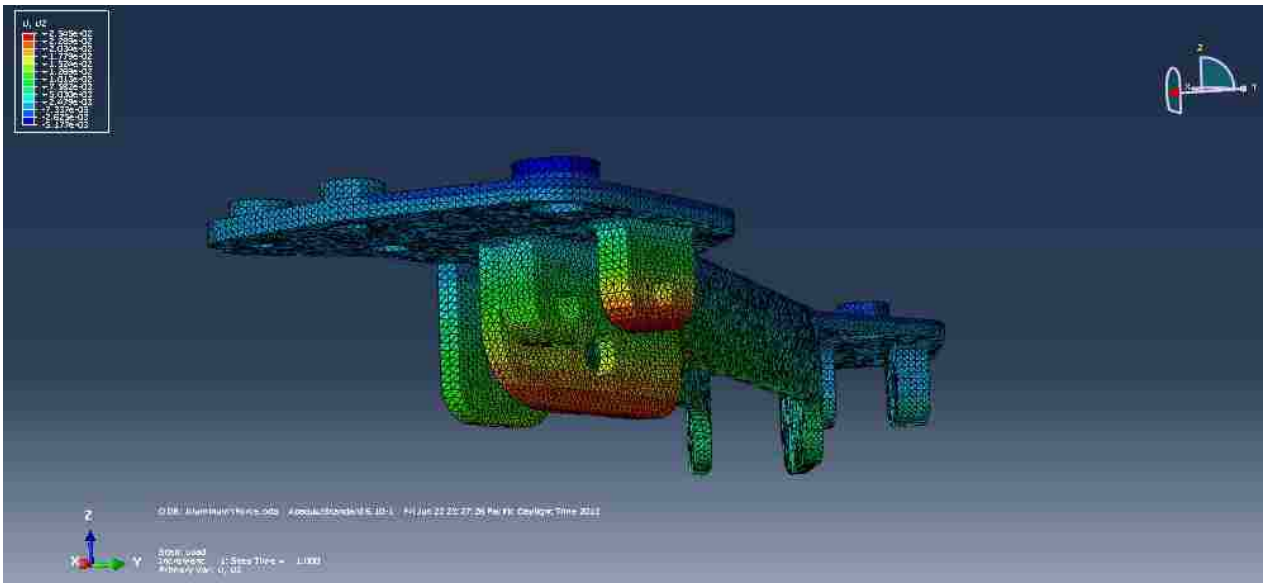

Figure 45: Aluminum model Upper lateral link - Displacements with force applied along y-direction

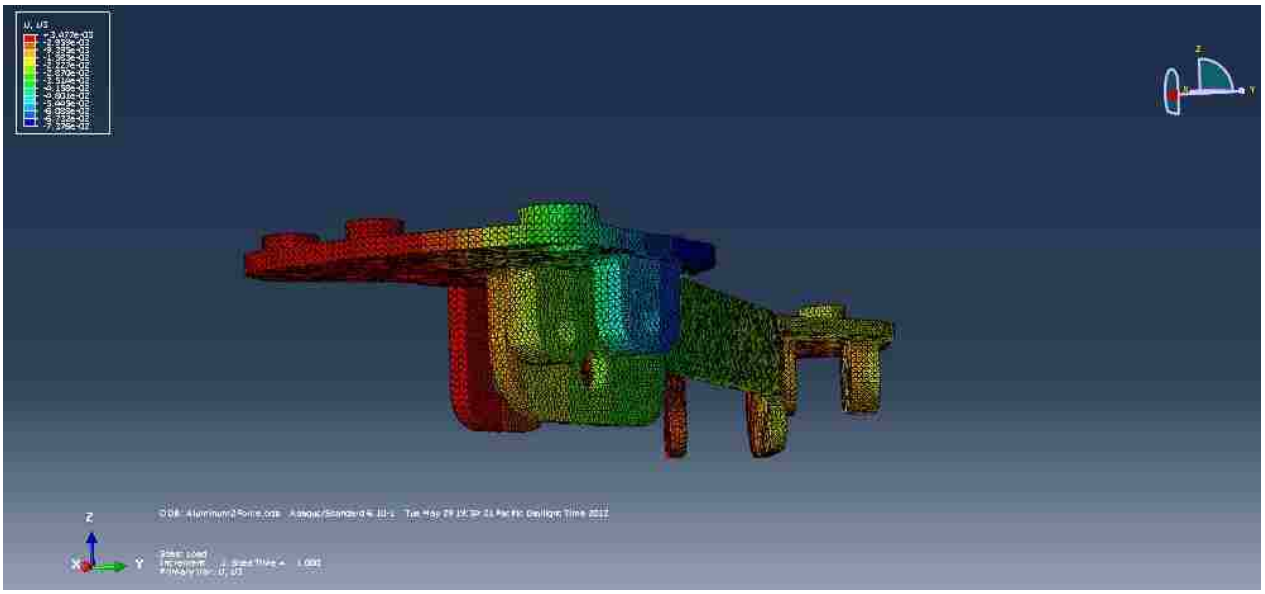

Figure 46: Aluminum model Upper lateral link - Displacements with force applied along z-direction

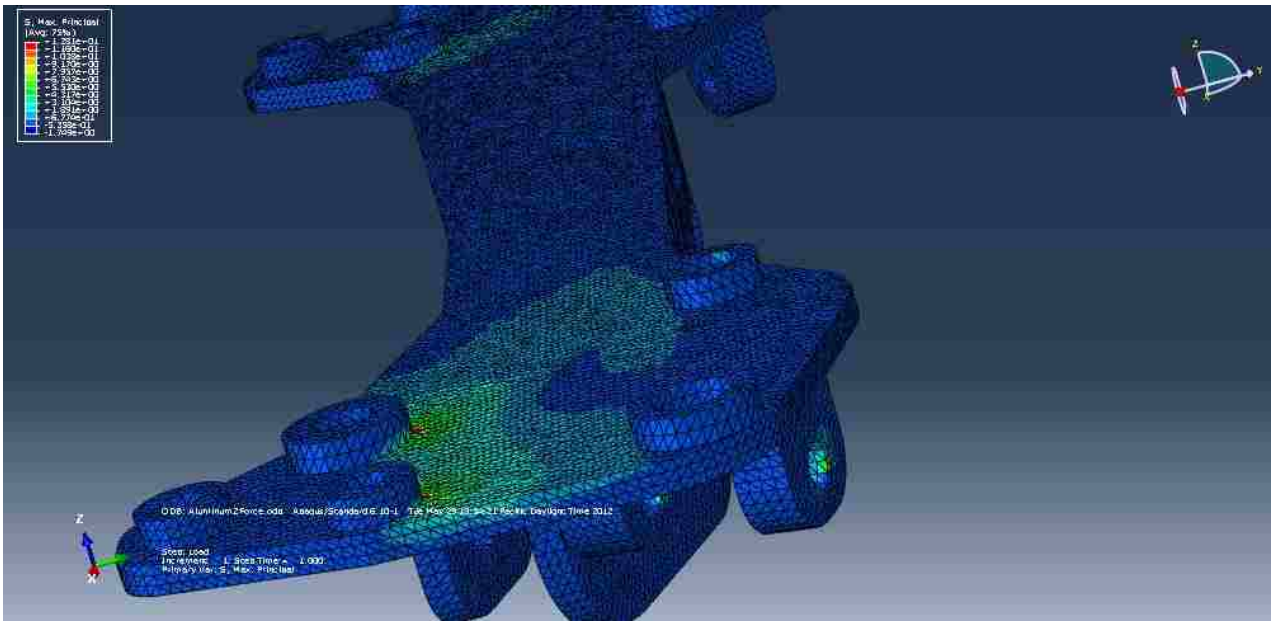

Figure 47: Aluminum model Lower lateral link - Stress distribution with force applied along x-direction

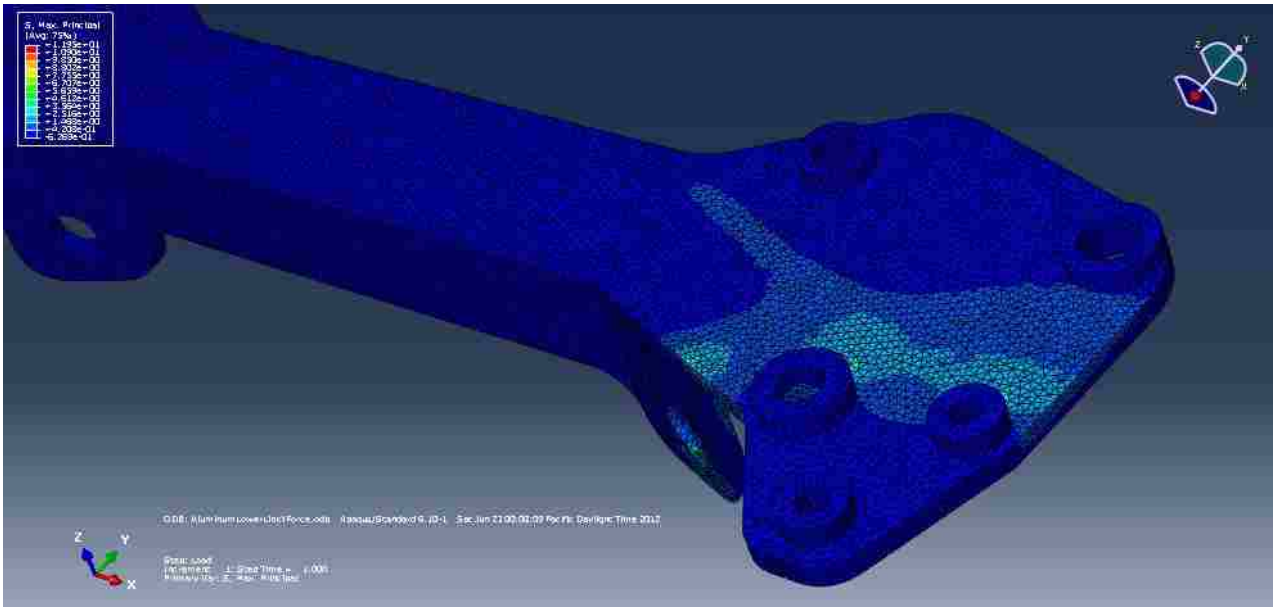

Figure 48: Aluminum model Lower lateral link - Stress distribution with force applied along y-direction

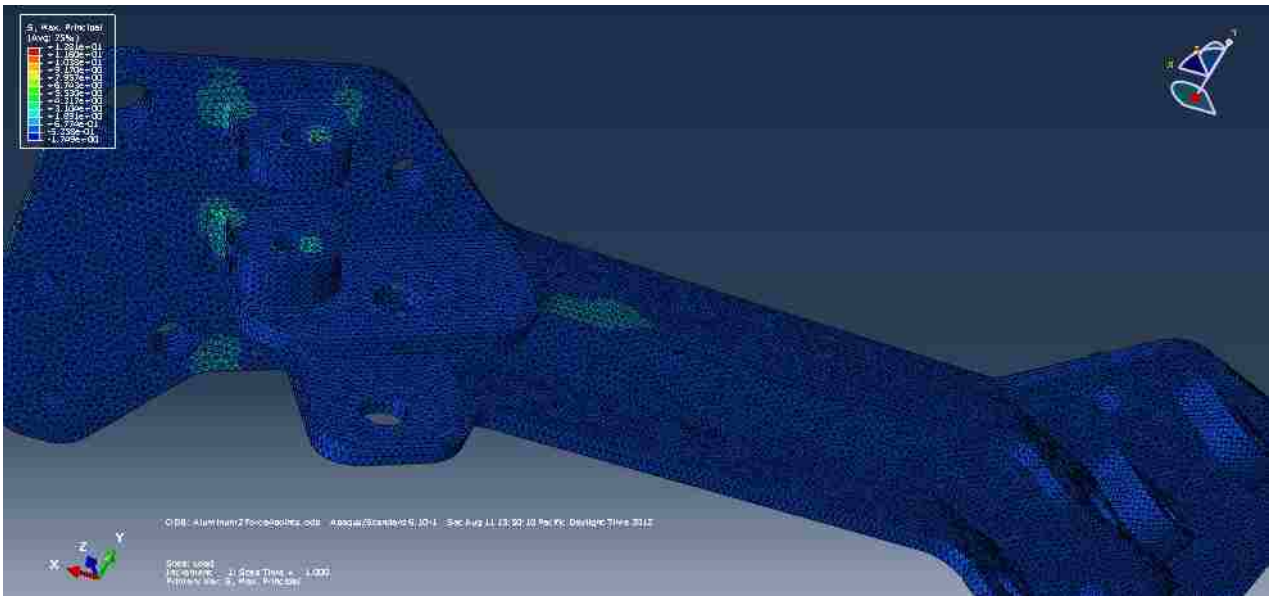

Figure 49: Aluminum model Lower lateral link - Stress distribution with force applied along z-direction

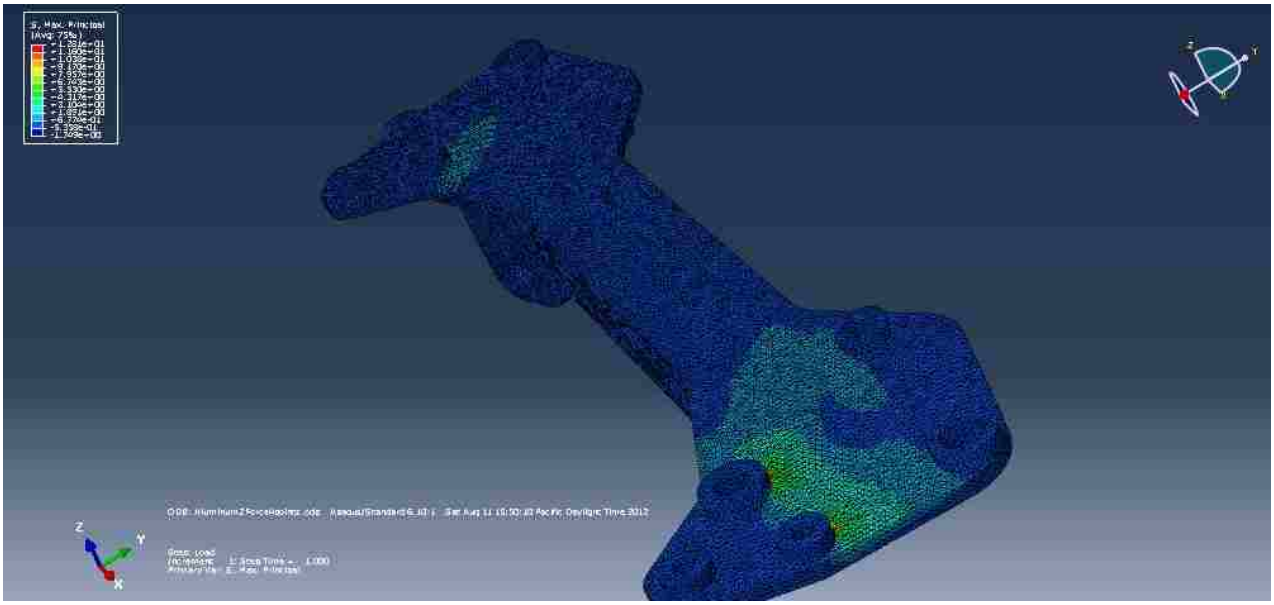

Figure 50: Aluminum model Upper lateral link - Stress distribution with force applied along x-direction

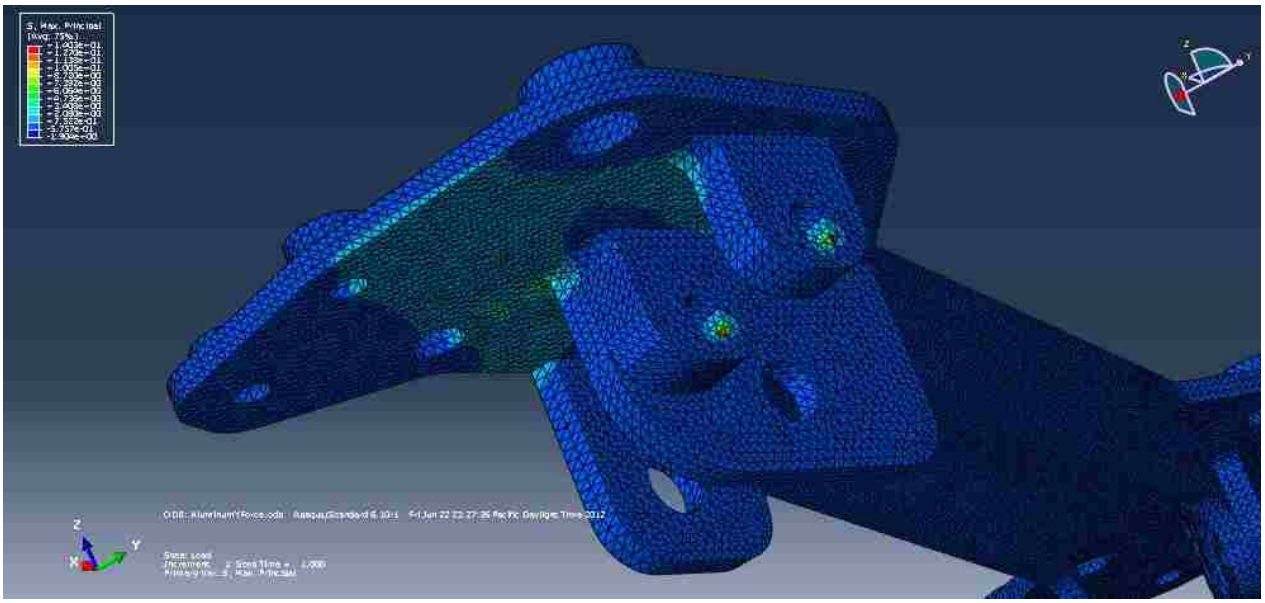

Figure 51: Aluminum model Upper lateral link - Stress distribution with force applied along y-direction

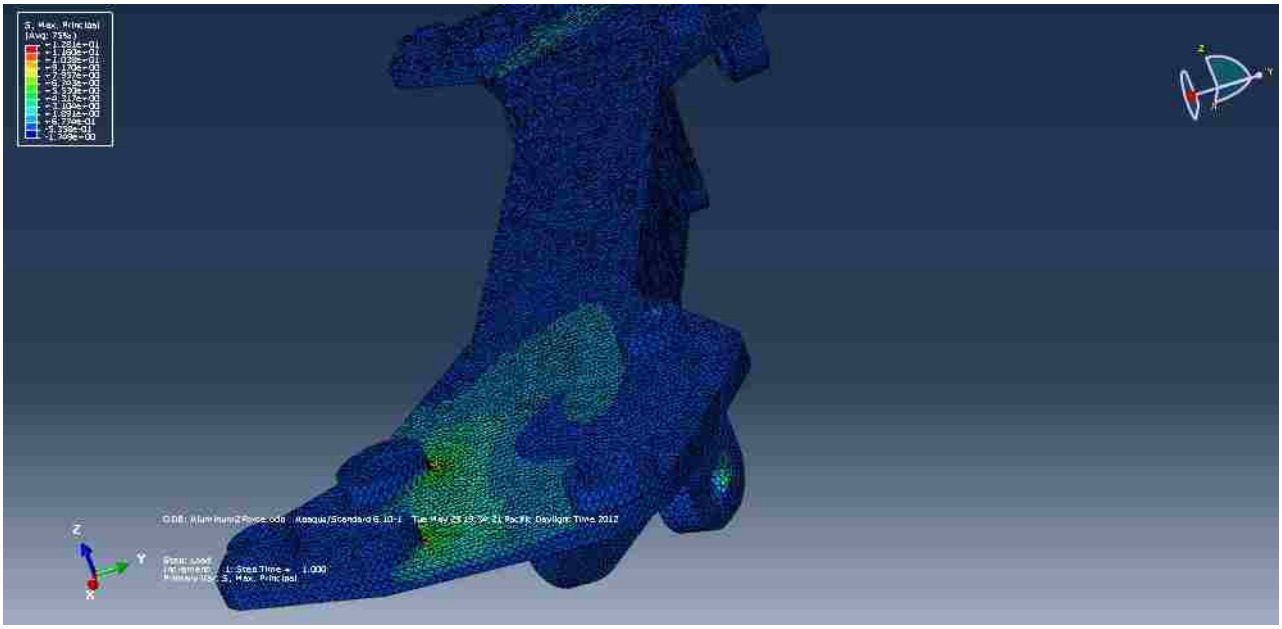

Figure 52: Aluminum model Upper lateral link - Stress distribution with force applied along z-direction

Figures 41 to 46 show the displacement fields in the cradle with different loads: the regions with red color represent the points where the displacements are higher in modulus (depending on the direction of the forces they can be either positive or negative), with the exceptions of Figures 44 and 46 where the red regions represent positive displacements that are lower than negative displacements in modulus.

With this specification, simulations show that the higher displacements occur at the lower extremity of the lower lateral link or of the lower extremity of the upper lateral link (Figures 41 to 46).

Combining the data of Table 8 relative to maximum displacements and Figures 41-46, it is possible to evaluate which regions of the cradle undergo higher values of displacements and their values. For example, with a force acting on the lower lateral link along x-direction Figure 41 shows that its lower region has the higher displacement, and it is equal to 7,83 E-03 mm.

Figures 47 to 52 show the stress distribution along the cradle with different load conditions; stress concentrations appear in coincidence with the constrained points of the cradle and at the points where forces are applied. Figures 47, 50 and 52 illustrate the most severe load conditions for the model; they represent the lower link loaded with force along x-direction and the upper link with forces along x and z directions, respectively.

Direction	Lower lateral link [N/mm]	Upper lateral link [N/mm]
X	42553	27393
Y	5714	5076
Z	16529	3077
	Maximum displacement [mm]	Maximum displacement [mm]
X	7,83E-03	9,01E-03
Y	4,98E-02	4,30E-02
Z	1,82E-02	7,38E-02

Table 8: Stiffness and maximum displacements of aluminum model along different directions

3.3 Development of composite model

The materials considered for the design of the composite model are the following: two carbon fiber reinforced polymers and one glass fiber composite; their mechanical characteristics are shown in the Tables 9 and 10. In Table 9 the highlighted column is a conventional carbon fiber reinforced polymer while a second carbon fiber polymer has been taken into account due to its higher Young's modulus.

Table 10 shows the properties of a glass fiber reinforced polymer, with lower mechanical properties with respect to the carbon fiber materials and with a higher density.

The composite part was designed with shell elements in order to define the layups of the layers made with composite materials.

The following step of the simulation phase is the definition of the material properties: in the Figure 53 it is shown how the properties of a composite material were defined. For a metal the type of elastic properties is set as isotropic; for a composite material it is necessary to choose lamina under the type of mechanical properties and specify the values for each field (E1, E2, Poisson ratio and shear modulus), where E1 and E2 are the Young moduli along 0° and 90° respectively.

The specification of the density is the same for both material types.

Mechanical Properties of Carbon Fibre Composite Materials, Fibre / Epoxy resin (120°C Cure)

Fibres @ 0° (UD), 0/90° (fabric) to loading axis, Dry, Room Temperature, Vf = 60% (UD), 50% (fabric)

	Symbol	Units	Std CF Fabric	HMCF Fabric	E glass Fabric	Kevlar Fabric	Std CF UD	HMCF UD	M55** UD	E glass UD	Kevlar UD	Boron UD
Young's Modulus 0°	E1	GPa	70	85	25	30	135	175	300	40	75	200
Young's Modulus 90°	E2	GPa	70	85	25	30	10	8	12	8	6	15
In-plane Shear Modulus	G12	GPa	5	5	4	5	5	5	5	4	2	5
Major Poisson's Ratio	v12		0.10	0.10	0.20	0.20	0.30	0.30	0.30	0.25	0.34	0.23
Ult. Tensile Strength 0°	Xt	MPa	600	350	440	480	1500	1000	1600	1000	1300	1400
Ult. Comp. Strength 0°	Xc	MPa	570	150	425	190	1200	850	1300	600	280	2800
Ult. Tensile Strength 90°	Yt	MPa	600	350	440	480	50	40	50	30	30	90
Ult. Comp. Strength 90°	Yc	MPa	570	150	425	190	250	200	250	110	140	280
Ult. In-plane Shear Stren.	S	MPa	90	35	40	50	70	60	75	40	60	140
Ult. Tensile Strain 0°	ext	%	0.85	0.40	1.75	1.60	1.05	0.55		2.50	1.70	0.70
Ult. Comp. Strain 0°	exc	%	0.80	0.15	1.70	0.60	0.85	0.45		1.50	0.35	1.40
Ult. Tensile Strain 90°	eyt	%	0.85	0.40	1.75	1.60	0.50	0.50		0.35	0.50	0.60
Ult. Comp. Strain 90°	eyc	%	0.80	0.15	1.70	0.60	2.50	2.50		1.35	2.30	1.85
Ult. In-plane shear strain	es	%	1.80	0.70	1.00	1.00	1.40	1.20		1.00	3.00	2.80
Thermal Exp. Co-ef. 0°	Alpha1	Strain/K	2.10	1.10	11.60	7.40	-0.30	-0.30	-0.30	6.00	4.00	18.00
Thermal Exp. Co-ef. 90°	Alpha2	Strain/K	2.10	1.10	11.60	7.40	28.00	25.00	28.00	35.00	40.00	40.00
Moisture Exp. Co-ef 0°	Beta1	Strain/K	0.03	0.03	0.07	0.07	0.01	0.01		0.01	0.04	0.01
Moisture Exp. Co-ef 90°	Beta2	Strain/K	0.03	0.03	0.07	0.07	0.30	0.30		0.30	0.30	0.30
Density		g/cc	1.60	1.60	1.90	1.40	1.60	1.60	1.65	1.90	1.40	2.00

** Calculated figures

Table 9: Carbon fiber reinforced polymers mechanical properties. Source: "Performance Composites LTD"

Property	*ASTM Standard*	*75°F*	*22°C*
Elastic Constants		*Msi*	*GPa*
Longitudinal Modulus, E_L	*D3039*	*7.7 - 8.5*	*53 - 59*
Transverse Modulus, E_T	*D3039*	*2.3 - 2.9*	*16 - 20*
Axial Shear Modulus, G_{LT}	*D3518*	*0.9 - 1.3*	*6 - 9*
Poisson's Ratio, u_{LT}	*D3039*	*0.26 - 0.28*	*0.26 - 0.28*
Strength Properties		*ksi*	*MPa*
Longitudinal Tension, F^{tu}_L	*D3039*	*230 - 290*	*1590 - 2000*
Longitudinal Compression, F^{cu}_L	*D3410*	*100 - 180*	*690 - 1240*
Transverse Tension, F^{tu}_T	*D3039*	*6 - 12*	*41 - 82*
Transverse Compression, F^{cu}_T	*D3410*	*16 - 29*	*110 - 200*
In-Plane Shear, F^{su}_{LT}	*D3518*	*9 - 24*	*62 - 165*
Interlaminar Shear, F^{su}	*D2344*	*8 - 15*	*55 - 103*
Longitudinal Flexural	*D790*	*180 - 250*	*1240 - 1720*
Longitudinal Bearing	*D953*	*68 - 80*	*469 - 552*
Ultimate Strains			
Longitudinal Tension, ϵ^{tu}_L	*D3039*	*2.7 - 3.5%*	
Longitudinal Compression, ϵ^{cu}_L	*D3410*	*1.1 - 1.8%*	
Transverse Tension, ϵ^{tu}_T	*D3039*	*0.25 - 0.50%*	
Transverse Compression, ϵ^{cu}_T	*D3410*	*1.1 - 2.0%*	
In-Plane Shear, γ^{su}_{LT}	*D3518*	*1.6 - 2.5%*	
Physical Properties			
Fiber Volume (%)	*D2734*	*57 - 63%*	*57-63%*
Density	*D792*	*lb/in³*	*g/cm³*
		0.071 - 0.073	*1.96 - 2.02*

Table 10: Glass fiber reinforced polymer mechanical properties. Source: "www.agy.com/technical_info"

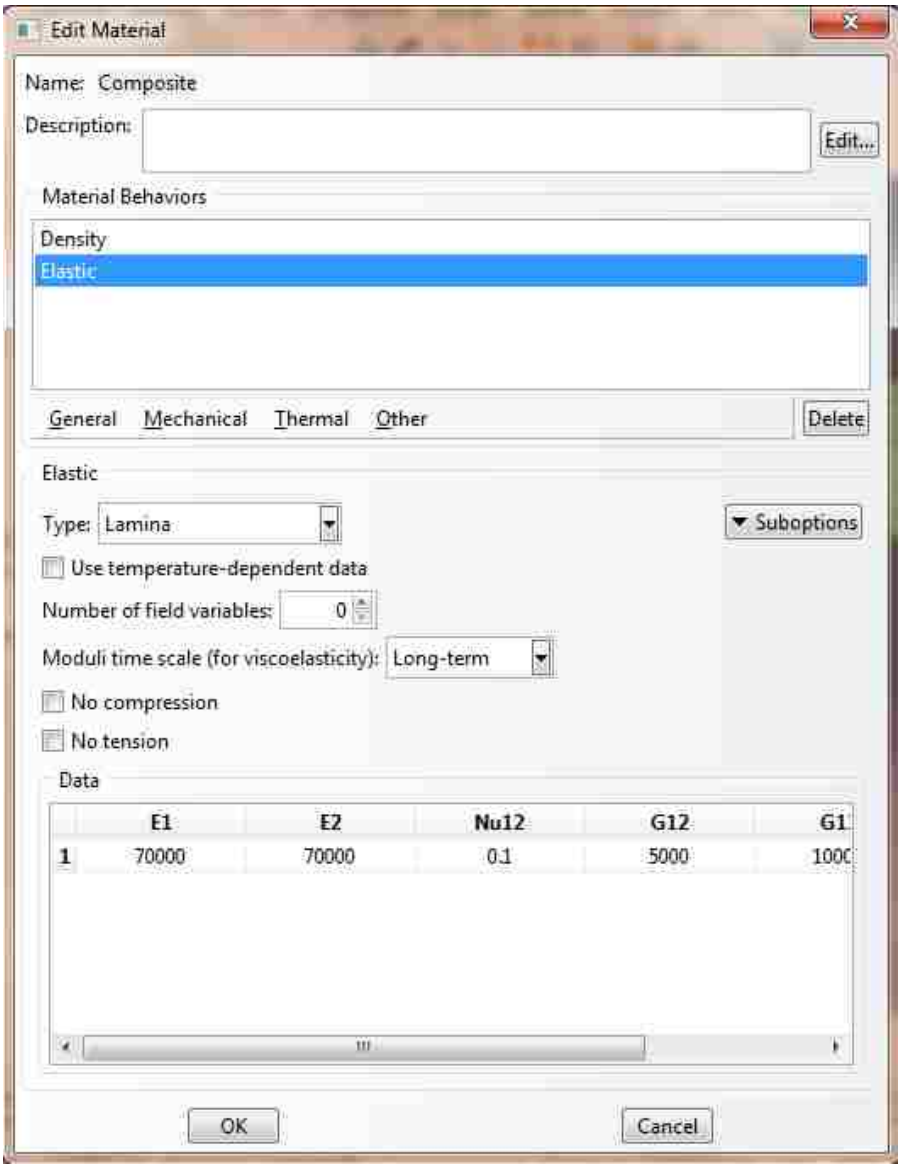

Figure 53: Definition of composite materials properties with Abaqus software

The materials described as "fabric" present the same Young moduli E1 and E2: this means that they have isotropic behavior along 0° and 90°. In the contrary, unidirectional composites have an E1 modulus much higher than E2, presenting an orthotropic behavior.

In order to describe an anisotropic material subject to a triaxial stress system, the compliance matrix with thirty-six terms is used [68]:

$$\begin{Bmatrix} \varepsilon_1 \\ \varepsilon_2 \\ \varepsilon_3 \\ \gamma_{23} \\ \gamma_{31} \\ \gamma_{12} \end{Bmatrix} = \begin{bmatrix} S_{11} & S_{12} & S_{13} & S_{14} & S_{15} & S_{16} \\ S_{21} & S_{22} & S_{23} & S_{24} & S_{25} & S_{26} \\ S_{31} & S_{32} & S_{33} & S_{34} & S_{35} & S_{36} \\ S_{41} & S_{42} & S_{43} & S_{44} & S_{45} & S_{46} \\ S_{51} & S_{52} & S_{53} & S_{54} & S_{55} & S_{56} \\ S_{61} & S_{62} & S_{63} & S_{64} & S_{65} & S_{66} \end{bmatrix} \begin{Bmatrix} \sigma_1 \\ \sigma_2 \\ \sigma_3 \\ \tau_{23} \\ \tau_{31} \\ \tau_{12} \end{Bmatrix} \quad (3)$$

where:

ε_1 is the direct strain in the x direction

ε_2 is the direct strain in the y direction

ε_3 is the direct strain in the z direction

γ_{23} is the shear strain in the yz plane

γ_{31} is the shear strain in the xz plane

γ_{12} is the shear strain in the xy plane

σ_1 is the direct stress in x direction

σ_2 is the direct stress in y direction

σ_3 is the direct stress in z direction

τ_{23} is the shear stress in the yz plane

τ_{31} is the shear stress in the xz plane

τ_{12} is the shear stress in the xy plane

In case of isotropic materials the number of constants of the matrix can be reduced using the following assumptions:

1. Shear stresses do not affect normal strains and normal stresses do not affect shear strains. This leads to: $S_{14}= S_{15}= S_{16}= S_{24}= S_{25}= S_{26}= S_{34}= S_{35}= S_{36}= 0$
2. Shear strains are only affected by shear stresses in the same plane. Hence: $S_{45}= S_{46}= S_{54}= S_{56}= S_{65}= S_{64}= 0$
3. The effect of σ_1 on ε_1 is the same as the effect of σ_2 on ε_2, etc. Hence: $S_{11}= S_{22}= S_{33}$
4. The effect of τ_{12} on γ_{12} is the same as the effect of τ_{23} on γ_{23}, etc. Hence: $S_{44}= S_{55}= S_{66}$

In this way for isotropic materials the matrix reduces to one in which there are only three constants S_{11}, S_{12} and S_{66}:

$$S_{11} = \frac{1}{E} \qquad S_{12} = -\frac{\upsilon}{E} \qquad S_{66} = \frac{1}{G} \tag{4}$$

However, with anisotropic materials the previous assumptions cannot be made and the following equations link the stresses to the strains [69] [70]:

$$E_1 = E_f * V_f + E_m * (1-V_f) \tag{5}$$

$$E_2 = E_f * E_m / [(\nu_f * E_m + (1- \nu_f) * E_f] \tag{6}$$

$$\nu_{12} = \nu_f * \nu_f + \nu_m * (1-\nu_f) \tag{7}$$

$$G_{12} = G_f * G_m / [(\nu_f * G_m + (1- \nu_f) * G_f] \tag{8}$$

Where:

E_f: Fiber elastic modulus along the main axis

E_m: Matrix elastic modulus

G_f: Fiber shear modulus

G_m: Matrix shear modulus

ν_f: Fiber Poisson ratio

ν_m: Matrix Poisson ratio

V_f: Fiber volume fraction

After the definition of the material, it is necessary to define the sections for the component. Sections define the thickness of the layers of material and it is possible to assign different sections to different parts of the component: this option has been exploited for the design of the third and definitive model where different sections have been assigned to the brackets and the reinforcement ribs of the cradle.

In Figure 54 the definition of sections for composite models with Abaqus is shown. The

type of section is a continuum shell, while for the aluminum model it is a solid homogeneous section.

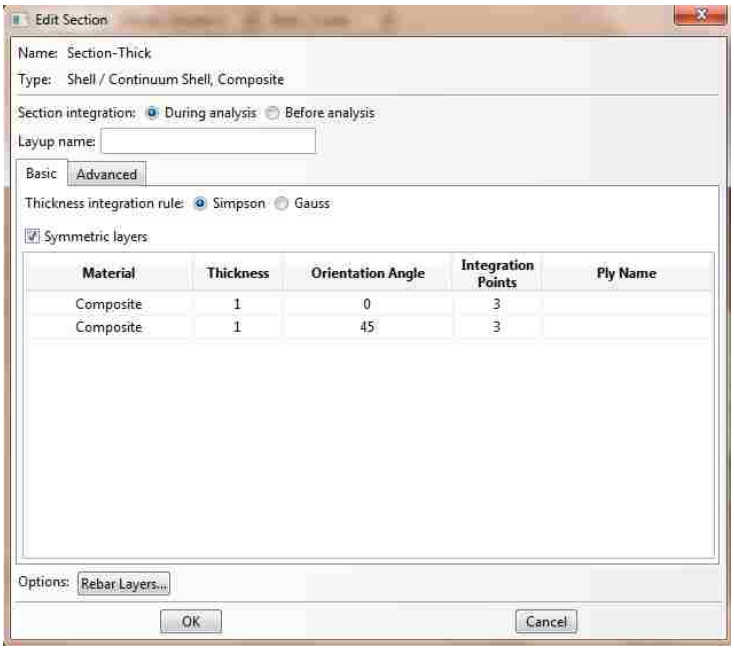

Figure 54: Definition of sections with Abaqus software

For the development of the composite layups the interaction forces between laminae has not been specified but it has been decided to keep the default values provided by Abaqus, including the number of integration points and the thickness integration rule (Simpson).

CHAPTER IV

ANALYSIS OF RESULTS

4.1 First Composite Solution

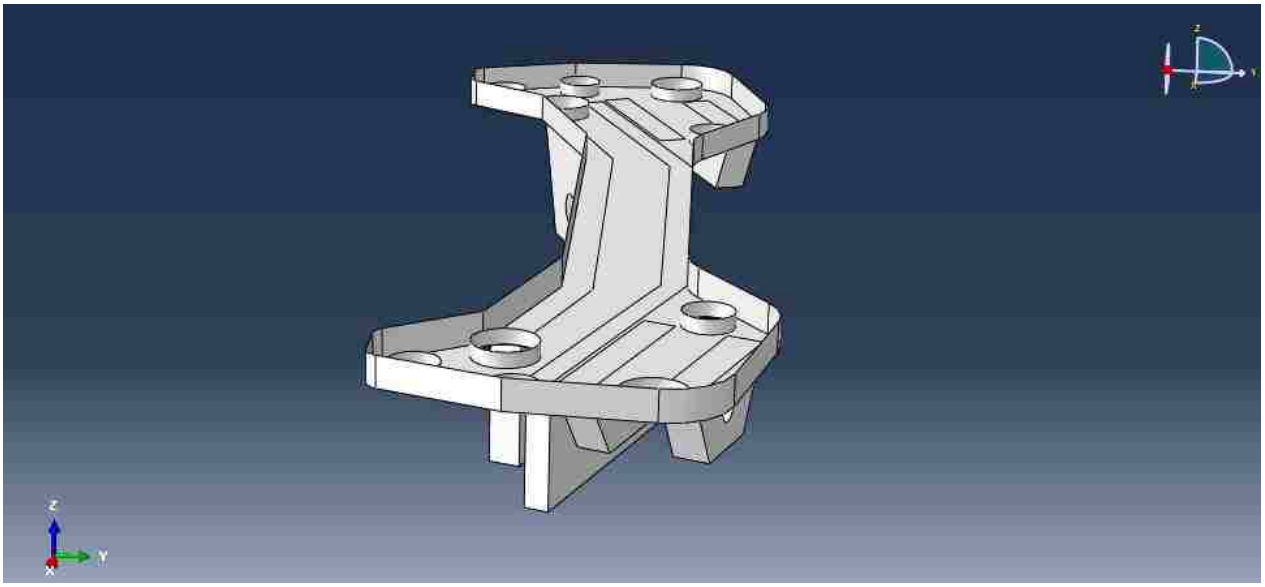

Figure 55: Model of composite solution A

In the design of the composite component, the starting point was the previous model realized with aluminum. The geometry reflects the same as that of the aluminum solution in terms of overall dimensions and brackets where the suspension arms are attached.

The model of this first solution is depicted in Figure 55.

As told before, the composite models have been designed using shell and not solid elements in order to define the layups of composite layers; in addition, this solution with conventional carbon fiber composite presents a lower weight with respect to the aluminum one due to the lower density of this material (2.16 kg vs. 4.12 kg).

As the first stage of the design, a rib along the border of the model has been realized (height of the reinforcement = 20 mm) with an overall thickness of the structure equal to 4 mm; the layup of the fibers is composed of a symmetric disposition of the fibers with an orientation of -45°/45° respect to the longitudinal axis of the component (x direction).
So in total there are 4 layers of composite material with this disposition: -45°/45°/45°/-45°.
The material chosen for this model and the others that will follow during this research is a conventional carbon fiber reinforced composite (the properties of this material are highlighted in the column of table 9), while the other two materials (high modulus carbon fiber and glass fiber) will be analyzed once the final geometry of the cradle is chosen after the first stage of the development of the model.
The performance of the component has been evaluated in terms of stiffness and its behavior compared with the aluminum model.

Direction	Lower lateral link [N/mm]	Upper lateral link [N/mm]
X	9020	9764
Y	1840	1976
Z	3540	952
	Maximum displacement [mm]	**Maximum displacement [mm]**
X	2,68E-02	2,12E-02
Y	1,31E-01	9,98E-02
Z	8,62E-02	2,70E-01

Table 11: Stiffness of first composite solution along different directions

Looking at the stiffness and maximum displacements of the composite model reported in Table 11, it can be seen that it presents lower values of stiffness compared to aluminum solution; since the model is much lighter than the aluminum one, the design approach will be to exploit the difference in terms of weight and to add ribs and increase the stiffness of the component in order to obtain comparable values of stiffness.

4.2 Second Composite Solution

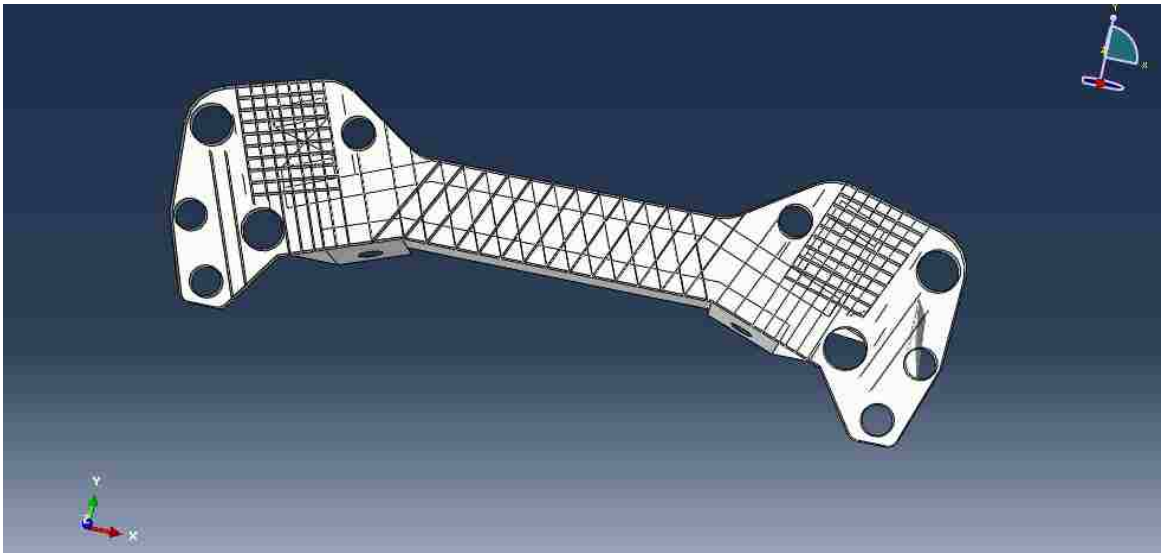

Figure 56: Model of composite solution B

With the design of this second model, ribs were added on the top surface of the cradle in order to increase the stiffness of the structure; they have been added in order to increase the overall stiffness of the cradle and to reduce the displacements in the structure (Figure 56). The orientation of the fibers and the overall thickness (4 mm) are the same as the previous model.

This model weighs 2.31 kg; Table 12 lists the stiffness values:

Direction	Lower lateral link [N/mm]	Upper lateral link [N/mm]
X	11236	11764
Y	1538	1942
Z	3313	1145
	Maximum displacement [mm]	**Maximum displacement [mm]**
X	3,05E-02	3,19E-02
Y	1,83E-01	1,10E-01
Z	3,10E-02	2,44E-01

Table 12: Stiffness of the second model along different directions

It can be seen that the addition of ribs to this configuration leads to improvements of the stiffness of the component: with respect to the previous solution, the stiffness of the upper lateral link is increased 20 % along x and z direction, while along y direction it is almost the same; regarding the lower lateral link its stiffness is increased of 24 % along x direction, while for y and z directions it results lowered of 17 % and 7 % respectively. However, comparing these values to the ones of the original model it can be seen that they are much lower.

The change in the orientation of the fibers did not bring significant improvements in terms of stiffness; for this reason a third model will be designed with a higher presence of ribs in the cradle and consideration of different thicknesses for the brackets and the central part of the cradle.

4.3 Third Composite Solution

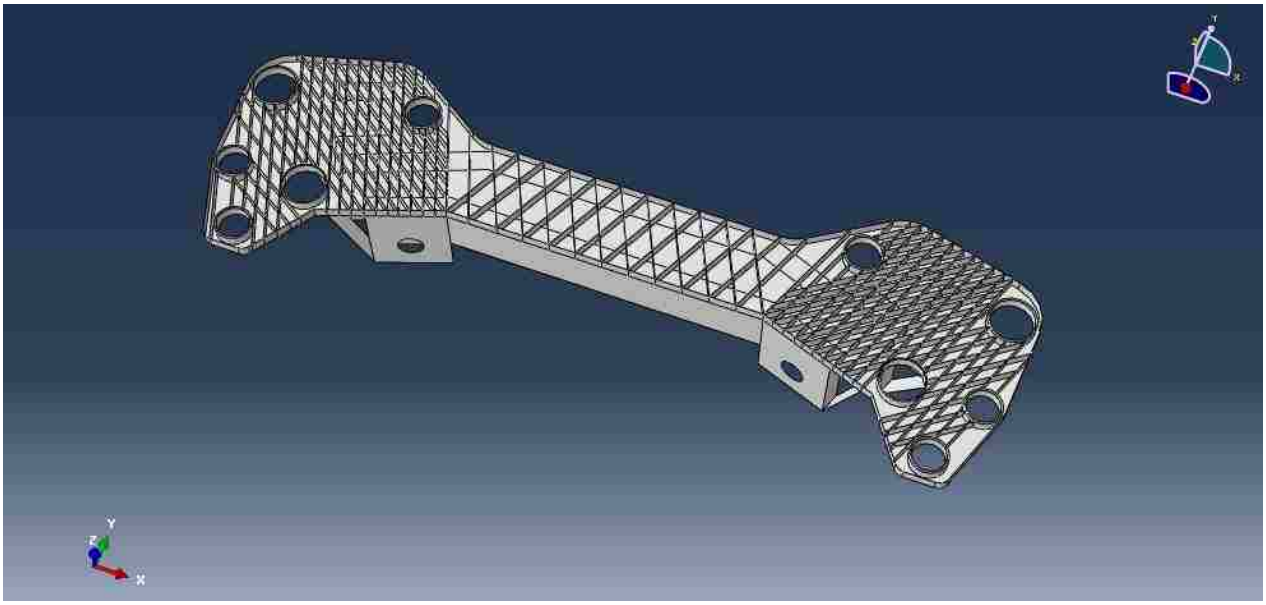

Figure 57: Model of composite solution C

With this design, additional ribs have been added all over the cradle with the same overall thickness (4 mm). The model of third solution is shown in Figure 57.

With respect to the second composite solution, in this model the number of the ribs is increased and they are oriented in a crosswise direction in order to improve the stiffness along all the directions, since the model undergoes loads applied in x, y and z axis.

All the other parameters are the same as the second design iteration.

The weight of this new model is 2.74 kg and in Table 13 the values relative to the stiffness and the maximum displacements are shown:

Direction	Lower lateral link [N/mm]	Upper lateral link [N/mm]
X	15357	16745
Y	2314	2857
Z	4520	1456
	Maximum displacement [mm]	**Maximum displacement [mm]**
X	2,81E-02	2,77E-02
Y	1,49E-01	8,04E-02
Z	1,98E-02	1,80E-01

Table 13: Stiffness of the third model along different directions

With respect to the second model, the stiffness of the upper lateral link is 43 % higher along x and y direction while along z directions it is 27 % higher; regarding the lower lateral link, stiffnesses are 36 % higher along x and z directions and 50 % higher along the y direction.

It can be seen that the trend of increasing stiffnesses leads to an increase of mechanical behavior of the component even if the values are still too low with respect to the aluminum design.

The next design change is to increase the thickness of the component in selected regions of the cradle (i. e. in the region of the brackets) up to 6 mm, maintaining all the other parameters as constant compared to the previous design iteration (material selection and orientation of the fibers).

It must be noted that the material chosen for the ribs added in the top face of the cradle is

chopped carbon fiber because only this kind of fiber can be put on the component through injection molding (while the rest of the cradle can be manufactured through compression molding of fabric prepregs).

The mechanical properties of chopped carbon fiber are much lower respect to fabric prepregs (10 GPa as E1 and E2 have been considered), and a dedicated section has been created with Abaqus software.

In this way, the weight of the cradle has increased up to the weight of the aluminum solution in order to exploit all the material of the model and then the stiffness of the third solution evaluated and the values are reported in Table 14:

Direction	Lower lateral link [N/mm]	Upper lateral link [N/mm]
X	48763	29400
Y	5756	7407
Z	18567	3420
	Maximum displacement [mm]	**Maximum displacement [mm]**
X	6,80E-03	9,75E-03
Y	7,23E-02	3,44E-02
Z	9,56E-03	9,45E-02

Table 14: Stiffness values of third composite solution. Fiber orientation -45°/45°symmetric

Analyzing the values reported above, it can be seen that the composite component presents higher values of stiffness respect to the aluminum version of the cradle, with the same weight. This result could be reached through the addition of more ribs and the increase of the thickness of the brackets.

In addition, the orientation of the fibers was modified to evaluate the influence of this parameter: a configuration with fibers oriented at 0°/90° symmetrically has been studied and the results of simulations are reported in Table 15.

Comparing the two solutions, it can be noted that the configuration with orientation of the fibers equal to -45°/45° symmetric leads to better performance along x direction, while

the orientation 0°/90° gives more stiffness along z direction for both the brackets. According to the direction that is considered more critical for the use of the component the consequent fiber orientation is chosen. Since the exact load profile of the component is not known, it has not been decided to choose a particular fiber orientation, but just analyze the effect of its variation on the stiffnesses reached by the component along different directions.

Direction	Lower lateral link [N/mm]	Upper lateral link [N/mm]
X	43562	22369
Y	4897	8130
Z	24589	4200
	Maximum displacement [mm]	Maximum displacement [mm]
X	6,80E-03	9,75E-03
Y	7,23E-02	3,45E-02
Z	9,56E-03	9,45E-02

Table 15: Stiffness values of third composite solution. Fiber orientation 0°/90° symmetric

Once these results were obtained, the thickness of the sections of the brackets were modified (the section of the reinforced ribs with chopped carbon fibers has not been modified) in order to achieve the same values of stiffness of the aluminum solution and weight savings were verified.

These iterative procedures lead to the definition of a threshold value of thickness that allows the composite model to have the same mechanical characteristics respect to aluminum in terms of stiffness: the value is equal to 5.2 mm with a corresponding weight of the component equal to 3.75 kg, allowing a reduction of 0.307 kg.

In Table 16 the results of simulations are reported:

Direction	Lower lateral link [N/mm]	Upper lateral link [N/mm]
X	44879	27612
Y	5021	6146
Z	16754	3032
	Maximum displacement [mm]	**Maximum displacement [mm]**
X	7,20E-03	9,20E-03
Y	6,70E-02	4,25E-02
Z	3,10E-02	9,60E-02

Table 16: Stiffness values of composite model with threshold value of thickness

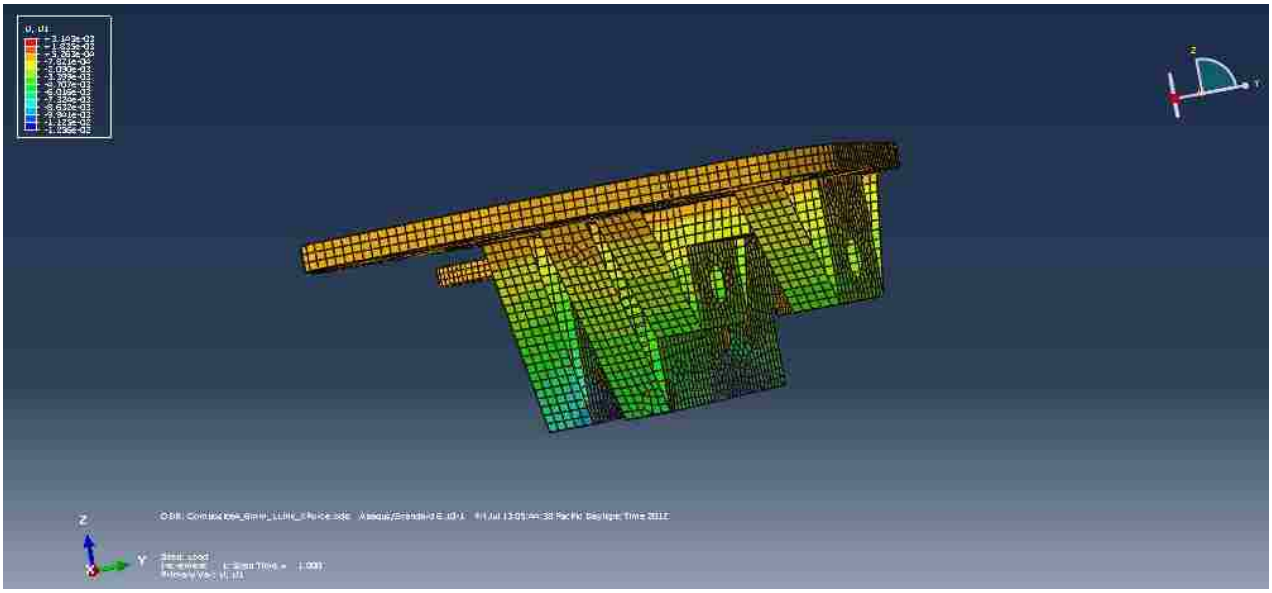

Figure 58: Composite Model C Lower Lateral Link - Displacements with force applied along x-direction

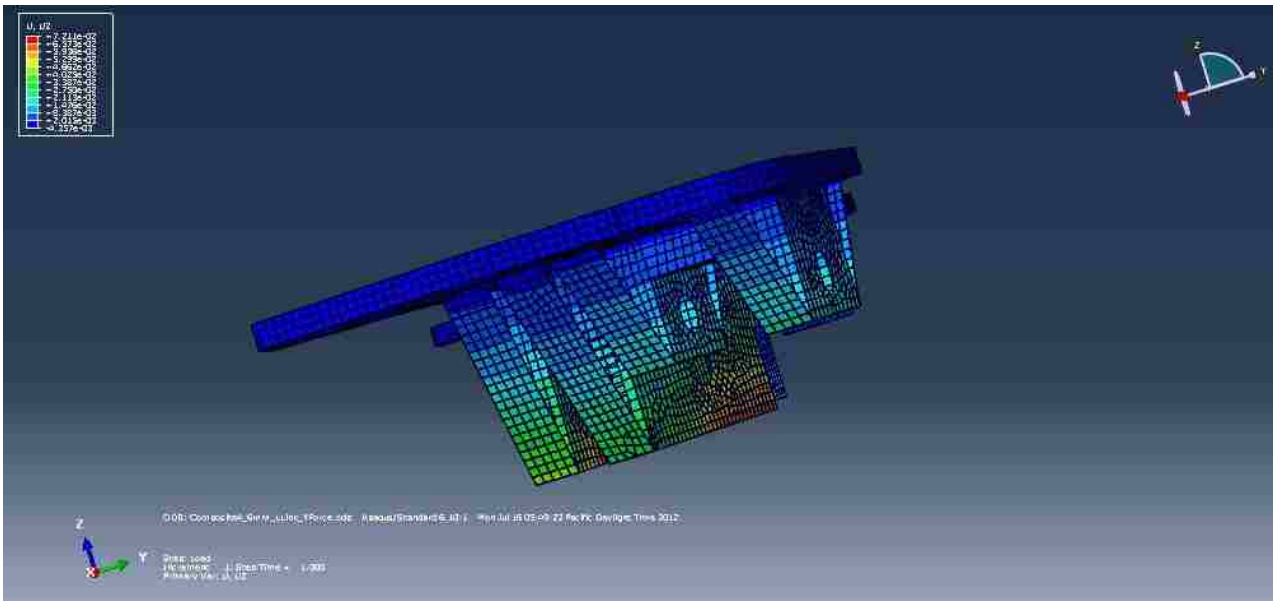

Figure 59: Composite Model C Lower Lateral Link - Displacements with force applied along y-direction

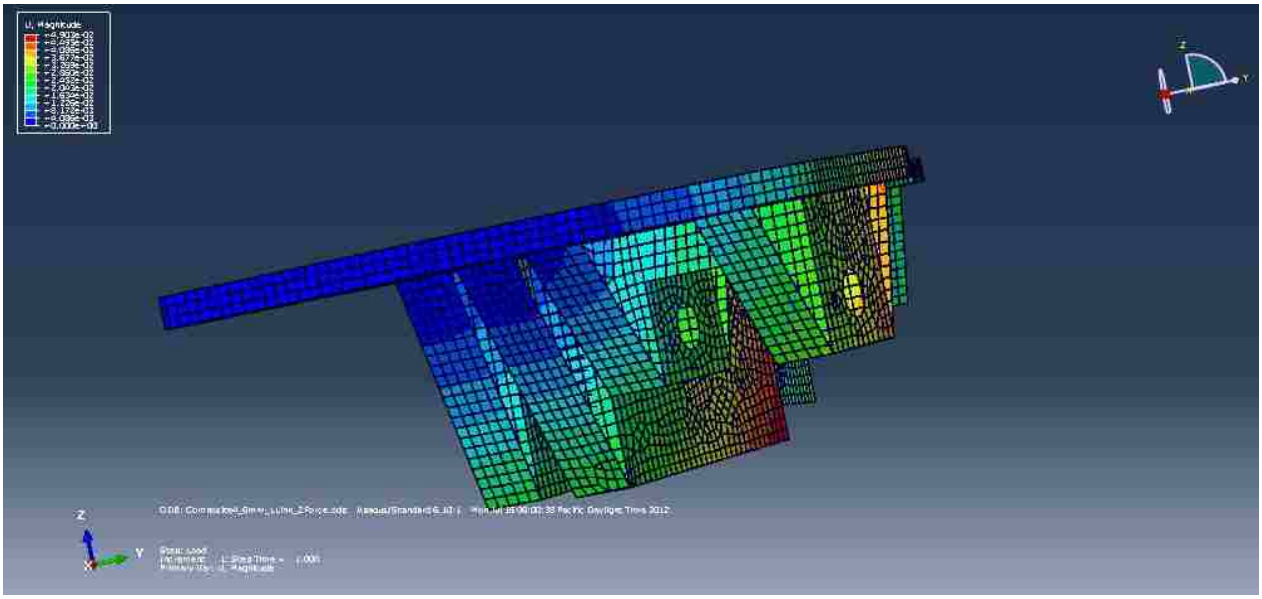

Figure 60: Composite Model C Lower Lateral Link - Displacements with force applied along z-direction

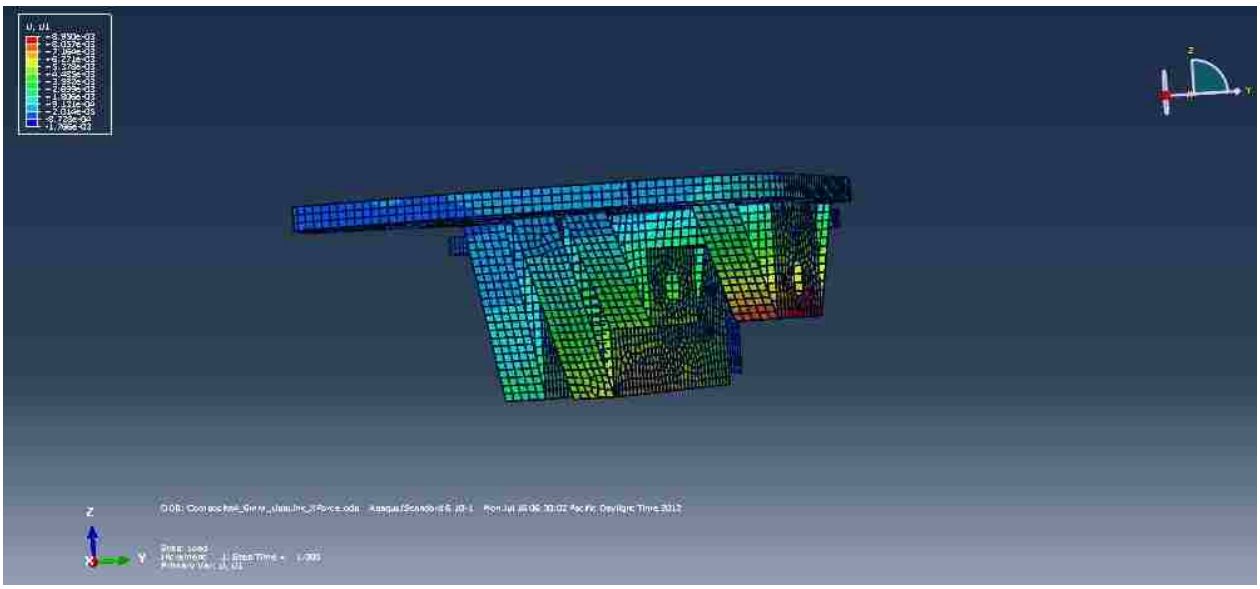

Figure 61: Composite Model C Upper Lateral Link - Displacements with force applied along x-direction

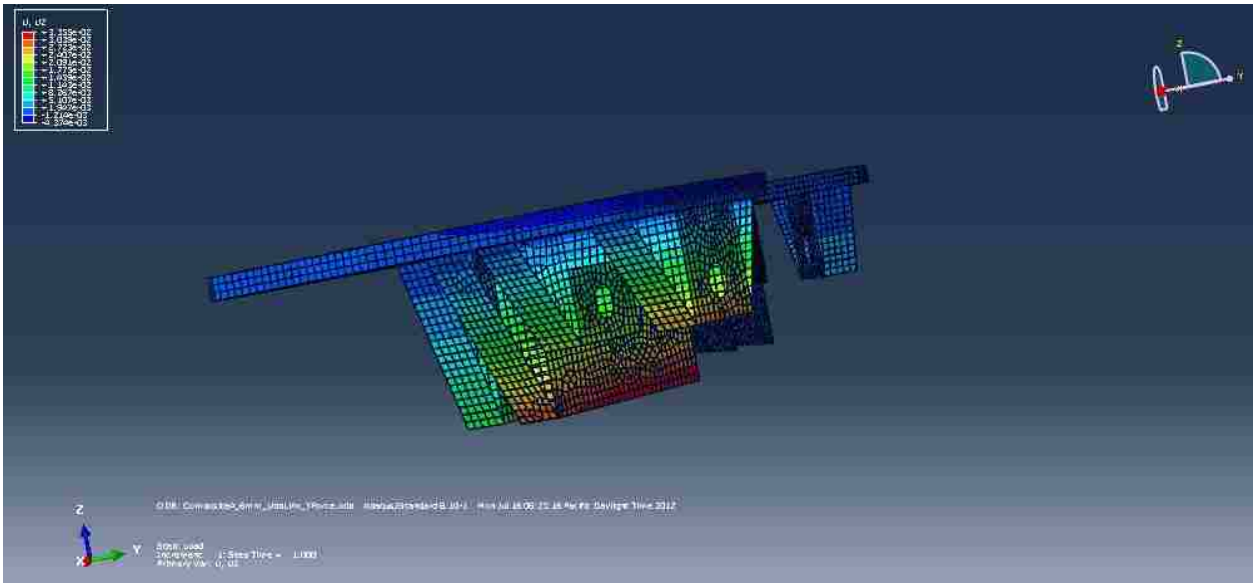

Figure 62: Composite Model C Upper Lateral Link - Displacements with force applied along y-direction

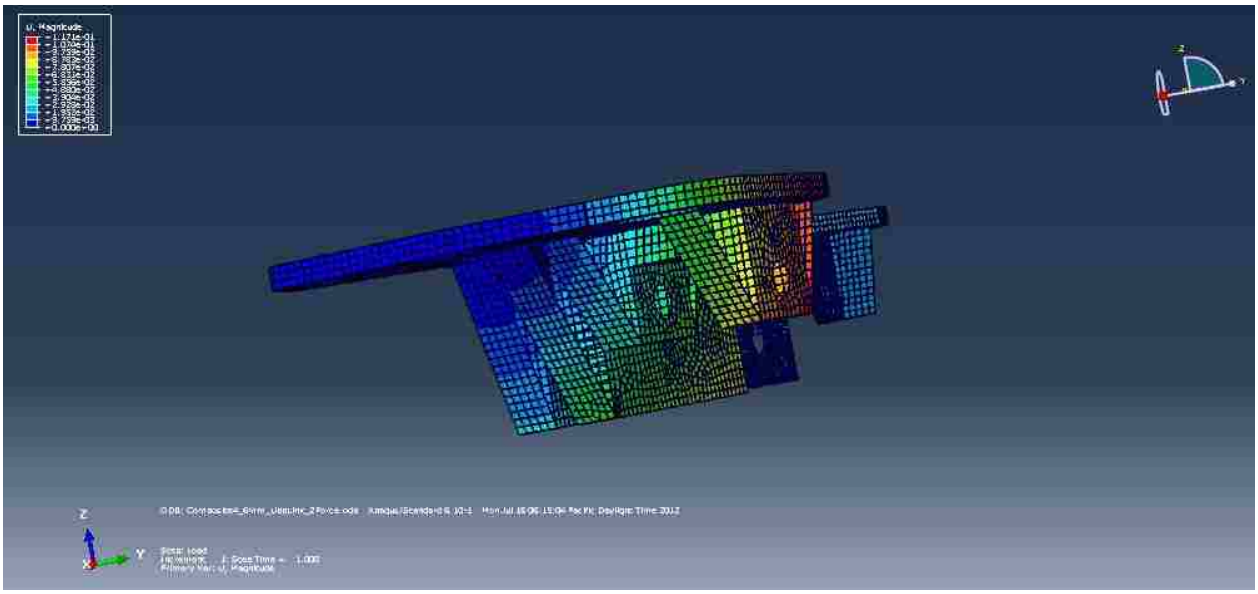

Figure 63: Composite Model C Upper Lateral Link - Displacements with force applied along z-direction

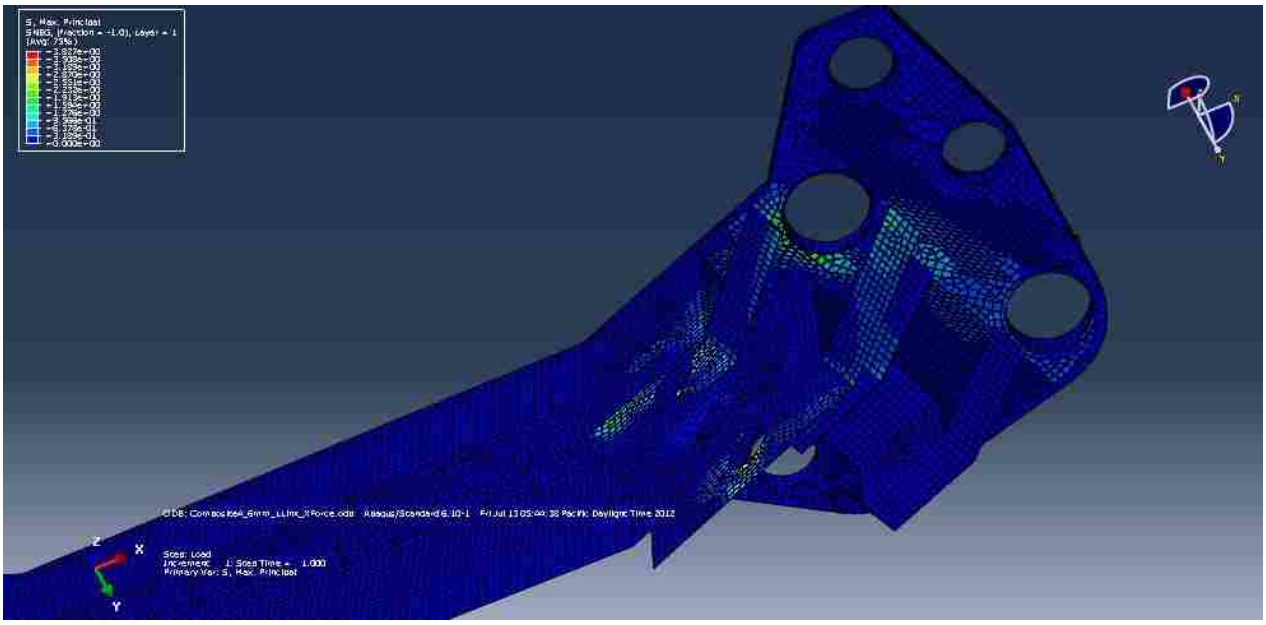

Figure 64: Composite Model C Lower Lateral Link - Stress distribution with force applied along x-direction

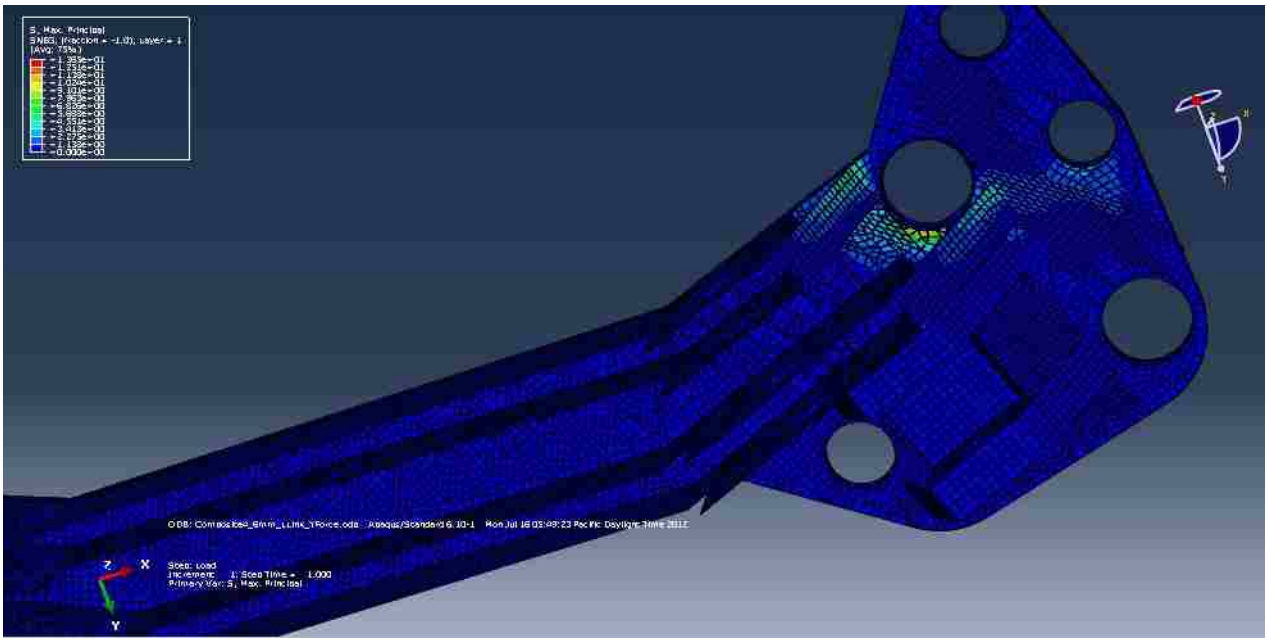

Figure 65: Composite Model C Lower Lateral Link - Stress distribution with force applied along y-direction

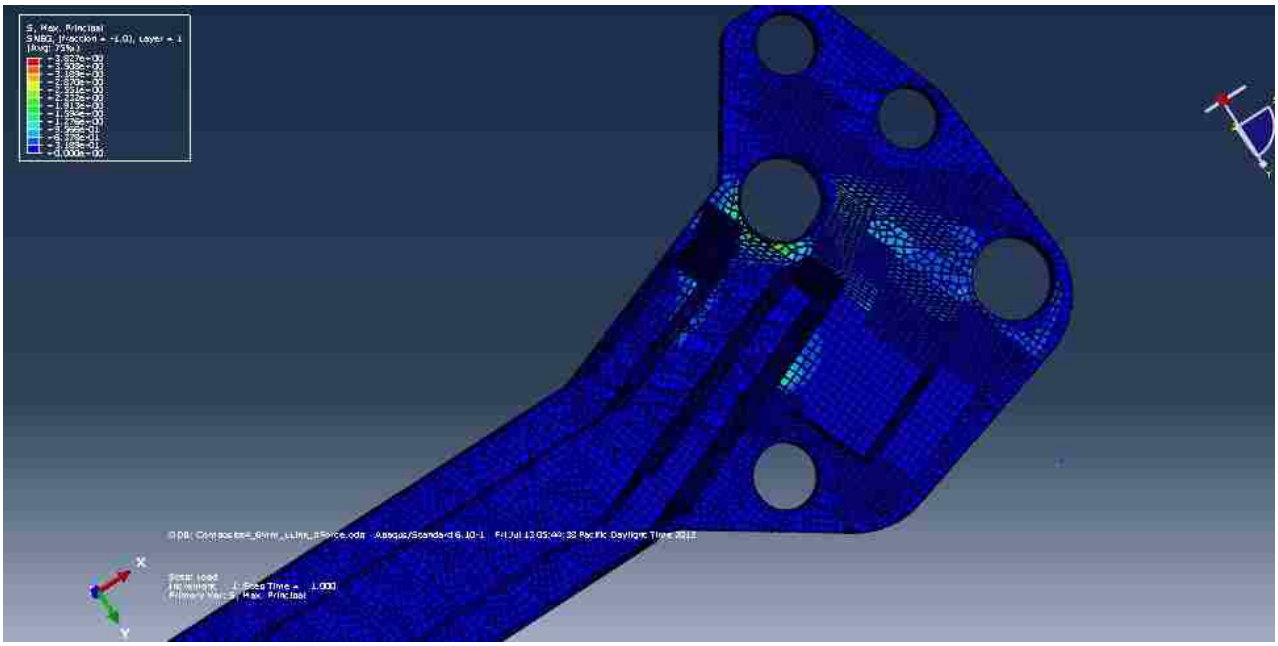

Figure 66: Composite Model C Lower Lateral Link - Stress distribution with force applied along z-direction

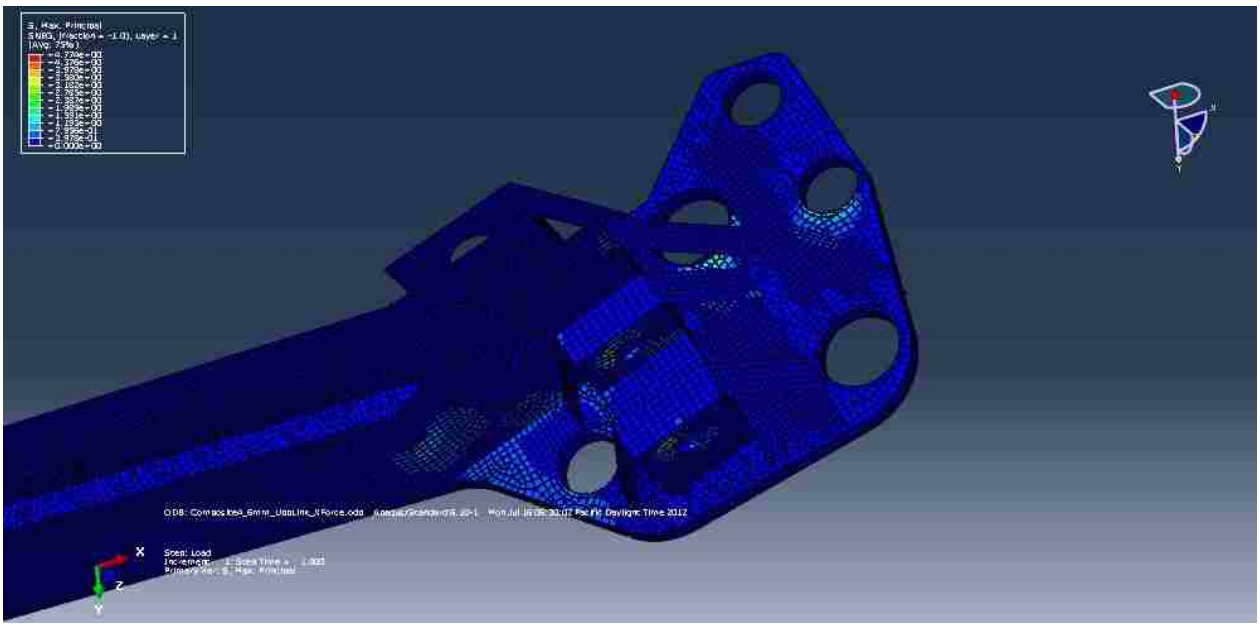

Figure 67: Composite Model C Upper Lateral Link - Stress distribution with force applied along x-direction

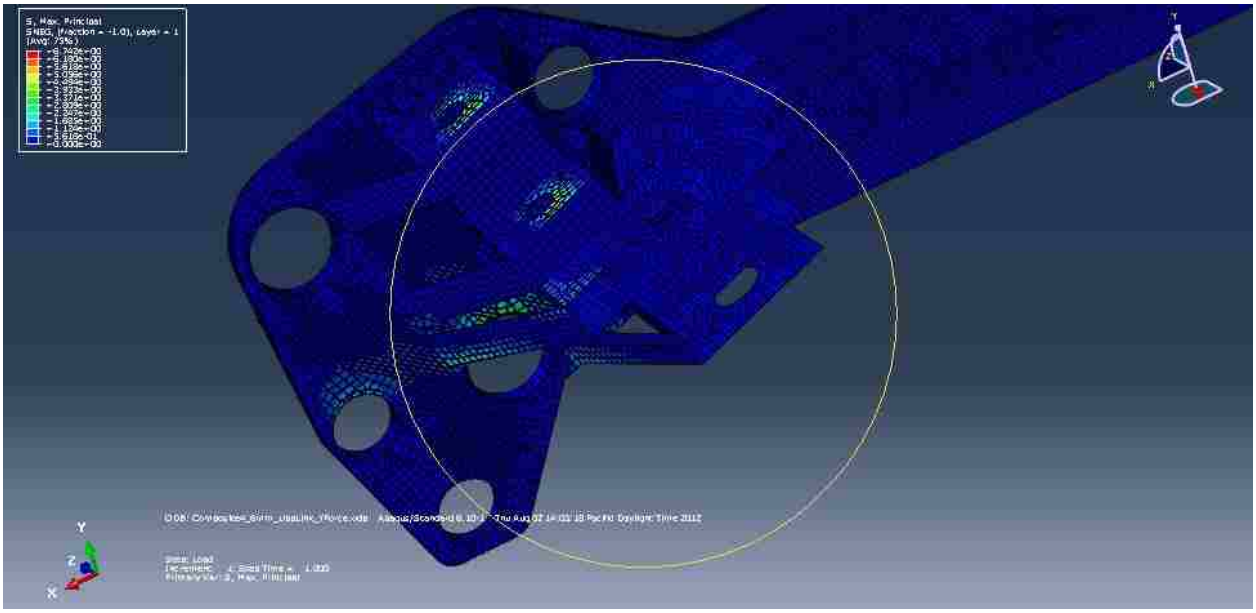

Figure 68: Composite Model C Upper Lateral Link - Stress distribution with force applied along y-direction

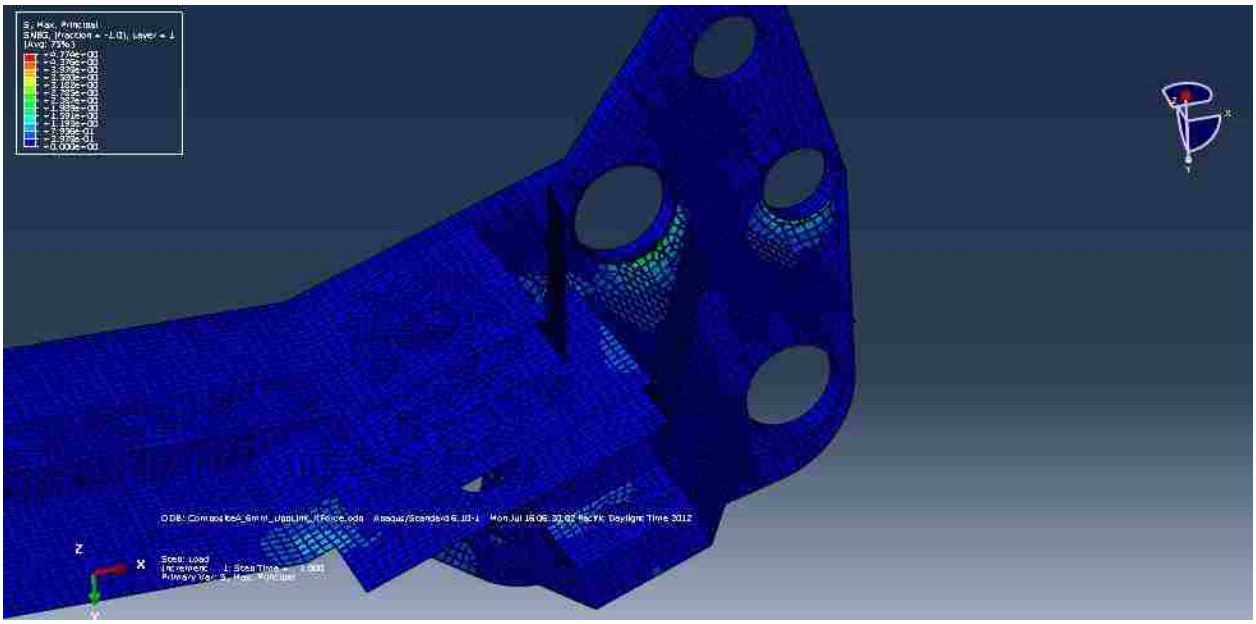

Figure 69: Composite Model C Upper Lateral Link - Stress distribution with force applied along z-direction

The solution with thickness equal to 5.2 mm has been chosen as the redesigned composite version for the analysis of displacements and stress distribution because it has comparable stiffness properties compared to the aluminum model previously analyzed and allows a weight saving of 0.307 kg as mentioned above.

Figures 58 to 63 show the displacements variation in the cradle: it can be noted that they present a pattern similar to the one that resulted from the analysis of the composite model, independently from the specific values: the regions subjected to higher displacements are the lower ones of the two lateral links (upper and lower).

Figure 58 shows higher displacements in the upper region of the cradle but only because they are positive: the highest displacements in the module are located in the lower link and they are negative so they are not shown as regions of maximum displacements (yellow to red colors). This situation does not happen for the other load cases where all the displacements have the same sign.

Figures 64 to 69 show the stress distribution along the cradle with different load

conditions: concentration of stresses is located again in correspondence of constrained points and where the loads are applied (lower and upper links). With respect to the aluminum model, this solution does not provide a gradual distribution of stresses: in the aluminum model the stress is distributed also to the regions close to the constrained points (Figures 47-52). In the composite model this distribution is not present and the stress is concentrated in the regions where the cradle is constrained, determining higher values of stresses (the peak reached in the composite model is 1.5 times the peak of the aluminum model). The values of stresses considered to evaluate the stress distribution are the maximum principal stresses, since the Von Mises stresses are not useful for analysis with composites.

The points where the stress concentration is higher are the points where delamination occurs in composites, so it is important to keep these values as low as possible.

Once the design for the model with conventional carbon fibers was determined, the same procedure described before was followed for the other materials: high modulus carbon fiber composite and glass fiber. In Tables 17 and 18 the results of the simulations are reported, without the images of the displacements and the stress distribution.

Direction	Lower lateral link [N/mm]	Upper lateral link [N/mm]
X	32456	16459
Y	2994	4538
Z	13567	2234
	Maximum displacement [mm]	**Maximum displacement [mm]**
X	9,23E-03	1,02E-02
Y	8,66E-02	4,54E-02
Z	6,88E-02	1,29E-01

Table 17: Stiffness values of glass fiber composite model. Fiber orientation 0/90°

The thickness of the layers has been kept constant so the weight of the component with glass fiber is equal to 5.03 kg (the density of the glass fiber composite is 1.9 g/cm^3).

It can be noted that the mechanical properties of this model are lower with respect to the

model with conventional carbon fiber composite and the same fiber orientation at 0°/90°; in order to achieve the same levels of stiffness the weight of the glass fiber composite has to be increased up to 5.9 kg, 43 % higher than the carbon fiber model.

Direction	Lower lateral link [N/mm]	Upper lateral link [N/mm]
X	52689	26897
Y	5873	9820
Z	29710	4986
	Maximum displacement [mm]	Maximum displacement [mm]
X	5,60E-03	8,15E-03
Y	5,93E-02	2,85E-02
Z	7,96E-03	7,64E-02

Table 18: Stiffness values of high modulus carbon fiber composite model. Fiber orientation 0/90°

In Table 18 the data relative for the model with high modulus carbon fiber composite material is reported, with the same weight of the model with conventional carbon fibers and fiber orientation equal to 0/90°: analyzing the values and comparing them to the model with a conventional carbon fiber composite, it can be noted that the latter are higher respect to the former with a ratio of about 1.21, that is the ratio between the Young moduli of the two materials, assuming the same epoxy matrix.

4.4 Torsional Stiffness

After having identified the most suitable design solution of a composite model for bending behavior, torsion behavior of this model was analyzed and compared to the aluminum model.

In order to simulate the behavior of the structure to torsion, it was decided to adopt the same approach used for the bending performance: unit loads were applied, but this time in the form of concentrated moments and not concentrated forces.

In Figure 70 it is shown how the moments were applied; it can be seen that the definition of the loads is very similar to the previous study case, with moments applied along the three different directions x, y and z. The grey arrows indicate the direction of the moment, according to the right hand rule.

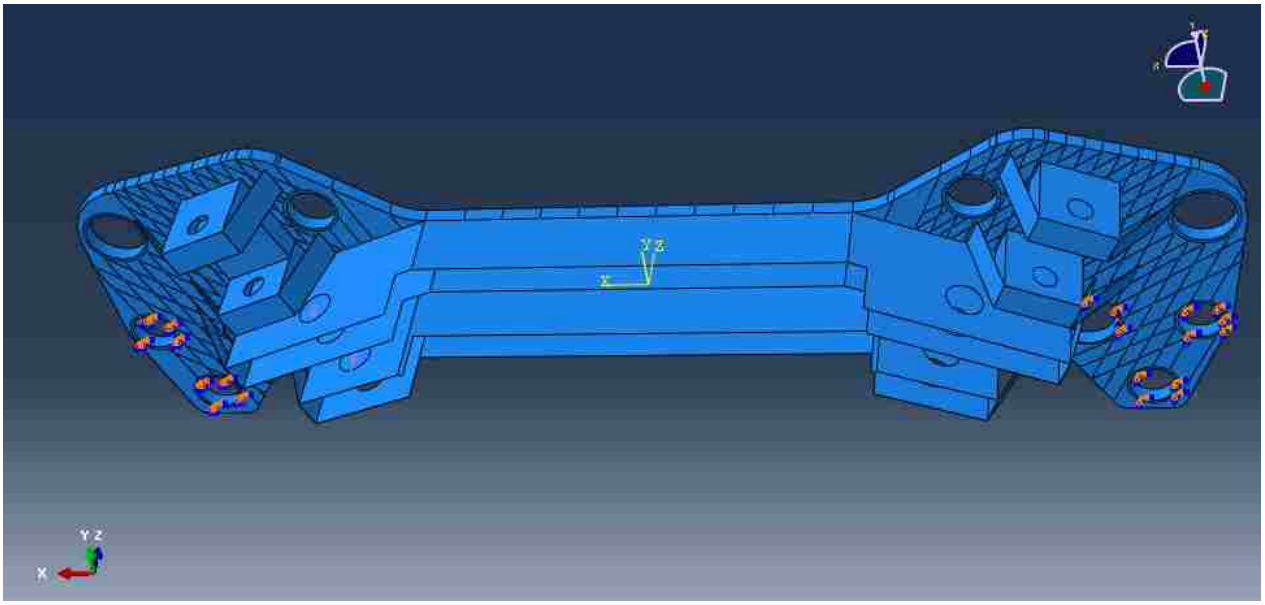

Figure 70: Location of applied loads- Moment acting on Lower Link along rz direction

In order to evaluate the torsional stiffness of the model and compare it to the data relative to the original model that have been given, the deflection of the points of the structure where the moments were applied were measured and then it was evaluated the correspondent angular displacement knowing the distance between the links.
For the aluminum model the following data were calculated through simulations:

Direction	Displacement Upper Link [mm]	Angle [rad]	Stiffness [Nmm/rad]
Rx	1,23E-03	2,05E-05	4,88E+06
Ry	1,96E-04	3,27E-06	3,06E+07
Rz	1,82E-04	3,03E-06	3,30E+07
	Displacement Lower Link [mm]	Angle [rad]	Stiffness [Nmm/rad]
Rx	1,42E-03	2,37E-05	4,23E+06
Ry	1,93E-04	3,22E-06	3,11E+07
Rz	2,17E-04	3,62E-06	2,76E+07

Table 19: Torsional stiffness of aluminum model

Analyzing the data of torsional stiffness of the simplified aluminum model reported in Table 19 it can be noted that they are one order of magnitude lower respect to the original model shown in Table 7, reflecting the same behavior of bending stiffness. This difference is mainly due to the simpler geometry and the lack of optimization that is beyond the scope of the current research. Moreover, the method used to evaluate the stiffness is not known and this is a further factor that does not allow a direct comparison between the two models (original and simplified).

Nevertheless, the values of torsional stiffness reflect the tendency of the original model, with higher values for ry and rz directions (one order of magnitude higher).

The composite models used to conduct the comparison are the conventional carbon fiber model with symmetric fiber orientation of -45°/45° that weighs 3.75 kg, whose bending characteristic has been described before, and the same model with glass fibers and with the same fiber orientation (weight of this last model equal to 5.9 kg).

Direction	Displacement Upper Link [mm]	Angle [rad]	Stiffness [Nmm/rad]
Rx	1,03E-03	1,71E-05	5,85E+06
Ry	1,85E-04	3,08E-06	3,24E+07
Rz	1,70E-04	2,83E-06	3,53E+07
	Displacement Lower Link [mm]	Angle [rad]	Stiffness [Nmm/rad]
Rx	1,30E-03	2,17E-05	4,62E+06
Ry	1,60E-04	2,67E-06	3,75E+07
Rz	1,95E-04	3,25E-06	3,08E+07

Table 20: Torsional stiffness of composite model with conventional carbon fiber

Direction	Displacement Upper Link [mm]	Angle [rad]	Stiffness [Nmm/rad]
Rx	1,34E-03	2,23E-05	4,48E+06
Ry	2,10E-04	3,50E-06	2,86E+07
Rz	1,96E-04	3,27E-06	3,06E+07
	Displacement Lower Link [mm]	Angle [rad]	Stiffness [Nmm/rad]
Rx	1,70E-03	2,83E-05	3,53E+06
Ry	2,60E-04	4,33E-06	2,31E+07
Rz	2,50E-04	4,17E-06	2,40E+07

Table 21: Torsional stiffness of composite model with glass fiber

Tables 20 and 21 show that the composite model with conventional carbon fiber presents higher values of torsional stiffness with respect to the model with glass fiber and with the same fiber orientation (-45°/45° symmetric), even if the model with glass fibers is much heavier than the carbon fiber one (5.9 kg versus 3.75, respectively).

Combining these data to the ones relative to bending stiffness shown in Table 16 it is possible to define the mechanical behavior of the model shown in Figure 57 made with conventional carbon fiber and epoxy matrix (data relative to the material available at table 8) with fiber orientation of -45° and 45° (symmetric layers) that weighs 3.75 kg.

From figure 71 to 76 the displacements in the composite model with conventional carbon

fiber in the presence of torsion are shown. Stress distribution data show very low values of stress concentrations in the component compared to the bending loads (one fourth), so their pattern has not been provided and analysis can be based on the previous data.

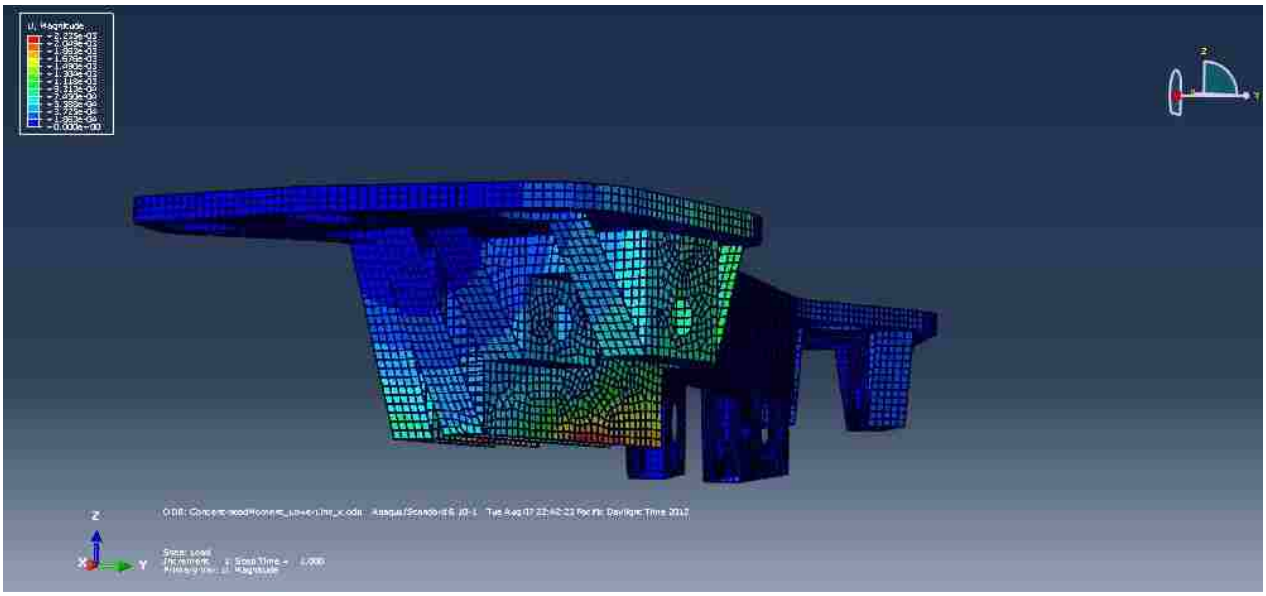

Figure 71: Composite Model C Lower Lateral Link - Displacements with moment applied along the rx direction

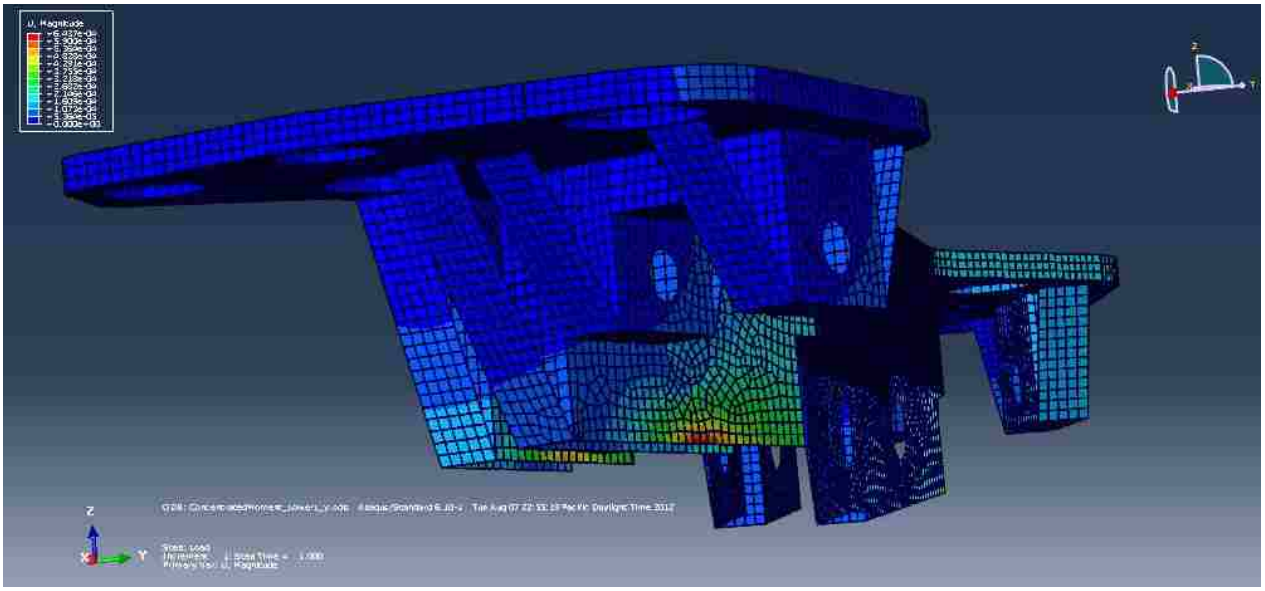

Figure 72: Composite Model C Lower Lateral Link - Displacements with moment applied along the ry direction

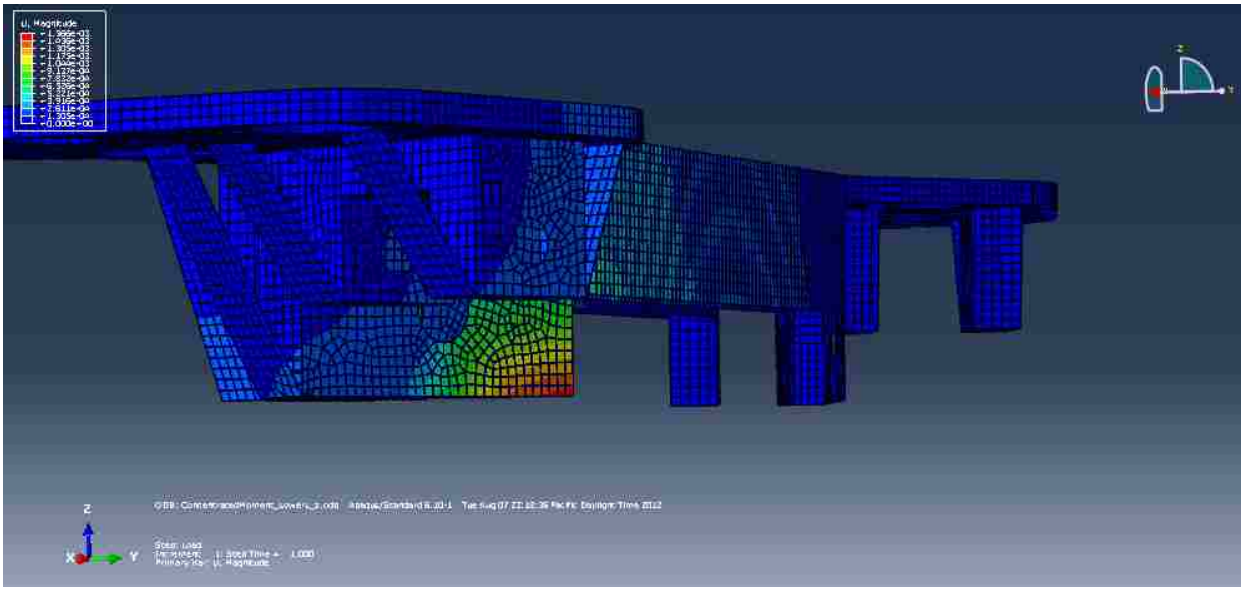

Figure 73: Composite Model C Lower Lateral Link - Displacements with moment applied along the rz direction

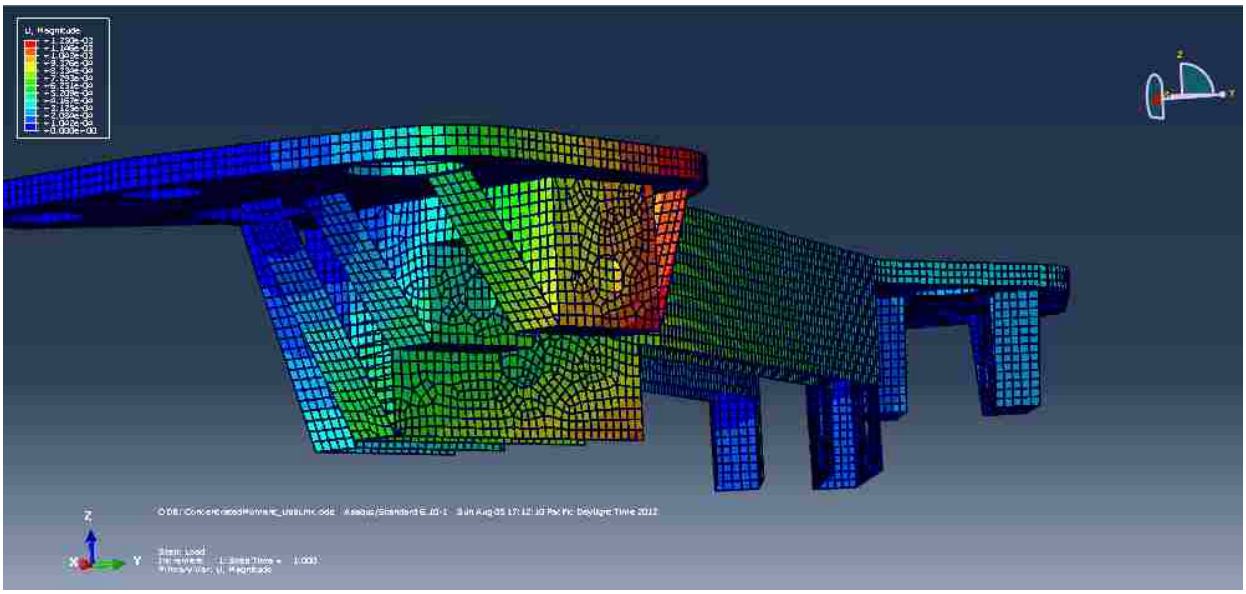

Figure 74: Composite Model C Upper Lateral Link - Displacements with moment applied along the rx direction

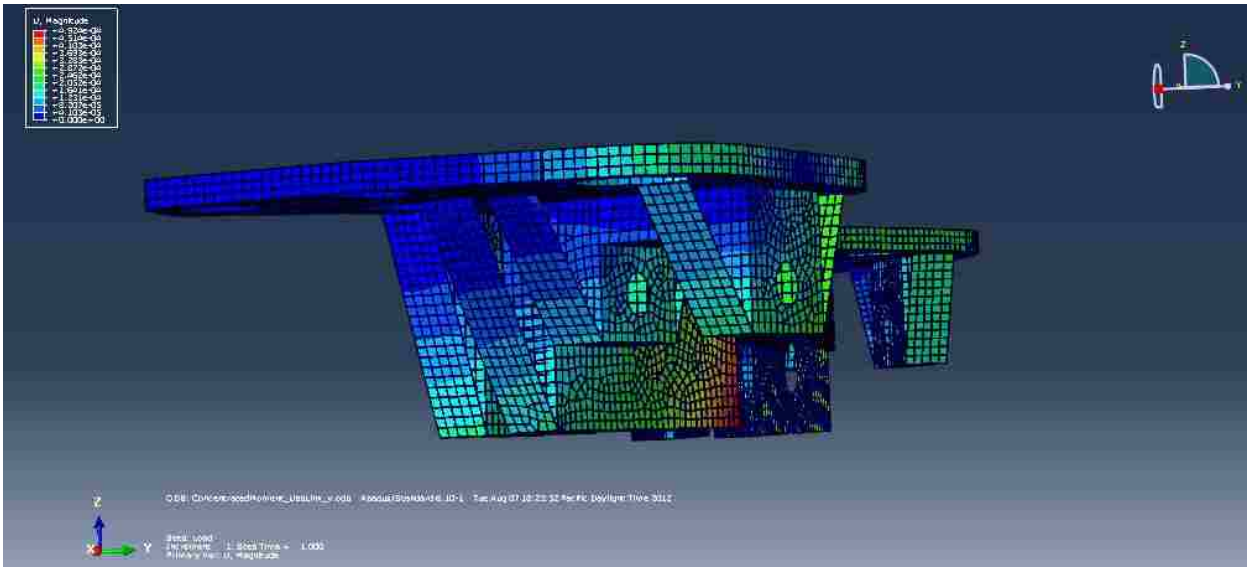

Figure 75: Composite Model C Upper Lateral Link - Displacements with moment applied along the ry direction

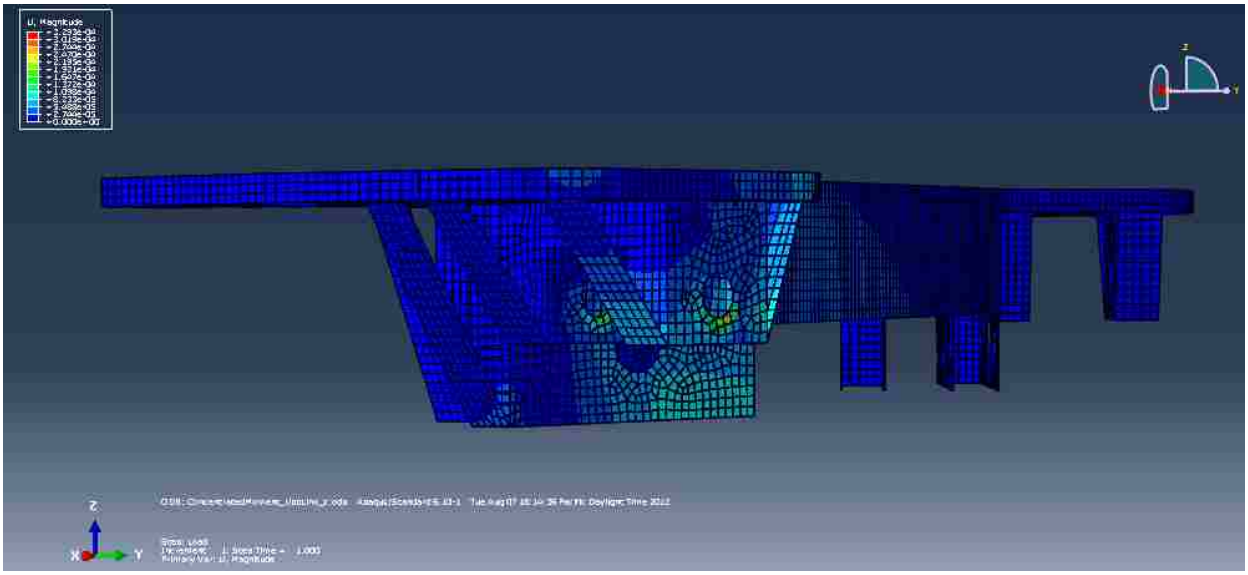

Figure 76: Composite Model C Upper Lateral Link - Displacements with moment applied along the rz direction

4.5 Summary of the Results

The following tables summarize the results obtained in each iteration illustrated in the previous chapters; the values of the stiffness and maximum displacements of each model are reported. The column "Percentage" indicates the relative value of each parameter (stiffness and displacements) in reference to the data of the aluminum model (Tables 8 and 19). For example, a percentage of 50% means that the value is half with respect to the same value of the aluminum model.

Direction	Lower lateral link [N/mm]	Percentage	Upper lateral link [N/mm]	Percentage
X	9020	21.2 %	9764	35.6 %
Y	1840	32.2 %	1976	38.9 %
Z	3540	21.4%	952	30.9%
	Maximumdisplacement[mm]	**Percentage**	**Maximumdisplacement[mm]**	**Percentage**
X	2,68E-02	342%	2,12E-02	235%
Y	1,31E-01	262%	9,98E-02	232%
Z	8,62E-02	474%	2,70E-01	365%

Table 22: Composite model A. Conventional carbon fiber. Fiber orientation -45°/45°. Weight 2.16 kg

Direction	Lower lateral link [N/mm]	Percentage	Upper lateral link [N/mm]	Percentage
X	11236	26.4 %	11764	42.9 %
Y	1538	26.9 %	1942	38.3 %
Z	3313	21.4%	1145	37.3%
	Maximumdisplacement[mm]	**Percentage**	**Maximumdisplacement[mm]**	**Percentage**
X	3,05E-02	389%	3,19E-02	354%
Y	1,83E-01	367%	7,80E-02	181%
Z	3,10E-02	170%	2,44E-01	330%

Table 23: Composite model B. Conventional carbon fiber. Fiber orientation -45°/45°. Weight 2.31 kg

Direction	Lower lateral link [N/mm]	Percentage	Upper lateral link [N/mm]	Percentage
X	15357	36.1 %	16745	61.1 %
Y	2314	40.4 %	2857	56.2 %
Z	4520	27.3%	1456	47.3%
	Maximumdisplacement[mm]	Percentage	Maximumdisplacement[mm]	Percentage
X	2,81E-02	359%	2,77E-02	307%
Y	1,49E-01	300%	8,04E-02	187%
Z	1,98E-02	109%	1,80E-01	244%

Table 24: Composite model C. Conventional carbon fiber. Fiber orientation -45°/45°. Weight 2.74 kg

Direction	Lower lateral link [N/mm]	Percentage	Upper lateral link [N/mm]	Percentage
X	48763	114.6%	29400	107.3%
Y	5756	100.3%	7407	145.9 %
Z	18567	112.3%	3420	111.1%
	Maximumdisplacement[mm]	Percentage	Maximumdisplacement[mm]	Percentage
X	6,80E-03	86,9%	9,75E-03	108.2%
Y	7,23E-02	145,3%	3,44E-02	80.0%
Z	9,56E-03	52,7%	9,45E-02	128.0%

Table 25: Composite model C. Conventional carbon fiber. Fiber orientation -45°/45°. Weight 4.11 kg

Direction	Lower lateral link [N/mm]	Percentage	Upper lateral link [N/mm]	Percentage
X	43562	102.3%	22369	81.7%
Y	4897	85.7%	8130	160.1 %
Z	24589	148.8%	4200	136.5%
	Maximumdisplacement[mm]	Percentage	Maximumdisplacement[mm]	Percentage
X	6,80E-03	86,9%	9,75E-03	108.2%
Y	7,23E-02	145,3%	3,45E-02	80.0%
Z	9,56E-03	52,7%	9,45E-02	128.0%

Table 26: Composite model C. Conventional carbon fiber. Fiber orientation 0°/90°. Weight 4.11 kg

Direction	Lower lateral link [N/mm]	Percentage	Upper lateral link [N/mm]	Percentage
X	44879	105.5%	27612	100.8%
Y	5021	87.9%	6146	121.1 %
Z	16754	101.4%	3032	98.5%
	Maximumdisplacement[mm]	Percentage	Maximumdisplacement[mm]	Percentage
X	7,20E-03	92.0%	9,20E-03	102.1%
Y	6,70E-02	134.6%	4,25E-02	98.9%
Z	3,12E-02	171.9%	9,60E-02	130.1%

Table 27: Composite model C. Conventional carbon fiber. Fiber orientation -45°/45°. Weight 3.75 kg

Direction	Lower lateral link [N/mm]	Percentage	Upper lateral link [N/mm]	Percentage
X	32456	76.3%	16459	60.1%
Y	2994	52.4%	4538	90.1%
Z	13567	82.1%	2234	72.6%
	Maximumdisplacement[mm]	Percentage	Maximumdisplacement[mm]	Percentage
X	9,23E-03	117.9%	1,02E-02	113.2%
Y	8,66E-02	174.0%	4,54E-02	105.6%
Z	6,88E-02	379.0%	1,29E-01	174.8%

Table 28: Composite model C. Glass fiber. Fiber orientation -45°/45°. Weight 5.03 kg

Direction	Lower lateral link [N/mm]	Percentage	Upper lateral link [N/mm]	Percentage
X	52689	123.8%	26897	98.2%
Y	5873	102.8%	9820	193.4%
Z	29710	179.7%	4986	162.0%
	Maximumdisplacement[mm]	Percentage	Maximumdisplacement[mm]	Percentage
X	5,60E-03	71.5%	8,15E-03	90.4%
Y	5,93E-02	119.2%	2,85E-02	66.3%
Z	7,96E-03	43.9%	7,64E-02	103.5%

Table 29: Composite model C. High modulus carbon fiber. Fiber orientation -45°/45°. Weight 4.11 kg

Direction	Stiffness Upper Link [Nmm/rad]	Percentage
Rx	5,85E+06	120%
Ry	3,24E+07	106%
Rz	3,53E+07	107%
	Stiffness Lower Link [Nmm/rad]	Percentage
Rx	4,62E+06	109%
Ry	3,75E+07	121%
Rz	3,08E+07	111%

Table 30: Torsion: composite model C. Conventional carbon fiber. Fiber orientation -45°/45°. Weight 3.75 kg

Direction	Stiffness Upper Link [Nmm/rad]	Percentage
Rx	4,48E+06	92%
Ry	2,86E+07	93%
Rz	3,06E+07	93%
	Stiffness Lower Link [Nmm/rad]	Percentage
Rx	3,53E+06	84%
Ry	2,31E+07	74%
Rz	2,40E+07	87%

Table 31: Torsion: composite model C. Glass fiber. Fiber orientation -45°/45°. Weight 5.03 kg

Starting from the simple geometry of design solution A and improving the model through the addition of ribs and increasing values of thicknesses, the model with conventional carbon fiber and design solution C has been developed, allowing a weight saving of 0.307 kg (7.45 %) and better performance respect to the aluminum model, in terms of both bending and torsional stiffness.

With reference to the displacements field, comparing the displacements of the aluminum model (Figures from 41 to 46) and the composite model with conventional carbon fibers (Figures from 58 to 63) the results show that they have the same pattern, with the similar location of regions subjected to higher displacements.

CHAPTER V

CONCLUSIONS AND RECOMMENDATIONS

5.1 Conclusions

In the previous chapters, the feasibility of the conversion of a structural component of the vehicle (rear suspension cradle) from aluminum to composite was presented.

Different design solutions with composite materials have been compared with an aluminum reference model in terms of bending and torsion stiffness. The results of the simulations summarized in Section 4.5 proved that the design solution C with conventional carbon fibers and an epoxy matrix resulted in a part with comparable mechanical performance with respect to the reference model allowing a 7.45 % weight savings (0.307 kg).

With reference to the results of the simulations and the considerations explained during the analysis of models in the previous chapters, the following conclusions can be stated:

1. The model with conventional carbon fibers and epoxy matrix results in a design comparable to the aluminum model in terms of bending and torsional stiffness (Tables 27 and 30) but stress distribution (Figures from 64 to 69) show that it has concentrated stresses that are 1.5 times higher than the peak stresses of the aluminum model. This leads to the possibility of delamination in these points so constrained points have to be properly designed or other design improvements should be studied to lower these values at these locations.
2. The model with glass fibers and epoxy matrix is shown to be unsuitable for this application due to the low mechanical properties (Tables 28 and 31) and the increased weight (5.03 kg).
3. The best mechanical performance has been obtained by the model with high modulus carbon fibers and epoxy matrix (Table 29) that has the same density of composite made with conventional carbon fiber (Table 8). Nevertheless, its application is limited

by the cost of the fibers, the preference is to choose the solution with conventional carbon fiber taking into account the high volume production required.

4. Comparing the displacements of the aluminum model (Figures from 41 to 46) and the composite model with conventional carbon fibers (Figures from 58 to 63) the results show that they have the same pattern, with the similar location of regions subjected to higher displacements.

Figures 77 to 80 provide a summary of the simulation results for lower and upper lateral links, with stiffness values along different directions are shown. With reference to the following Figures, the abbreviation CCF stand for conventional carbon fiber, HMCF stands for high modulus carbon fiber while GF means glass fiber. The epoxy matrix is common for all the fibers.

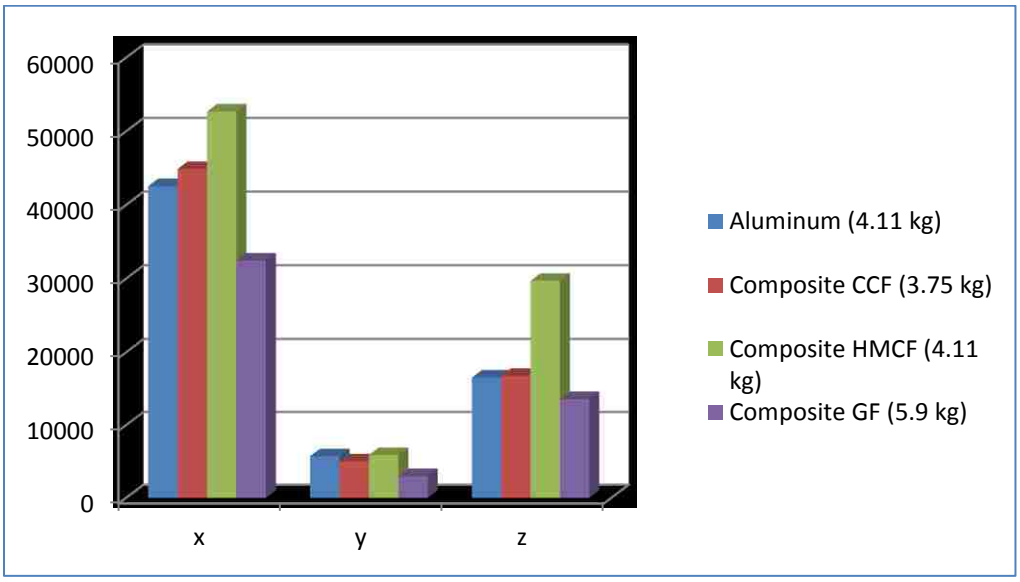

Figure 77: Summary of results: Bending stiffness of Lower Lateral Link [N/mm]

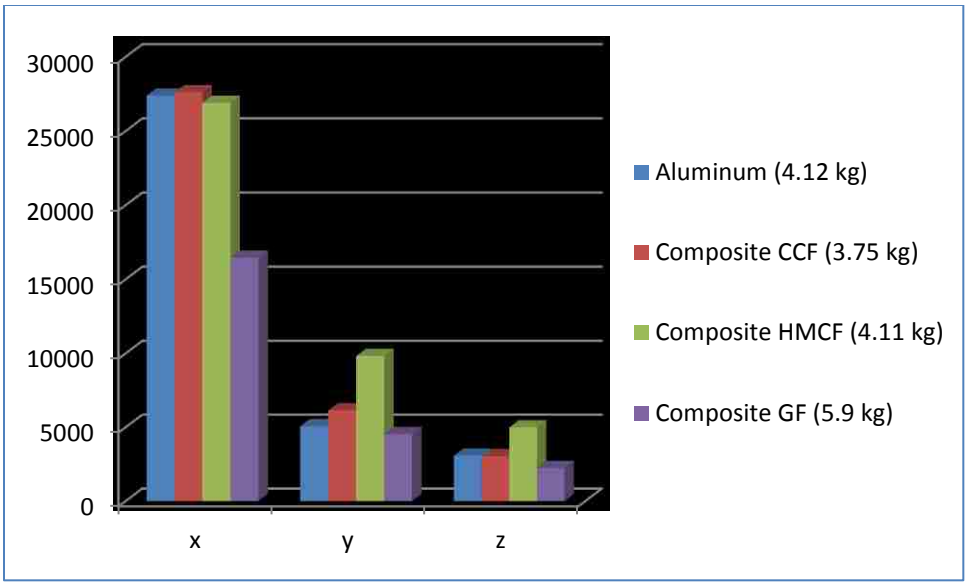

Figure 78: Summary of results: Bending stiffness of Upper Lateral Link [N/mm]

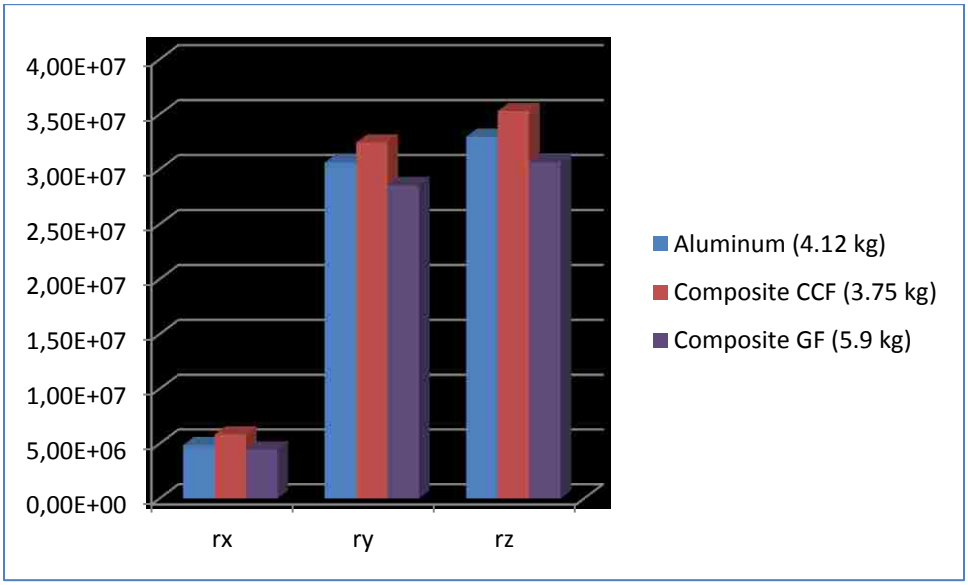

Figure 79: Summary of results: Torsional stiffness of Lower Lateral Link [Nmm/rad]

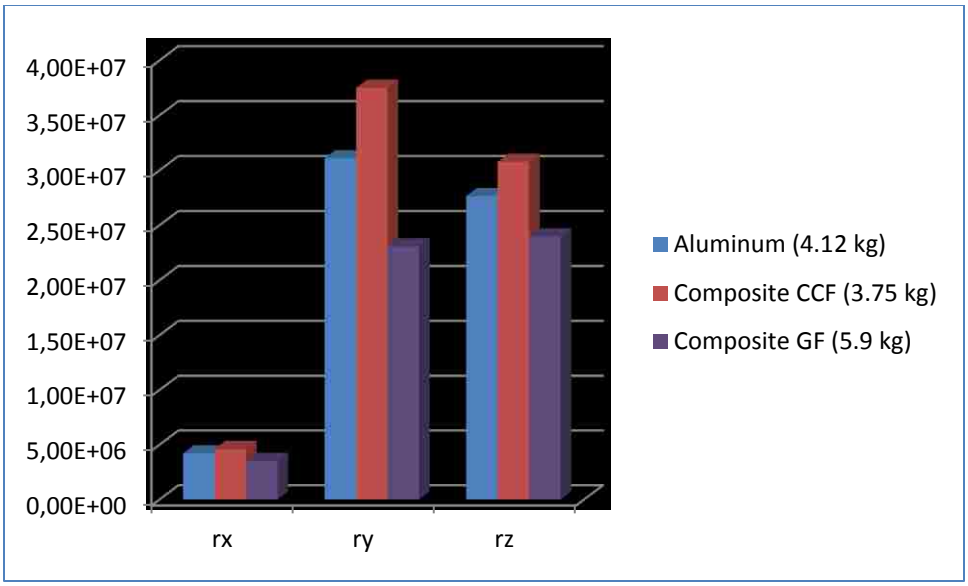

Figure 80: Summary of results: Torsional stiffness of Upper Lateral Link [Nmm/rad]

During the design phase manufacturing processes suitable for high volume production have been taken into account: in particular, for the production of the composite model C with conventional carbon fiber two processes are necessary. They have been identified as the compression molding of the cradle with its geometry and then injection molding of the ribs present on the top surface.

Referring to the model of the component shown in Figure 57, the addition of stiffener ribs on the top surface through injection molding does not allow the use of the same standard carbon fiber fabrics (Table 9) utilized for the rest of the cradle, but chopped carbon fibers with reduced mechanical properties is necessary. This aspect has been taken into account defining a different section for the ribs, as explained in the chapters before.

The cost and the times for the production of the component have not been investigated, but at the present state of art compression molding and injection molding are the most suitable for high volume productions.

Regarding the recyclability of the component, since a carbon fiber reinforced epoxy has been chosen pyrolysis represents the most effective solution for this kind of component. The description of the processes has been provided in the section 2.6. With reference to the Table 1, pyrolysis allows high retention of mechanical properties and there is the

opportunity to recover mechanical feedstock from the resin. Moreover, no chemical solvents are used. Pyrolysis has been experimented to be conducted in commercial-scale plant with high quantities of material recycled (up to 2000 t/year).

Other processes could be used, especially chemical recovery of the fibers but they are applied in pilot scale or laboratory plants, so they are not useful for high volumes of material recycling.

Future developments of the study could be conducted both in the design analysis of the component and in the characterization of the most suitable manufacturing process; in particular the following steps can be followed to improve the present model:

- Knowing the load conditions applied for the model of the actual component, reproduce the same conditions on the composite model and improve the design with the adoption of other stiffener members (corrugated, ribs with different disposition) in order to obtain comparable performance.

- Once the requirements for the component are known, conduct stress analysis on the component and verify if the model can operate without the onset of delamination. This kind of analysis has not been conducted since the loads have been applied to calculate the stiffness of the component and they do not represent the actual in-service load profile of the cradle.

- Having access to detailed information regarding costs of material and equipment, provide a cost analysis of the manufacturing processes mentioned previously and compare it to the cost of production of the current component.

- Knowing specific data of recycling processes provide a costs estimate to recycle the component using pyrolysis process and verify if it is suitable for a high volume production.

REFERENCES

1. Sehanobish, K. (2009). A vision for carbon fiber in the automotive market. Retrieved from http://www.compositesworld.com/columns/a-vision-for-carbon-fiber-in-the-automotive-market
2. Cole, G.S., Sherman A.M. (1995). Lightweight materials for automotive applications. *Materials Characterization, 3, 3-9.* doi:10.1016/1044-5803(95)00063-1
3. Stewart, R. (2003). New developments help composites compete. *Reinforced Plastics*, 47 (2), 27-31. Retrieved from www.reinforcedplastics.com,
4. Stewart, R. (2009). Lightweighting the automotive market. *Reinforced Plastics*, 53 (2), 14-16, 18-19, 21. doi: 10.1016/S0034-3617(09)70078-5
5. Stewart, R. (2010). Automotive composites offer lighter solutions. Retrieved from www.reinforcedplastics.com
6. Stewart, R. (2011). Thermoplastic composites- recyclable and fast to process. Retrieved from www.reinforcedplastics.com,
7. Kim, H., Keoleian, G., Skerlos, S. (2010) Economic assessment of Greenhouse gas emissions reduction by vehicle lightweighting using aluminum and high-strength steel. *Journal of Industrial Ecology*, 15 (1), 64-80, doi: 10.1111/j.1530-9290.2010.00288.x
8. Cheah, L., Heywood, J., Kirchain, R., (2009). The energy impact of U.S. passenger vehicle Fuel Economy Standards. Retrieved from http://web.mit.edu/sloan-auto-lab/research/beforeh2/files/IEEE-ISSST-cheah.pdf
9. Sloan, J. (2012). Automotive evolution or real revolution? Retrieved from http://www.compositesworld.com/columns/automotive-evolution-or-real-revolution
10. Brosius, D., (2004). Corvette gets leaner with carbon fiber hood. Retrieved from http://www.compositesworld.com/articles/corvette-gets-leaner-with-carbon-fiber-hood

11. Black, S. (2006). Innovative composite design may replace aluminum chassis. Retrieved from http://www.compositesworld.com/articles/innovative-composite-design-may-replace-aluminum-chassis
12. Beardmore, P., Johnson, C. F., (2003). The potential for composites in structural automotive applications. *Composites Science and Technology*, 26 (4), 251-281, doi: 10.1016/0266-3538(86)90002-3
13. Della Volpe, D. (2008). Modellazione del trasporto di acqua in strutture composite sandwich per applicazioni aeronautiche. Retrieved from http://www.fedoa.unina.it/3851/
14. Garcia, E., Wardle, B., Hart, A. (2008). Joining prepreg composite interfaces with aligned carbon nanotubes. *Composites Part A: Applied Science and Manufacturing*, 39 (6), 1065-1070, doi: 10.1016/j.compositesa.2008.03.011
15. Zucchelli, A., Focarete, M. L., Gualandi, C., Ramakrishna, S., (2010). Electrospun nanofibers for enhancing structural performance of composite materials. *Polymers Advanced Technologies.* doi: 10.1002/pat.183
16. Yamamoto, N., Hart, A., Garcia, E., Wicks, S., Duong, H. M., Slocum, A., Wardle, B., (2008). High-yield growth and morphology control of aligned carbon nanotubes on ceramic fibers for multifunctional enhancement of structural composites. *Carbon.* 47 (3), 551-560. doi: 10.1016/j.carbon.2008.10.030
17. Hayashi, T., Endo, M., (2011). Carbon nanotubes as structural material and their application in composites. *Composites Part B. Engineering.* 42 (8), 2151-2157. doi: 10.1016/j.compositesb.2011.05.011
18. Department of Defense of US. (1997). Composite materials handbook.
19. A. Alloatti, G.Alvino, "Progetto di un Sedile in Materiale Composito per Vettura di Formula SAE", 2010
20. Compere, A. L., Griffith, W. L., Leitten Jr., C. F., Shaffer, J. T., "Low cost carbon fiber from renewable resources. Oak Ridge National Laboratory. Retrieved from http://www.ornl.gov/~webworks/cppr/y2001/pres/111380.pdf
21. Baker, F. S., (2010). Low cost carbon fiber from renewable resources. WashingtonDC.

Retrievedfromhttp://www1.eere.energy.gov/vehiclesandfuels/pdfs/merit_review_2010/lightweight_materials/lm005_baker_2010_o.pdf

22. Lasell, D., DeBoer, B., Dimensional capability of carbon fiber reinforced epoxy exterior automotive products. *Vermont Composites Inc.* Retrieved from http://www.speautomotive.com/SPEA_CD/SPEA2005/pdf/g/g3.pdf
23. Lasell, D. M. High volume production of carbon fiber reinforced epoxy. retrieved from http://www.speautomotive.com/SPEA_CD/SPEA2010/pdf/ET/ET7.pdf
24. Lasell, D. M. A unique approach to the high volume production of carbon fiber reinforced epoxy structural components. *Think Composites L.L.C.* Retrieved from http://www.thinkcompositesllc.com/HIGH_VOLUME_PRODUCTION_OF_CARBON_FIBER_REINFORCED_EPOXY_STRUCTURAL_COMPONENTS.pdf
25. Arnold, F., Thoman, S., (1996). B-Staging of toughned epoxy composites. Retrieved from http://www.thinkcompositesllc.com
26. www.machinedesign.com . Date of access February 2012
27. www.sinotech.com . Date of access February 2012
28. Todd, R. H., Allen, D. K., Alting, L. (1994). Manufacturing processes reference guide. Industrial Press Inc.
29. Peterson, C. W., Ehnert, G., Liebold, K., Horsting, K., Kuhfusz, R., (2001). Compression molding ASM handbook. Menzolit-Fibron GmbH, Germany
30. www.alexpb.com, Date of Access February 2012
31. www.substech.com Date of Access February 2012
32. Bryce, D. M., (1996). Plastic injection molding: manufacturing process fundamentals. SME
33. www.rtmcomposites.com, Date of Access February 2012
34. Caspe, R. J., Coenen, V. L., Nesbitt, A., Day, R.J., Wilkinson, A. N., (2008). Through-Thickness Melding of Advanced CFRP for aerospace applications. University of Manchester. Retrieved from http://www.iccm-central.org/Proceedings/ICCM17proceedings/Themes/Behaviour/JOINING%20OF%20ADV%20COMP/F16.16%20Caspe.pdf

35. Corbett, T., Forrest, M., Law, H., Fox, B. L., (2004). Melding: A New Alternative to adhesive bonding. Retrieved from server-web.com/whitepapers/-Melding_ALTERNATIVE_adhesive_bonding_SAMPE2005.pdf
36. Griffiths, B., Noble, N., (2004). Processing and Tooling for Low Cost, Rapid Curing of Composites Structures. Retrieved from server-web.com/newsMedia/-media/January 2004 QS SAMPE Article.pdf
37. Li, X., Li, G., Wang, C. H., (2011). Optimization of Composite Sandwich Structures Subjected to Combined Torsion and Bending Stiffness Requirements. *Applied Composite Materials.* 19 (2), 117-126. doi: 10.1007/s10443-010-9185-4
38. Pimenta, S., Pinho, S. T., (2010). Recycling Carbon Fiber Reinforced Polymers for Structural Applications: Technology Review and Market Outlook. *Waste Management.* 31 (2), 378-392. doi: 10.1016/j.wasman.2010.09.019
39. Carberry, W., (2008). Airplane Recycling Efforts Benefit Boeing Operators. Retrievedfromhttp://130.76.96.105/commercial/aeromagazine/articles/qtr_4_08/pdfs/AERO_Q408_article02.pdf
40. Roberts, A., (2007). Rapid growth forecast for carbon fiber market. *reinforced Plastics.* 51 (2), 10-13. doi: 10.1016/S0034-3617(07)70051-6
41. Carberry, W., (2009). Aerospace's role in the development of the recycled carbon fiber supply chain. Retrieved from http://www.iom3.org/news/lifeline-waste-carbon-fibres
42. Astrom, B. T., (1997). Manufacturing of Polymer Composites. Chapman & Hall.
43. Wong, K. H., Pickering, S. J., Brooks, R., (2007). Recycled carbon fiber reinforced polypropylene composites: effect of coupling agents on mechanical properties. Improved Sustainability and Environmental Performance, Net Composites, Barcelona, Spain
44. Connor, M. L., (2008). Characterization of Recycled Carbon Fibers and Their Formation of Composites Using Injection Molding. North Carolina State University.Retrievedfromhttp://repository.lib.ncsu.edu/ir/bitstream/1840.16/673/1/etd.pdf

45. Allen, B. E., (2008). Characterization of reclaimed Carbon Fibers and their Integration into New Thermoset Polymer Matrices via Existing Composite Fabrication Techniques.
46. Pickering, S. J., Turner, T. A., Warrior, N. A., (2006). Molding Compound Development Using Recycled Carbon Fibers". *Composites part B. Engineering.* 42 (3), 517-525. doi: 10.1016/j.compositesb.2010.11.010
47. Pickering, S. J., Turner, T. A., Warrior, N. A, (2009). Development of High Value Composite Materials Using Recycled Carbon Fiber. Collaborative Research and Development. Retrieved from http://www.bis.gov.uk/files/file34992.pdf
48. Pickering, S. J., Turner, T. A., Warrior, N. A, (2009). AFRECAR and HIRECAR Project Results. Hamburg, Germany. Retrieved from http://tradefairs.fibre2fashion.com/postfairreport/pdf/12708.pdf
49. BIS, (2009). The UK Composite Strategy. Retrieved from http://www.bis.gov.uk/~/media/BISCore/corporate/docs/C/Composites-Strategy.pdf
50. Line, S., (2009). Commercialization of the carbon fiber recycling process.
51. Alsop, S. H., (2009). Pyrolysis off-gas processing. Baltimore, MD. Retrieved from http://www.sampe.org/store/paper.aspx?pid=5633
52. Marsh, G., (2008). Reclaiming value from post-use carbon composite. *Reinforced Plastics.* 52 (7), 36-39. doi: 10.1016/S0034-3617(08)70242-X
53. Hunter, T., (2009). A recycler's perspective on recycling carbon fiber prepreg productionscrap.Retrievedfromhttp://www.reinforcedplastics.com/view/8116/launching-the-carbon-fibre-recycling-industry/
54. George, P. E., (2009). End user perspective: perspective on carbon fiber recycling from a major end user.
55. McConnel, V. P., (2010). Launching the carbon fiber recycling industry. *Reinforced Plastics.* 54 (2), 33-37. doi: 10.1016/S0034-3617(10)70063-1
56. Wood, K., (2010). Carbon fiber reclamation: going commercial. Retrieved from http://www.compositesworld.com/articles/carbon-fiber-reclamation-going-commercial

57. Curry, R., (2010). Successful research program allows high performance brake discs to be manufactured at lower cost. Retrieved from http://www.prlog.org/10475702-successful-research-programme-allows-high-performance-brake-discs-to-be-manufactured-at-lower-cost.html
58. Howarth, J., Jeschke, M., (2009). Advanced non-woven materials from recycled carbon fiber. Conference, IntertechPira,Hamburg, Germany.
59. Panesar, S., (2009). Converting composite waste into high quality reusable carbon fiber.
60. Pickering, S. J. (2006). Recycling technologies for thermoset composite materials-current status. *Composites Part A. Applied Science and Manufacturing.* 37 (8), 106-1215. doi: 10.1016/j.compositesa.2005.05.030
61. Ellison, G. C., McNaught, R., (2000). The use of natural fibers in nonwoven structures for applications as automotive component substrates. Retrieved from http://www.ienica.net/usefulreports/auto.pdf
62. Pickering, S. J., Robinson, P., Pimenta, S., Pinho, S. T., (2010). Applications for recycled carbon fiber. *Waste Management*. 31 (2), 378-392. doi: 10.1016/j.wasman.2010.09.019
63. Berger, L. Program summary of the ACC automotive composites underbody. retrievedfromhttp://www.speautomotive.com/SPEA_CD/SPEA2011/pdf/DDSU/DDSU1.pdf
64. Zhang, J., He, S., Walton, I. H., Kajla, A., Wang, C.H., (2012). Lightweight stiffened composite structure with superior bending strength and stiffness for automotive floor applications. *Sustainable Automotive Technologies 2012.* doi: 10.1007/978-3-642-24145-1_11
65. Knakal, C. W., Shah, B., Berger, L. Manufacturing scenarios and challenges with a fabric SMC automotive underbody. Retrieved from http://www.speautomotive.com/SPEA_CD/SPEA2011/pdf/DDSU/DDSU1.pdf
66. Knakal, C. W., Shah, B., Berger, L. Material properties of a fabric sheet molding compound for a structural composite underbody.

67. Fuchs, H., Gillund, E. Status of the composite underbody component and assembly structural test-analysis correlation, *Multimatic Engineering.* Retrieved fromhttp://www.speautomotive.com/SPEA_CD/SPEA2011/pdf/DDSU/DDSU5.pdf
68. Benham, P.P., Crawford R.J., Mechanics of engineering materials. Longman Scientific and Technical. 1987
69. http://www.substech.com/dokuwiki/punbb/ upload/viewtopic.php?id=7
70. http://www.tech.plym.ac.uk/sme/MATS324/MATS324A2%20E-G-nu.htm

VITA AUCTORIS

NAME	Davide Scuccimarra
PLACE OF BIRTH	Teramo, Italy
YEAR OF BIRTH	1988
EDUCATION	Liceo Scientifico Einstein, Teramo 2002 – 2007 Politecnico di Torino 2007 – 2010 Bachelor Degree Politecnico di Torino 2010 – 2012 Master Degree University of Windsor, Canada 2011 – 2012 M. A. Sc.